TWO NOVEL EFFICIENT ALGORITHMS FOR PARAMETERIZED MAGNETOHYDRODYNAMIC FLOW ENSEMBLE SIMULATION

A Thesis

by

JULIÁN VICENTE MIRANDA

Submitted to Texas A&M International University
in partial fulfillment of the requirements
for the degree of

MASTER OF SCIENCE

August 2023

Major Subject: Mathematics

TWO NOVEL EFFICIENT ALGORITHMS FOR PARAMETERIZED MAGNETOHYDRODYNAMIC FLOW ENSEMBLE SIMULATION

A Thesis

by

JULIÁN VICENTE MIRANDA

Submitted to Texas A&M International University
in partial fulfillment of the requirements
for the degree of

MASTER OF SCIENCE

Approved as to style and content by:

Chair of Committee,	Muhammad Mohebujjaman
Committee Members,	Ruchang Lin
	Saqib Hussain
	Khaled Enab
	Rohitha Goonatilake
Head of Department,	Rohitha Goonatilake

August 2023

Major Subject: Mathematics

ABSTRACT

Two Novel Efficient Algorithms for Parameterized Magnetohydrodynamic Flow Ensemble Simulation

(August 2023)

Julián Vicente Miranda, B. S., Mathematics; 2022

Chair of Committee: Dr. Muhammad Mohebujjaman

We propose, analyze, and test two efficient and accurate, fully-discrete algorithms for computing the solution of stochastic magnetohydrodynamic (MHD) flow problems having random noises within the initial conditions, boundary conditions, forcing functions, and viscosity parameters. The stable decoupled algorithms use the Elsässer variable formulations and a decoupling of the ensemble MHD system into two Oseen-type sub-problems for each realization. For each of the sub-problems, the first algorithm uses a grad-div stabilization and ensemble eddy-viscosity terms in conjunction with penalty-projection based splitting method and provides unconditional stability, and first order accuracy in time. The second algorithm is second order accurate in timein practice, and optimally accurate in space. Both algorithms are designed in a way that at each time step the finite element assembly of the system provides the same coefficient matrix for each of the J realizations but with different right-hand-side vectors. The stability and convergence theorems of both algorithms are ascertained rigorously. The numerical tests are given to support the predicted convergence rates using some manufactured analytical solutions. Finally, we test the penalty-projection scheme on benchmark channel flow over a step, and a regularized lid-driven problems, and found it works well.

ACKNOWLEDGEMENTS

I would like to start by thanking the National Science Foundation (NSF-DMS-2213274) for providing the resources needed to complete this thesis. The NSF supported me with my cost of tuition, a laptop to work on, and all the software necessary in order to complete this thesis. I would also like to thank my advisor Dr.Muhammad Mohebujjaman. I have worked closely with him for over a year now and have learned so much. He has been a tremendous help throughout this thesis and without him, none of this would be possible. I would also like to thank the thesis committee for advising and encouraging me throughout the proposal and thesis process. They asked tough questions, and gave helpful criticism which ultimately made this thesis better. I would also like to thank Texas A&M International University (TAMIU) and the Department of Mathematics and Physics for allowing me to use the cluster computer for running simulations. Because of this, I was able to run multiple simulations at a time allowing me to fine tune parameters at a faster rate. I would like to thank Dr.Rohitha Goonatilake for the insight and suggestions he has given me throughout the editing process. Finally, and most of all, I want to thank my parents. Without their love and support, none of this would be ever possible.

TABLE OF CONTENTS

Page

ABSTRACT ii
ACKNOWLEDGEMENTS iii
TABLE OF CONTENTS iv
LIST OF TABLES v
LIST OF FIGURES vi
INTRODUCTION 1
NOTATION AND PRELIMINARIES 5
FULLY DISCRETE AND DECOUPLED FIRST ORDER IN TIME ENSEMBLE SCHEME 7
GRAD-DIV STABILIZE PENALTY PROJECTION ALGORITHM 11
NUMERICAL EXPERIMENTS 27
CONVERGENCE RATE VERIFICATION 28
CHANNEL FLOW OVER A STEP 31
LID-DRIVEN CAVITY 34
THE IMPLICIT-EXPLICIT ENSEMBLE SCHEME 38
FULLY DISCRETE θ SCHEME 39
NUMERICAL EXPERIMENTS 53
CONVERGENCE RATE VERIFICATION 54
COMPARISON TABLES 58
CONCLUSION AND FUTURE WORKS 60
REFERENCES 61
APPENDIX 64
G-CALCULATIONS FOR θ SCHEME 64
VITA 66

LIST OF TABLES

Page

Table (2.1): Temporal Convergence for SPP-Scheme at $\epsilon = 0.0$ 28
Table (2.2): Temporal Convergence for SPP-Scheme at $\epsilon = 0.001$ 28
Table (2.3): Temporal Convergence for SPP-Scheme at $\epsilon = 0.01$ 28
Table (2.4): Spatial Convergence for SPP-Scheme at $\epsilon = 0.0$ 29
Table (2.5): Spatial Convergence for SPP-Scheme at $\epsilon = 0.001$ 29
Table (2.6): Spatial Convergence for SPP-Scheme at $\epsilon = 0.01$ 29
Table (3.1): Temporal Convergence for θ-Scheme at $\epsilon = 0.0$ 53
Table (3.2): Temporal Convergence for θ-Scheme at $\epsilon = 0.0001$ 53
Table (3.3): Temporal Convergence for θ-Scheme at $\epsilon = 0.01$ 54
Table (3.4): Temporal Convergence for θ-Scheme at $\epsilon = 0.05$ 54
Table (3.5): Temporal Convergence for θ-Scheme at $\epsilon = 0.1$ 54
Table (3.6): Spatial Convergence for θ-Scheme at $\epsilon = 0.0$ 55
Table (3.7): Spatial Convergence for θ-Scheme at $\epsilon = 0.0001$ 55
Table (3.8): Spatial Convergence for θ-Scheme at $\epsilon = 0.001$ 55
Table (3.9): Spatial Convergence for θ-Scheme at $\epsilon = 0.05$ 56
Table (3.10): Spatial Convergence for θ-Scheme at $\epsilon = 0.1$ 56
Table (4.1): 2-Norm γ Convergence for SPP-Scheme using 1^{st} set of $(\nu_j, \nu_{m,j})$ 57
Table (4.2): 2-Norm γ Convergence for SPP-Scheme using 2^{nd} set of $(\nu_j, \nu_{m,j})$ 57
Table (4.3): ∞-Norm γ Convergence for SPP-Scheme using 3^{rd} set of $(\nu_j, \nu_{m,j})$ 57
Table (4.4): ∞-Norm γ Convergence for SPP-Scheme using 4^{th} set of $(\nu_j, \nu_{m,j})$ 58

LIST OF FIGURES

Page

Figure (1.1): Image of MHD blood pump 1

Figure (1.2): Image of liquid-metal flow in channels 2

Figure (2.1): Velocity ensemble average solutions; SPP-FEM and BE-MHD comparison 31

Figure (2.2): Magnetic field ensemble average solutions; SPP-FEM and BE-MHD comparison 32

Figure (2.3): Velocity strength for lid driven cavity solution at $s = 0.0$ 34

Figure (2.4): Velocity strength for lid driven cavity solution at varying s 35

Figure (2.5): Magnetic field for lid driven cavity solution at varying s 36

Key words. Magnetohydrodynamics, Uncertainty quantification, Penalty-projection method, fast ensemble calculation, second order scheme, Backward-euler, finite element method, Elsässer variables

1 Introduction

Magnetohydrodynamics (MHD) is the study of the interaction of electrically conducting fluids and imposed magnetic fields. When an electrically conducting fluid, such as an ionized gas or liquid metal, moves in a magnetic field, the magnetic field polarizes the fluid which induces a current density in the fluid and creates a second magnetic field. This second magnetic field adds to the original magnetic field and changes the magnetic field. This resultant magnetic field interacts with the induced current density and creates a force that opposes the movement of the flow. One of the major benefits of utilizing MHD flow is that it requires no moving parts to produce a flow in the electrically conducting fluid.. Such precision is necessary for many applications such as weather forecasting [28, 34], liquid metal cooling of nuclear reactors such as the *Tokamak* [5, 18, 40], process metallurgy [11, 12], artificial heart [44], and MHD propulsion [30, 31].

Fig. 1.1: The test device with an AC MHD blood pump a: the general schematic of the experimental device; b: Longitudinal view of the pump body; c: the pump body is schematic diagram and internal structure diagram. [44]

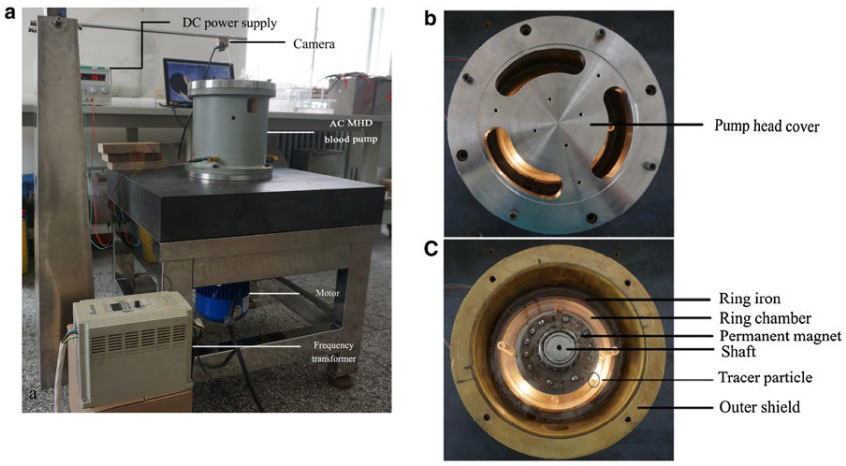

Fig. 1.2: Magnetohydrodynamics of liquid-metal flow in channels. [5]

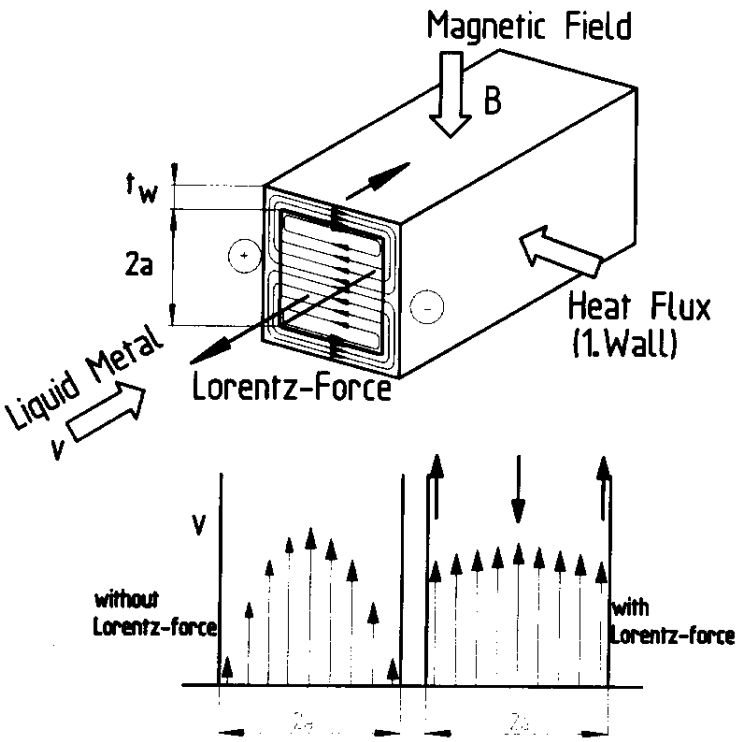

One of the many applications of MHD can be used to simulate plasma propulsion [2, 39, 41]. Electromagnetic plasma propulsion systems offer high exhaust velocities and produce higher thrust densities than space-charge limited electric propulsion systems [39]. These systems use magnetic fields to accelerate and expel plasma, enabling efficient propulsion within a vacuum. Another use of MHD can be seen in the field of geophysics [7]. MHD can be observed within the Earth's fluid core causing geomagnetic field generation. The MHD system is presented as the nonlinear coupling of the momentum equation to the Maxwell's equation of the magnetic field.

We will be using the following system of governing equations from [6, 26] to formulate the governing equations for our stochastic MHD system:

$$\begin{aligned} \boldsymbol{u}_t + (\boldsymbol{u}\cdot\nabla)\boldsymbol{u} - s(\boldsymbol{B}\cdot\nabla)\boldsymbol{B} - \nu\Delta\boldsymbol{u} + \nabla p &= f, && (1.1)\\ \nabla\cdot\boldsymbol{u} &= 0, && (1.2)\\ \boldsymbol{B}_t + (\boldsymbol{u}\cdot\nabla)\boldsymbol{B} - (\boldsymbol{B}\cdot\nabla)\boldsymbol{u} - \nu,\Delta\boldsymbol{B} + \nabla\lambda &= \nabla\times\boldsymbol{g}, && (1.3)\\ \nabla\cdot\boldsymbol{B} &= 0. && (1.4) \end{aligned}$$

In order to present a realistic MHD flow model, random noise in the initial and boundary conditions, forcing functions and diffusion parameters must be considered. To approximate the randomness and

produce accurate solution statistics of the stochastic MHD system, we consider J time dependent, nonlinear coupled systems of PDE's [6, 11, 26, 36] as follows:

$$\begin{aligned}
\boldsymbol{u}_{j,t} + \boldsymbol{u}_j \cdot \nabla \boldsymbol{u}_j - s\boldsymbol{B}_j \cdot \nabla \boldsymbol{B}_j - \nu_j \Delta \boldsymbol{u}_j + \nabla p_j &= \boldsymbol{f}_j(\boldsymbol{x}, t), \text{ in } \Omega \times (0, T], && (1.5)\\
\boldsymbol{B}_{j,t} + \boldsymbol{u}_j \cdot \nabla \boldsymbol{B}_j - \boldsymbol{B}_j \cdot \nabla \boldsymbol{u}_j - \nu_{m,j} \Delta \boldsymbol{B}_j + \nabla \lambda_j &= \nabla \times \boldsymbol{g}_j(\boldsymbol{x}, t), \text{ in } \Omega \times (0, T], && (1.6)\\
\nabla \cdot \boldsymbol{u}_j &= 0, \text{ in } \Omega \times (0, T], && (1.7)\\
\nabla \cdot \boldsymbol{B}_j &= 0, \text{ in } \Omega \times (0, T], && (1.8)\\
\boldsymbol{u}_j(\boldsymbol{x}, 0) &= \boldsymbol{u}_j^0(\boldsymbol{x}), \text{ in } \Omega, && (1.9)\\
\boldsymbol{B}_j(\boldsymbol{x}, 0) &= \boldsymbol{B}_j^0(\boldsymbol{x}), \text{ in } \Omega, && (1.10)
\end{aligned}$$

where $\boldsymbol{u}_j$, $\boldsymbol{B}_j$, p_j, and λ_j denote the velocity, magnetic field, pressure, and artificial magnetic pressure solutions, respectively, for each j-th candidate of the ensemble utilizing different initial conditions $\boldsymbol{u}_j^0$ and $\boldsymbol{B}_j^0$, kinematic viscosity ν_j, magnetic diffusivity $\nu_{m,j}$, and forcing functions $\boldsymbol{f}_j$, and $\nabla \times \boldsymbol{g}_j$. The index $j = 1, 2, \cdots, J$, and J represents the number of realization used to approximate the randomness of the data. The convex polygonal or polyhedral simulation domain is denoted by $\Omega \in \mathbb{R}^d (d = 2 \text{ or } 3)$ with boundary $\partial\Omega$, t is the time variable, T is the simulation time, $\boldsymbol{x}$ is the spatial variable, and s is the coupling number. We will consider homogeneous Dirichlet boundary conditions for simplicity of our analysis.

One of the main difficulties in simulating MHD flow is solving the fully coupled systems (1.5) to (1.10) (together with the appropriate boundary conditions), where the velocity and magnetic fields are nonlinearly coupled through the coupling parameter s. Computing long-time simulation in the convection-dominated regime with high spatial resolution of a fully coupled MHD system (even assuming no noise present in the data) is computationally challenging and quite demanding even with the advanced super computing facilities. As the common decoupled algorithms often fail unless a very small time-step size is used. To avoid this issue, an excellent idea was proposed by Trenchea in [42] which decouples the MHD system rewriting them in terms of Elsässer variables, which greatly decreases the computational complexity within the system [13, 14, 29]. Studies have shown that MHD systems with Elsässer variables allow us to propose decoupled stable simulation algorithm [1, 19, 35, 36, 42, 43], thus decreasing the

computational cost. The following substitutions are used to get the Elsässer variables formulation:

$$\begin{aligned}
\boldsymbol{v}_j &:= \boldsymbol{u}_j + \sqrt{s}\boldsymbol{B}_j,\\
\boldsymbol{w}_j &:= \boldsymbol{u}_j - \sqrt{s}\boldsymbol{B}_j,\\
\boldsymbol{f}_{1,j} &:= \boldsymbol{f}_j + \sqrt{s}\nabla \times \boldsymbol{g}_j,\\
\boldsymbol{f}_{2,j} &:= \boldsymbol{f}_j - \sqrt{s}\nabla \times \boldsymbol{g}_j,\\
q_j &:= p_j + \sqrt{s}\lambda_j,\\
r_j &:= p_j - \sqrt{s}\lambda_j,
\end{aligned}$$

together with the initial and boundary conditions to produce:

$$\boldsymbol{v}_{j,t} + \boldsymbol{w}_j \cdot \nabla \boldsymbol{v}_j - \frac{\nu_j + \nu_{m,j}}{2}\Delta \boldsymbol{v}_j - \frac{\nu_j - \nu_{m,j}}{2}\Delta \boldsymbol{w}_j + \nabla q_j = \boldsymbol{f}_{1,j}, \tag{1.11}$$

$$\boldsymbol{w}_{j,t} + \boldsymbol{v}_j \cdot \nabla \boldsymbol{w}_j - \frac{\nu_j + \nu_{m,j}}{2}\Delta \boldsymbol{w}_j - \frac{\nu_j - \nu_{m,j}}{2}\Delta \boldsymbol{v}_j + \nabla r_j = \boldsymbol{f}_{2,j}, \tag{1.12}$$

$$\nabla \cdot \boldsymbol{v}_j = \nabla \cdot \boldsymbol{w}_j = 0. \tag{1.13}$$

The computational cost of the above system = $J\times$ one MHD system. We will be utilizing the break through idea proposed by Jiang and Layton idea in [22] for computing ensemble average of the solutions to reduce the large computational cost of (1.11)-(1.13). We will propose a decoupled scheme of the system enabling the algorithm to solve two identical Oseen-type [46] sub-problems simultaneously at each time-step. This will save on computer memory and system matrix assembly and factorization/preconditioner are needed only once per time-step.

Computing long-time simulations of fully coupled MHD ensemble systems is computationally arduous and expensive. Therefore, decoupled algorithms which can reuse the global system matrix at each time-step for all J realizations are computationally attractive. First-order time-stepping partitioned algorithms with small time-step restrictions are studied at low magnetic Reynolds number in a reduced MHD system in [24]. Decoupled, and unconditionally stable algorithm for the evolutionary full MHD ensemble system in Elsässer variables are investigated in [36].

This thesis will investigate three efficient algorithms for the Uncertainty Quantification (UQ) of MHD flows. The fully discrete and decoupled first order in time ensemble scheme, grad-div stabilize penalty projection finite element algorithm and implicit-explicit second order time-stepping ensemble scheme (fully discrete $\boldsymbol{\theta}$-scheme). The first algorithms is our preliminary algorithm from [37]. We will leverage this information to aid in the development of other algorithms and assess their accuracy and convergence rates in comparison to this one. The other two algorithms each contain four subsections. We

show each of their stability analysis, convergence, numerical experiments, convergence rate verification, and finally their appropriate tables and figures. Following these sections, we will show tables comparing the convergence rates between the BE-MHD and SPP-FEM algorithms.

1.1 Notations and Preliminaries

The usual $L^2(\Omega)$ norm and inner product are denoted by $\|.\|$ and $(.,.)$, respectively. Similarly, the $L^p(\Omega)$ norms and the Sobolev $W_p^k(\Omega)$ norms are $\|.\|_{L^p}$ and $\|.\|_{W_p^k}$, respectively for $k \in \mathbb{N}$, $1 \leq p \leq \infty$. The Sobolev space $W_2^k(\Omega)$ is represented by $H^k(\Omega)$ with norm $\|.\|_k$. The vector-valued spaces are defined by

$$\boldsymbol{L}^p(\Omega) = (L^p(\Omega))^d, \text{ and } \boldsymbol{H}^k(\Omega) = (H^k(\Omega))^d.$$

For $\boldsymbol{X}$ being a normed function space in Ω, $L^p(0,T;\boldsymbol{X})$ is the space of all functions defined on $(0,T]\times\Omega$ for which the following norm

$$\|\boldsymbol{u}\|_{L^p(0,T;\boldsymbol{X})} = \left(\int_0^T \|\boldsymbol{u}\|_{\boldsymbol{X}}^p dt\right)^{\frac{1}{p}}, \quad p \in [1,\infty)$$

is finite. For $p=\infty$, the usual modification is used in the definition of this space. The natural function spaces for our problem are

$$\begin{aligned}
\boldsymbol{X} &:= \boldsymbol{H}_0^1(\Omega) = \{\boldsymbol{v} \in \boldsymbol{L}^p(\Omega) : \nabla \boldsymbol{v} \in L^2(\Omega)^{d\times d}, \boldsymbol{v} = \boldsymbol{0} \text{ on } \partial\Omega\},\\
\boldsymbol{Y} &:= \{\boldsymbol{v} \in \boldsymbol{H}^1(\Omega) : \boldsymbol{v}\cdot\hat{\boldsymbol{n}} = 0 \text{ on } \partial\Omega\},\\
Q &:= L_0^2(\Omega) = \{q \in L^2(\Omega) : \int_\Omega q\, d\boldsymbol{x} = 0\}.
\end{aligned}$$

Recall that the Poincaré inequality holds in $\boldsymbol{X}$. There exists C depending only on Ω satisfying for all $\boldsymbol{\varphi} \in \boldsymbol{X}$,

$$\|\boldsymbol{\varphi}\| \leq C\|\nabla\boldsymbol{\varphi}\|.$$

The divergence-free velocity space is given by

$$\boldsymbol{V} := \{\boldsymbol{v} \in \boldsymbol{X} : (\nabla\cdot\boldsymbol{v}, q) = 0, \forall q \in Q\}.$$

We define the trilinear form $b : \boldsymbol{X}\times\boldsymbol{X}\times\boldsymbol{X} \to \mathbb{R}$ by

$$b(\boldsymbol{u},\boldsymbol{v},\boldsymbol{w}) := (\boldsymbol{u}\cdot\nabla\boldsymbol{v},\boldsymbol{w}),$$

and the explicitly skew symmetrized trilinear form $b^* : \boldsymbol{X} \times \boldsymbol{X} \times \boldsymbol{X} \to \mathbb{R}$ by

$$b^*(\boldsymbol{u}, \boldsymbol{v}, \boldsymbol{w}) := \frac{1}{2}\big((\boldsymbol{u} \cdot \nabla \boldsymbol{v}, \boldsymbol{w}) - (\boldsymbol{u} \cdot \nabla \boldsymbol{w}, \boldsymbol{v})\big).$$

Note that $b^*(\boldsymbol{u}, \boldsymbol{v}, \boldsymbol{v}) = 0$, and if $\|\nabla \cdot \boldsymbol{u}\| = 0$, then $(\boldsymbol{u} \cdot \nabla \boldsymbol{v}, \boldsymbol{w}) = b^*(\boldsymbol{u}, \boldsymbol{v}, \boldsymbol{w})$. Moreover, $b^*(\boldsymbol{u}, \boldsymbol{v}, \boldsymbol{w})$ satisfies the following bound [17]:

$$|b^*(\boldsymbol{u}, \boldsymbol{v}, \boldsymbol{w})| \leq C(\Omega)\|\nabla \boldsymbol{u}\|\|\nabla \boldsymbol{v}\|\|\nabla \boldsymbol{w}\|, \quad \text{for any } \ \boldsymbol{u}, \boldsymbol{v}, \boldsymbol{w} \in \boldsymbol{X}. \tag{1.14}$$

The conforming finite element spaces are denoted by $\boldsymbol{X}_h \subset \boldsymbol{X}$ and $Q_h \subset Q$, and we assume a regular triangulation $\tau_h(\Omega)$, where h is the maximum triangle diameter. We assume that $(\boldsymbol{X}_h, Q_h)$ satisfies the usual discrete *inf-sup* condition

$$\inf_{q_h \in Q_h} \sup_{\boldsymbol{v}_h \in \boldsymbol{X}_h} \frac{(q_h, \nabla \cdot \boldsymbol{v}_h)}{\|q_h\|\|\nabla \boldsymbol{v}_h\|} \geq \beta > 0, \tag{1.15}$$

where β is independent of h. The space of discretely divergence-free functions is defined as

$$\boldsymbol{V}_h := \{\boldsymbol{v}_h \in \boldsymbol{X}_h : (\nabla \cdot \boldsymbol{v}_h, q_h) = 0, \ \ \forall q_h \in Q_h\}.$$

Consider a shape-regular, simplicial, and conforming triangulation of Ω denoted as $\mathcal{T}_h$. In this context, each simplex T in the triangulation has a diameter $h_T = \text{diam}(T)$ and $h := \max_{T \in \mathcal{T}_h}$. We define $\mathcal{P}_k$ as the space of piecewise polynomials with respect to the triangulation $\mathcal{T}_h$, where the degree does not exceed k. Additionally, we use $\boldsymbol{\mathcal{P}}_k := [\mathcal{P}_k]^d$ to represent the corresponding vector-valued polynomial space.

For simplicity of our analysis, we will use the Scott-Vogelius (SV) finite element pair $(\boldsymbol{X}_h, Q_h) = \big((P_k)^d, P_{k-1}^{disc}\big)$, which satisfies the *inf-sup* condition under certain conditions, such as when the mesh is created as a barycenter refinement of a regular mesh and the polynomial degree $k \geq d$ [3, 45]. Our analysis can be extended without difficulty to any *inf-sup* stable element choice, although with minor additional technical detail. Since the SV element is point-wise divergence free, the discrete pressure terms vanish from the analysis. But if we use a finite element pair which is only weakly divergence free, for example, the Taylor-Hood element, then we must need to handle the pressure involving terms in the analysis. Since, in this case, the orthogonal property of the discrete pressure and velocity spaces may not hold true.

We have the following approximation properties in $(\boldsymbol{X}_h, Q_h)$ [8]:

$$\inf_{\boldsymbol{v}_h \in \boldsymbol{X}_h} \|\boldsymbol{u} - \boldsymbol{v}_h\| \leq Ch^{k+1}|\boldsymbol{u}|_{k+1}, \quad \boldsymbol{u} \in \boldsymbol{H}^{k+1}(\Omega), \tag{1.16}$$

$$\inf_{\boldsymbol{v}_h \in \boldsymbol{X}_h} \|\nabla(\boldsymbol{u} - \boldsymbol{v}_h)\| \leq Ch^{k}|\boldsymbol{u}|_{k+1}, \quad \boldsymbol{u} \in \boldsymbol{H}^{k+1}(\Omega), \tag{1.17}$$

$$\inf_{q_h \in Q_h} \|p - q_h\| \leq Ch^{k}|p|_{k}, \quad p \in H^{k}(\Omega), \tag{1.18}$$

where $|\cdot|_r$ denotes the H^r or $\boldsymbol{H}^r$ seminorm.

We will assume the mesh is sufficiently regular for the inverse inequality to hold, and with this and the *inf-sup* assumption, we have approximation properties

$$\|\nabla(\boldsymbol{u} - P^{L^2}_{\boldsymbol{V}_h}(\boldsymbol{u}))\| \leq Ch^{k}|\boldsymbol{u}|_{k+1}, \quad \boldsymbol{u} \in \boldsymbol{H}^{k+1}(\Omega), \tag{1.19}$$

$$\inf_{\boldsymbol{v}_h \in \boldsymbol{V}_h} \|\nabla(\boldsymbol{u} - \boldsymbol{v}_h)\| \leq Ch^{k}|\boldsymbol{u}|_{k+1}, \quad \boldsymbol{u} \in \boldsymbol{H}^{k+1}(\Omega), \tag{1.20}$$

where $P^{L^2}_{\boldsymbol{V}_h}(\boldsymbol{u})$ is the L^2 projection of $\boldsymbol{u}$ into $\boldsymbol{V}_h$.

The following lemma for the discrete Grönwall inequality was given in [20].

Lemma 1.1. *Let Δt, $\mathcal{D}$, a_n, b_n, c_n, d_n be non-negative numbers for $n = 1, \cdots, M$ such that*

$$a_M + \Delta t \sum_{n=1}^{M} b_n \leq \Delta t \sum_{n=1}^{M-1} d_n a_n + \Delta t \sum_{n=1}^{M} c_n + \mathcal{D} \quad \textit{for } M \in \mathbb{N},$$

then for all $\Delta t > 0$,

$$a_M + \Delta t \sum_{n=1}^{M} b_n \leq exp\left(\Delta t \sum_{n=1}^{M-1} d_n\right)\left(\Delta t \sum_{n=1}^{M} c_n + \mathcal{D}\right) \quad \textit{for } M \in \mathbb{N}.$$

1.2 Fully Discrete and Decoupled First Order in Time Ensemble Scheme

To solve the MHD system in (1.11) to (1.13) efficiently, a decoupled, fully discrete, first-order accurate time-stepping algorithm is proposed in [31]. The algorithm is efficient because of its following features: (1) It decouples the system (1.11) to (1.13) into two Oseen-type sub-problems, which can be solved simultaneously and both have a much smaller block system matrix than the original MHD problem. (2) The two sub-problems are identical. (3) At each time-step, each of the sub-problems, shares a common system matrix for all of its realizations but with different right-hand-side vectors, which saves a huge computer memory and assembling time. Thus, if we want to use a direct solver, the LU decomposition (or its variant) of the system matrix needs to be computed only once at each time-step. On the other hand, if we want to use Krylov subspace methods, the precondition we need to build only once at each

time-step. Moreover, it can take advantage of the block linear solvers, and the computational cost could be reduced to the level of solving a single MHD system without noise in the data.

Algorithm 1: Fully discrete and decoupled Backward-Euler MHD (BE-MHD) ensemble scheme [37]

Given time-step $\Delta t > 0$, end time $T > 0$, initial conditions $\boldsymbol{v}_j^0, \boldsymbol{w}_j^0 \in \boldsymbol{V}_h$ and $\boldsymbol{f}_{1,j}, \boldsymbol{f}_{2,j} \in L^2\left(0, T; \boldsymbol{H}^{-1}(\Omega)\right)$ for $j = 1, 2, \cdots, J$. Set $M = T/\Delta t$ and for $n = 1, \cdots, M-1$, to compute as follows:

Step 1: Find $\boldsymbol{v}_{j,h}^{n+1} \in \boldsymbol{V}_h$ satisfying, for all $\boldsymbol{\chi}_{j,h} \in \boldsymbol{V}_h$:

$$\begin{aligned}
&\left(\frac{\boldsymbol{v}_{j,h}^{n+1} - \boldsymbol{v}_{j,h}^{n}}{\Delta t}, \boldsymbol{\chi}_{j,h}\right) + b\left(< \boldsymbol{w}_h >^n, \boldsymbol{v}_{j,h}^{n+1}, \boldsymbol{\chi}_{j,h}\right) + \frac{\bar{\nu} + \bar{\nu}_m}{2}\left(\nabla \boldsymbol{v}_{j,h}^{n+1}, \nabla \boldsymbol{\chi}_{j,h}\right) \\
&+ \left(2\nu_T(\boldsymbol{w}_h^{'}, t^n)\nabla \boldsymbol{v}_{j,h}^{n+1}, \nabla \boldsymbol{\chi}_{j,h}\right) = \left(\boldsymbol{f}_{1,j}(t^{n+1}), \boldsymbol{\chi}_{j,h}\right) - b\left(\boldsymbol{w}_{j,h}^{'n}, \boldsymbol{v}_{j,h}^{n}, \boldsymbol{\chi}_{j,h}\right) \\
&- \frac{\nu_j - \nu_{m,j}}{2}\left(\nabla \boldsymbol{w}_{j,h}^{n}, \nabla \boldsymbol{\chi}_{j,h}\right) - \frac{\nu_j^{'} + \nu_{m,j}^{'}}{2}\left(\nabla \boldsymbol{v}_{j,h}^{n}, \nabla \boldsymbol{\chi}_{j,h}\right). \qquad (1.21)
\end{aligned}$$

Step 2: Find $\boldsymbol{w}_{j,h}^{n+1} \in \boldsymbol{V}_h$ satisfying, for all $\boldsymbol{l}_{j,h} \in \boldsymbol{V}_h$:

$$\begin{aligned}
&\left(\frac{\boldsymbol{w}_{j,h}^{n+1} - \boldsymbol{w}_{j,h}^{n}}{\Delta t}, \boldsymbol{l}_{j,h}\right) + b\left(< \boldsymbol{v}_h >^n, \boldsymbol{w}_{j,h}^{n+1}, \boldsymbol{l}_{j,h}\right) + \frac{\bar{\nu} + \bar{\nu}_m}{2}\left(\nabla \boldsymbol{w}_{j,h}^{n+1}, \nabla \boldsymbol{l}_{j,h}\right) \\
&+ \left(2\nu_T(\boldsymbol{v}_h^{'}, t^n)\nabla \boldsymbol{w}_{j,h}^{n+1}, \nabla \boldsymbol{l}_{j,h}\right) = \left(\boldsymbol{f}_{2,j}(t^{n+1}), \boldsymbol{l}_{j,h}\right) - b\left(\boldsymbol{v}_{j,h}^{'n}, \boldsymbol{w}_{j,h}^{n}, \boldsymbol{l}_{j,h}\right) \\
&- \frac{\nu_j - \nu_{m,j}}{2}\left(\nabla \boldsymbol{v}_{j,h}^{n}, \nabla \boldsymbol{l}_{j,h}\right) - \frac{\nu_j^{'} + \nu_{m,j}^{'}}{2}\left(\nabla \boldsymbol{w}_{j,h}^{n}, \nabla \boldsymbol{l}_{j,h}\right). \qquad (1.22)
\end{aligned}$$

Where $\boldsymbol{v}_{j,h}^n, \boldsymbol{w}_{j,h}^n, q_{j,h}^n$, and $r_{j,h}^n$ denote approximations of $\boldsymbol{v}_j(\cdot, t^n), \boldsymbol{w}_j(\cdot, t^n), q_j(\cdot, t^n)$, and $r_j(\cdot, t^n)$, respectively. The ensemble mean and fluctuation about the mean are defined as follows:

$$\begin{aligned}
< \boldsymbol{u}_h >^n &:= \frac{1}{J}\sum_{j=1}^{J} \boldsymbol{u}_{j,h}^n, \quad \boldsymbol{u}_{j,h}^{'n} := \boldsymbol{u}_{j,h}^n - < \boldsymbol{u}_h >^n, \\
\bar{\nu} &:= \frac{1}{J}\sum_{j=1}^{J} \nu_j, \quad \nu_j^{'} := \nu_j - \bar{\nu}, \text{ and} \\
\bar{\nu}_m &:= \frac{1}{J}\sum_{j=1}^{J} \nu_{j,m}, \quad \nu_{j,m}^{'} := \nu_{j,m} - \bar{\nu}_m.
\end{aligned}$$

The eddy viscosity term, which is $O(\Delta t)$, is defined using mixing length phenomenology, following

[23], and is given by

$\nu_T(\boldsymbol{z}^{'}, t^n) := \mu\Delta t(l_{\boldsymbol{z}}^n)^2$, where $(l_{\boldsymbol{z}}^n)^2 = \sum_{j=1}^{J} |\boldsymbol{z}_j^{'n}|^2$ is a scalar quantity, and $|\cdot|$ denotes length of a vector.

Assumption 1.1. *Assume the true solution $\boldsymbol{v}_j, \boldsymbol{w}_j \in L^2(0,T;\boldsymbol{H}^2(\Omega))$. We also assume there exists a constant C_* which is independent of h, Δt, and γ such that for sufficiently small h and Δt, the solutions of the Algorithm 1 satisfies*

$$\max_{1\le n\le M}\Big(\|\nabla \boldsymbol{v}_{j,h}^n\|_{L^3} + \|\nabla \boldsymbol{w}_{j,h}^n\|_{L^3} + \|\boldsymbol{v}_{j,h}^n\|_\infty + \|\boldsymbol{w}_{j,h}^n\|_\infty\Big) \le C_*, \ \ \textit{for all } \ j = 1, 2, \cdots, J.$$

Define $\alpha_j := \bar{\nu}+\bar{\nu}_m - |\nu_j - \nu_{m,j}| - |\nu_j^{'} + \nu_{m,j}^{'}|$, for $j = 1, 2, \cdots, J$, then the stability of the Algorithm 1 can be given as below [37]:

Theorem 1.2. *Suppose $\boldsymbol{f}_{1,j}, \boldsymbol{f}_{2,j} \in L^2\left(0,T;\boldsymbol{H}^{-1}(\Omega)\right)$, and $\boldsymbol{v}_{j,h}^0$, $\boldsymbol{w}_{j,h}^0 \in \boldsymbol{H}^1(\Omega)$, then the solutions to the Algorithm 1 are stable: For any $\Delta t > 0$, if $\alpha_j > 0$, and $\mu > \frac{1}{2}$*

$$\begin{aligned}\|\boldsymbol{v}_{j,h}^M\|^2 + \|\boldsymbol{w}_{j,h}^M\|^2 + \frac{\bar{\nu}+\bar{\nu}_m}{2}\Delta t\Big(\|\nabla \boldsymbol{v}_{j,h}^M\|^2 + \|\nabla \boldsymbol{w}_{j,h}^M\|^2\Big) + \frac{\alpha_j\Delta t}{2}\sum_{n=0}^{M-1}\Big(\|\nabla \boldsymbol{v}_{j,h}^n\|^2 + \|\nabla \boldsymbol{w}_{j,h}^n\|^2\Big)\\ \le \|\boldsymbol{v}_{j,h}^0\|^2 + \|\boldsymbol{w}_{j,h}^0\|^2 + \frac{\bar{\nu}+\bar{\nu}_m}{2}\Delta t\Big(\|\nabla \boldsymbol{v}_{j,h}^0\|^2 + \|\nabla \boldsymbol{w}_{j,h}^0\|^2\Big)\\ + \frac{2\Delta t}{\alpha_j}\sum_{n=0}^{M-1}\Big(\|\boldsymbol{f}_{1,j}(t^{n+1})\|_{-1}^2 + \|\boldsymbol{f}_{2,j}(t^{n+1})\|_{-1}^2\Big).\end{aligned}$$

It is proved in [37] that the discrete ensemble average solution to the Algorithm 1 converges to the true ensemble average under assumed regularity assumptions. The theory shows that the first-order temporal BE-MHD Algorithm 1 is optimally accurate for 2D and shows a sub-optimal convergence in 3D due to the introduction of the ensemble eddy-viscosity term.

Theorem 1.3. *Assume $(\boldsymbol{v}_j, \boldsymbol{w}_j, q_j, r_j)$ satisfying (1.11)-(1.13) with regularity assumptions $\boldsymbol{v}_j, \boldsymbol{w}_j \in L^2\big(0,T;\boldsymbol{H}^{k+1}(\Omega)\big)$, $\boldsymbol{v}_{j,t}, \boldsymbol{w}_{j,t} \in L^2\big(0,T,\boldsymbol{H}^2(\Omega)\big)$, $\boldsymbol{v}_{j,tt}, \boldsymbol{w}_{j,tt} \in L^2\big(0,T,\boldsymbol{L}^2(\Omega)\big)$ for $j = 1, 2, \cdots, J$, then the ensemble average solution $(<\boldsymbol{v}_h>, <\boldsymbol{w}_h>)$ to the Algorithm 1 converges to the true ensemble average solution: For any $\Delta t > 0$, if $\alpha_j > 0$, and $\mu > \frac{1}{2}$, one has*

$$\begin{aligned}\| <\boldsymbol{v}>(T) - <\boldsymbol{v}_h>^M \|^2 + \| <\boldsymbol{w}>(T) - <\boldsymbol{w}_h>^M \|^2 + \frac{\alpha_j\Delta t}{2}\sum_{n=1}^{M}\Big(\|\nabla\big(<\boldsymbol{v}>(t^n) - <\boldsymbol{v}_h>^n\big)\|^2\\ + \|\nabla\big(<\boldsymbol{w}>(t^n) - <\boldsymbol{w}_h>^n\big)\|^2\Big) \le C\, exp\Big(\frac{CT}{\alpha_j}\Big(1 + \frac{\Delta t^2}{J}\Big)\Big)\Big(\Delta t^2 + h^{2k} + h^{2k}\Delta t^2\\ + h^{2-d}\Delta t^2 + h^{2k-1}\Delta t + h^{2k+2}\Big).\end{aligned}$$

The BE-MHD algorithm solves a saddle-point problem at each time, which leads to solve a 2×2 block system with stable finite element pair. This needs still a huge computation cost for computing ensemble solution of realistic flow problems in the convection-dominated regime with high spatial resolution. This motivates us to propose a more efficient penalty-projection based splitting algorithm.

2 Grad-div Stabilize Penalty Projection Finite Element Algorithm

Now, we present and analyze an efficient, fully discrete, and decoupled penalty-projection time stepping scheme with grad-div stabilization terms for computing MHD flow ensemble. To introduce splitting, we define an additional velocity space: $\boldsymbol{Y}_h := (\boldsymbol{P}_k)^d \cap \boldsymbol{H}_0^{div}(\Omega)^d$.

The importance and benifits of this algorithms includes 1) Step 1 (2.1) and Step 3 (2.4) can be represented as $A[x_1|x_2|\cdots|x_j] = [b_1|b_2|\cdots|b_j]$. For direct solver, we need only one LU-factorization at each time-step. 2) For iterative solver, we need to build preconditioner only once for each time-step and can re-use for all realization. Moreover, can take advantage of block linear solvers. 3) For Step 2 (2.2) and Step 4 (2.5), the system matrix is symmetric-positive definite and can be solved by the conjugate-gradient method. 4) The BE-MHD algorithm is useful since it solves velocity and magnetic field separately, however the benefit of using the SPP-FEM Algorithm is that we will be solving for velocity, magnetic field, and pressure separately. This will save time when computing the system matrix, which is a very time consuming process. 5) As $\lambda \to \infty$, SPP-FEM solution converges to BE-MHD algorithm's solution.

The scheme is defined below.

Algorithm 2: Stabilized Penalty Projection - Finite Element Method (SPP-FEM)

Given time-step $\Delta t > 0$, end time $T > 0$, stabilization parameter $\gamma > 0$, initial conditions $\boldsymbol{v}_j^0, \boldsymbol{w}_j^0 \in \boldsymbol{V}_h$ and $\boldsymbol{f}_{1,j}, \boldsymbol{f}_{2,j} \in L^2\left(0,T;\boldsymbol{H}^{-1}(\Omega)\right)$ for $j = 1, 2, \cdots, J$. Set $M = T/\Delta t$ and for $n = 1, \cdots, M-1$, to compute:

Step 1: Find $\hat{\boldsymbol{v}}_{j,h}^{n+1} \in \boldsymbol{X}_h$ satisfying, for all $\boldsymbol{\chi}_{j,h} \in \boldsymbol{X}_h$:

$$\begin{aligned}
&\left(\frac{\hat{\boldsymbol{v}}_{j,h}^{n+1} - \tilde{\boldsymbol{v}}_{j,h}^{n}}{\Delta t}, \boldsymbol{\chi}_{j,h}\right) + b\left(< \hat{\boldsymbol{w}}_h >^n, \hat{\boldsymbol{v}}_{j,h}^{n+1}, \boldsymbol{\chi}_{j,h}\right) + \frac{\bar{\nu} + \bar{\nu}_m}{2}\left(\nabla \hat{\boldsymbol{v}}_{j,h}^{n+1}, \nabla \boldsymbol{\chi}_{j,h}\right) \\
&+ \gamma\left(\nabla \cdot \hat{\boldsymbol{v}}_{j,h}^{n+1}, \nabla \cdot \boldsymbol{\chi}_{j,h}\right) + \left(2\nu_T(\hat{\boldsymbol{w}}_h^{'}, t^n)\nabla \hat{\boldsymbol{v}}_{j,h}^{n+1}, \nabla \boldsymbol{\chi}_{j,h}\right) = \left(\boldsymbol{f}_{1,j}(t^{n+1}), \boldsymbol{\chi}_{j,h}\right) \\
&- b\left(\hat{\boldsymbol{w}}_{j,h}^{'n}, \hat{\boldsymbol{v}}_{j,h}^{n}, \boldsymbol{\chi}_{j,h}\right) - \frac{\nu_j - \nu_{m,j}}{2}\left(\nabla \hat{\boldsymbol{w}}_{j,h}^{n}, \nabla \boldsymbol{\chi}_{j,h}\right) - \frac{\nu_j^{'} + \nu_{m,j}^{'}}{2}\left(\nabla \hat{\boldsymbol{v}}_{j,h}^{n}, \nabla \boldsymbol{\chi}_{j,h}\right). \qquad (2.1)
\end{aligned}$$

Step 2: Find $(\tilde{\boldsymbol{v}}_{j,h}^{n+1}, \hat{q}_{j,h}^{n+1}) \in \boldsymbol{Y}_h \times Q_h$ satisfying for all $(\boldsymbol{v}_{j,h}, q_{j,h}) \in \boldsymbol{Y}_h \times Q_h$,

$$\left(\frac{\tilde{\boldsymbol{v}}_{j,h}^{n+1} - \hat{\boldsymbol{v}}_{j,h}^{n+1}}{\Delta t}, \boldsymbol{v}_{j,h}\right) - (\hat{q}_{j,h}^{n+1}, \nabla \cdot \boldsymbol{v}_{j,h}) = 0, \qquad (2.2)$$

$$(\nabla \cdot \tilde{\boldsymbol{v}}_{j,h}^{n+1}, q_{j,h}) = 0. \qquad (2.3)$$

Step 3: Find $\hat{\boldsymbol{w}}_{j,h}^{n+1} \in \boldsymbol{X}_h$ satisfying, for all $\boldsymbol{l}_{j,h} \in \boldsymbol{X}_h$:

$$\begin{aligned}
&\left(\frac{\hat{\boldsymbol{w}}_{j,h}^{n+1} - \tilde{\boldsymbol{w}}_{j,h}^{n}}{\Delta t}, \boldsymbol{l}_{j,h}\right) + b\left(< \hat{\boldsymbol{v}}_h >^n, \hat{\boldsymbol{w}}_{j,h}^{n+1}, \boldsymbol{l}_{j,h}\right) + \frac{\bar{\nu} + \bar{\nu}_m}{2}\left(\nabla \hat{\boldsymbol{w}}_{j,h}^{n+1}, \nabla \boldsymbol{l}_{j,h}\right) \\
&+ \gamma\left(\nabla \cdot \hat{\boldsymbol{w}}_{j,h}^{n+1}, \nabla \cdot \boldsymbol{l}_{j,h}\right) + \left(2\nu_T(\hat{\boldsymbol{v}}_h^{'}, t^n)\nabla \hat{\boldsymbol{w}}_{j,h}^{n+1}, \nabla \boldsymbol{l}_{j,h}\right) = \left(\boldsymbol{f}_{2,j}(t^{n+1}), \boldsymbol{l}_{j,h}\right) \\
&- b\left(\hat{\boldsymbol{v}}_{j,h}^{'n}, \hat{\boldsymbol{w}}_{j,h}^{n}, \boldsymbol{l}_{j,h}\right) - \frac{\nu_j - \nu_{m,j}}{2}\left(\nabla \boldsymbol{v}_{j,h}^{n}, \nabla \boldsymbol{l}_{j,h}\right) - \frac{\nu_j^{'} + \nu_{m,j}^{'}}{2}\left(\nabla \boldsymbol{w}_{j,h}^{n}, \nabla \boldsymbol{l}_{j,h}\right). \qquad (2.4)
\end{aligned}$$

Step 4: Find $(\tilde{\boldsymbol{w}}_{j,h}^{n+1}, \hat{\lambda}_{j,h}^{n+1}) \in \boldsymbol{Y}_h \times Q_h$ satisfying for all $(\mathbf{s}_{j,h}, r_{j,h}) \in \boldsymbol{Y}_h \times Q_h$,

$$\left(\frac{\tilde{\boldsymbol{w}}_{j,h}^{n+1} - \hat{\boldsymbol{w}}_{j,h}^{n+1}}{\Delta t}, \mathbf{s}_{j,h}\right) - (\hat{\lambda}_{j,h}^{n+1}, \nabla \cdot \mathbf{s}_{j,h}) = 0, \qquad (2.5)$$

$$(\nabla \cdot \tilde{\boldsymbol{w}}_{j,h}^{n+1}, r_{j,h}) = 0, \qquad (2.6)$$

Since $\boldsymbol{X}_h \subset \boldsymbol{Y}_h$, we can choose $\boldsymbol{v}_{j,h} = \boldsymbol{\chi}_{j,h}$ in (2.2), $\mathbf{s}_{j,h} = \boldsymbol{l}_{j,h}$ in (2.5) and combine them with equations (2.1) and (2.4), respectively, to get

$$\left(\frac{\hat{\boldsymbol{v}}_{j,h}^{n+1}-\hat{\boldsymbol{v}}_{j,h}^{n}}{\Delta t},\boldsymbol{\chi}_{j,h}\right)+b\Big(<\hat{\boldsymbol{w}}_h>^n,\hat{\boldsymbol{v}}_{j,h}^{n+1},\boldsymbol{\chi}_{j,h}\Big)+\frac{\bar{\nu}+\bar{\nu}_m}{2}\Big(\nabla\hat{\boldsymbol{v}}_{j,h}^{n+1},\nabla\boldsymbol{\chi}_{j,h}\Big)$$
$$+\gamma\Big(\nabla\cdot\hat{\boldsymbol{v}}_{j,h}^{n+1},\nabla\cdot\boldsymbol{\chi}_{j,h}\Big)+\Big(2\nu_T(\hat{\boldsymbol{w}}_h^{'},t^n)\nabla\hat{\boldsymbol{v}}_{j,h}^{n+1},\nabla\boldsymbol{\chi}_{j,h}\Big)-\Big(\hat{q}_{j,h}^{n},\nabla\cdot\boldsymbol{\chi}_{j,h}\Big)=\Big(\boldsymbol{f}_{1,j}(t^{n+1}),\boldsymbol{\chi}_{j,h}\Big)$$
$$-b\Big(\hat{\boldsymbol{w}}_{j,h}^{'n},\hat{\boldsymbol{v}}_{j,h}^{n},\boldsymbol{\chi}_{j,h}\Big)-\frac{\nu_j-\nu_{m,j}}{2}\Big(\nabla\hat{\boldsymbol{w}}_{j,h}^{n},\nabla\boldsymbol{\chi}_{j,h}\Big)-\frac{\nu_j^{'}+\nu_{m,j}^{'}}{2}\Big(\nabla\hat{\boldsymbol{v}}_{j,h}^{n},\nabla\boldsymbol{\chi}_{j,h}\Big),\tag{2.7}$$

and

$$\left(\frac{\hat{\boldsymbol{w}}_{j,h}^{n+1}-\hat{\boldsymbol{w}}_{j,h}^{n}}{\Delta t},\boldsymbol{l}_{j,h}\right)+b\Big(<\hat{\boldsymbol{v}}_h>^n,\hat{\boldsymbol{w}}_{j,h}^{n+1},\boldsymbol{l}_{j,h}\Big)+\frac{\bar{\nu}+\bar{\nu}_m}{2}\Big(\nabla\hat{\boldsymbol{w}}_{j,h}^{n+1},\nabla\boldsymbol{l}_{j,h}\Big)$$
$$+\gamma\Big(\nabla\cdot\hat{\boldsymbol{w}}_{j,h}^{n+1},\nabla\cdot\boldsymbol{l}_{j,h}\Big)+\Big(2\nu_T(\hat{\boldsymbol{v}}_h^{'},t^n)\nabla\hat{\boldsymbol{w}}_{j,h}^{n+1},\nabla\boldsymbol{l}_{j,h}\Big)-\Big(\hat{\lambda}_{j,h}^{n+1},\nabla\cdot\boldsymbol{l}_{j,h}\Big)=\Big(\boldsymbol{f}_{2,j}(t^{n+1}),\boldsymbol{l}_{j,h}\Big)$$
$$-b\Big(\hat{\boldsymbol{v}}_{j,h}^{'n},\hat{\boldsymbol{w}}_{j,h}^{n},\boldsymbol{l}_{j,h}\Big)-\frac{\nu_j-\nu_{m,j}}{2}\Big(\nabla\boldsymbol{v}_{j,h}^{n},\nabla\boldsymbol{l}_{j,h}\Big)-\frac{\nu_j^{'}+\nu_{m,j}^{'}}{2}\Big(\nabla\boldsymbol{w}_{j,h}^{n},\nabla\boldsymbol{l}_{j,h}\Big).\tag{2.8}$$

2.1 Stability Analysis

We now prove stability and well-posedness for the Algorithm 2.

Theorem 2.1. *(Unconditional Stability) Let* $\big(\hat{\boldsymbol{v}}_{j,h}^{n+1},\hat{q}_{j,h}^{n+1},\hat{\boldsymbol{w}}_{j,h}^{n+1},\hat{\lambda}_{j,h}^{n+1}\big)$ *be the solution of Algorithm 2 and* $\boldsymbol{f}_{1,j},\boldsymbol{f}_{2,j}\in L^2\big(0,T;\boldsymbol{H}^{-1}(\Omega)\big)$*, and* $\boldsymbol{v}_{j,h}^0,\ \boldsymbol{w}_{j,h}^0\in\boldsymbol{H}^1(\Omega)$*. Then for all* $\Delta t>0$*, if* $\alpha_j>0$*, and* $\mu>1$*, we have the following stability bound:*

$$\|\hat{\boldsymbol{v}}_{j,h}^{M}\|^2+\|\hat{\boldsymbol{w}}_{j,h}^{M}\|^2+\frac{\bar{\nu}+\bar{\nu}_m}{2}\Delta t\Big(\|\nabla\hat{\boldsymbol{v}}_{j,h}^{M}\|^2+\|\nabla\hat{\boldsymbol{w}}_{j,h}^{M}\|^2\Big)+2\gamma\Delta t\sum_{n=0}^{M-1}\Big(\|\nabla\cdot\hat{\boldsymbol{v}}_{j,h}^{n+1}\|^2+\|\nabla\cdot\hat{\boldsymbol{w}}_{j,h}^{n+1}\|^2\Big)$$
$$+\frac{\alpha_j\Delta t}{2}\sum_{n=0}^{M-1}\Big(\|\nabla\hat{\boldsymbol{v}}_{j,h}^{n}\|^2+\|\nabla\hat{\boldsymbol{w}}_{j,h}^{n}\|^2\Big)\le\frac{2\Delta t}{\alpha_j}\sum_{n=0}^{M-1}\Big(\|\boldsymbol{f}_{1,j}(t^{n+1})\|^2+\|\boldsymbol{f}_{2,j}(t^{n+1})\|^2\Big)$$
$$+\|\hat{\boldsymbol{v}}_{j,h}^{0}\|^2+\|\hat{\boldsymbol{w}}_{j,h}^{0}\|^2+\frac{\bar{\nu}+\bar{\nu}_m}{2}\Delta t\Big(\|\nabla\hat{\boldsymbol{v}}_{j,h}^{0}\|^2+\|\nabla\hat{\boldsymbol{w}}_{j,h}^{0}\|^2\Big).\tag{2.9}$$

Proof: Taking $\boldsymbol{\chi}_{j,h}=\hat{\boldsymbol{v}}_{j,h}^{n+1}$ in (2.1) and $\boldsymbol{l}_{j,h}=\hat{\boldsymbol{w}}_{j,h}^{n+1}$ in (2.4), we obtain

$$\left(\frac{\hat{\boldsymbol{v}}_{j,h}^{n+1}-\tilde{\boldsymbol{v}}_{j,h}^{n}}{\Delta t},\hat{\boldsymbol{v}}_{j,h}^{n+1}\right)+\frac{\bar{\nu}+\bar{\nu}_m}{2}\|\nabla\hat{\boldsymbol{v}}_{j,h}^{n+1}\|^2+\gamma\|\nabla\cdot\hat{\boldsymbol{v}}_{j,h}^{n+1}\|^2$$
$$+\Big(2\nu_T(\hat{\boldsymbol{w}}_h^{'},t^n)\nabla\hat{\boldsymbol{v}}_{j,h}^{n+1},\nabla\hat{\boldsymbol{v}}_{j,h}^{n+1}\Big)=\Big(\boldsymbol{f}_{1,j}(t^{n+1}),\hat{\boldsymbol{v}}_{j,h}^{n+1}\Big)$$
$$-\Big(\hat{\boldsymbol{w}}_{j,h}^{'n}\cdot\nabla\hat{\boldsymbol{v}}_{j,h}^{n},\hat{\boldsymbol{v}}_{j,h}^{n+1}\Big)-\frac{\nu_j-\nu_{m,j}}{2}\Big(\nabla\hat{\boldsymbol{w}}_{j,h}^{n},\nabla\hat{\boldsymbol{v}}_{j,h}^{n+1}\Big)-\frac{\nu_j^{'}+\nu_{m,j}^{'}}{2}\Big(\nabla\hat{\boldsymbol{v}}_{j,h}^{n},\nabla\hat{\boldsymbol{v}}_{j,h}^{n+1}\Big),\tag{2.10}$$

and

$$\left(\frac{\hat{\boldsymbol{w}}_{j,h}^{n+1}-\tilde{\boldsymbol{w}}_{j,h}^{n}}{\Delta t},\boldsymbol{l}_{j,h}\right)+\frac{\bar{\nu}+\bar{\nu}_m}{2}\|\nabla\hat{\boldsymbol{w}}_{j,h}^{n+1}\|^2+\gamma\|\nabla\cdot\hat{\boldsymbol{w}}_{j,h}^{n+1}\|^2$$
$$+\Big(2\nu_T(\hat{\boldsymbol{v}}_h^{'},t^n)\nabla\hat{\boldsymbol{w}}_{j,h}^{n+1},\nabla\hat{\boldsymbol{w}}_{j,h}^{n+1}\Big)=\Big(\boldsymbol{f}_{2,j}(t^{n+1}),\hat{\boldsymbol{w}}_{j,h}^{n+1}\Big)$$
$$-\Big(\hat{\boldsymbol{v}}_{j,h}^{'n}\cdot\nabla\hat{\boldsymbol{w}}_{j,h}^{n},\hat{\boldsymbol{w}}_{j,h}^{n+1}\Big)-\frac{\nu_j-\nu_{m,j}}{2}\Big(\nabla\hat{\boldsymbol{v}}_{j,h}^{n},\nabla\hat{\boldsymbol{w}}_{j,h}^{n+1}\Big)-\frac{\nu_j^{'}+\nu_{m,j}^{'}}{2}\Big(\nabla\hat{\boldsymbol{w}}_{j,h}^{n},\nabla\hat{\boldsymbol{w}}_{j,h}^{n+1}\Big). \tag{2.11}$$

Using polarization identity and $(2\nu_T(\hat{\boldsymbol{w}}_h^{'},t^n)\nabla\hat{\boldsymbol{v}}_{j,h}^{n+1},\nabla\hat{\boldsymbol{v}}_{j,h}^{n+1})=2\mu\Delta t\|l_{\hat{\boldsymbol{w}},h}^{n}\nabla\boldsymbol{v}_{j,h}^{n+1}\|^2$, we get

$$\frac{1}{2\Delta t}\Big(\|\hat{\boldsymbol{v}}_{j,h}^{n+1}\|^2-\|\tilde{\boldsymbol{v}}_{j,h}^{n}\|^2+\|\hat{\boldsymbol{v}}_{j,h}^{n+1}-\tilde{\boldsymbol{v}}_{j,h}^{n}\|^2\Big)+\frac{\bar{\nu}+\bar{\nu}_m}{2}\|\nabla\hat{\boldsymbol{v}}_{j,h}^{n+1}\|^2+\gamma\|\nabla\cdot\hat{\boldsymbol{v}}_{j,h}^{n+1}\|^2$$
$$+2\mu\Delta t\|l_{\hat{\boldsymbol{w}},h}^{n}\nabla\hat{\boldsymbol{v}}_{j,h}^{n+1}\|^2=\Big(\boldsymbol{f}_{1,j}(t^{n+1}),\hat{\boldsymbol{v}}_{j,h}^{n+1}\Big)-b\Big(\hat{\boldsymbol{w}}_{j,h}^{'n},\hat{\boldsymbol{v}}_{j,h}^{n},\hat{\boldsymbol{v}}_{j,h}^{n+1}\Big)$$
$$-\frac{\nu_j-\nu_{m,j}}{2}\Big(\nabla\hat{\boldsymbol{w}}_{j,h}^{n},\nabla\hat{\boldsymbol{v}}_{j,h}^{n+1}\Big)-\frac{\nu_j^{'}+\nu_{m,j}^{'}}{2}\Big(\nabla\hat{\boldsymbol{v}}_{j,h}^{n},\nabla\hat{\boldsymbol{v}}_{j,h}^{n+1}\Big), \tag{2.12}$$

and

$$\frac{1}{2\Delta t}\Big(\|\hat{\boldsymbol{w}}_{j,h}^{n+1}\|^2-\|\tilde{\boldsymbol{w}}_{j,h}^{n}\|^2+\|\hat{\boldsymbol{w}}_{j,h}^{n+1}-\tilde{\boldsymbol{w}}_{j,h}^{n}\|^2\Big)+\frac{\bar{\nu}+\bar{\nu}_m}{2}\|\nabla\hat{\boldsymbol{w}}_{j,h}^{n+1}\|^2+\gamma\|\nabla\cdot\hat{\boldsymbol{w}}_{j,h}^{n+1}\|^2$$
$$+2\mu\Delta t\|l_{\hat{\boldsymbol{v}},h}^{n}\nabla\hat{\boldsymbol{w}}_{j,h}^{n+1}\|^2=\Big(\boldsymbol{f}_{2,j}(t^{n+1}),\hat{\boldsymbol{w}}_{j,h}^{n+1}\Big)-b\Big(\hat{\boldsymbol{v}}_{j,h}^{'n},\hat{\boldsymbol{w}}_{j,h}^{n},\hat{\boldsymbol{w}}_{j,h}^{n+1}\Big)$$
$$-\frac{\nu_j-\nu_{m,j}}{2}\Big(\nabla\hat{\boldsymbol{v}}_{j,h}^{n},\nabla\hat{\boldsymbol{w}}_{j,h}^{n+1}\Big)-\frac{\nu_j^{'}+\nu_{m,j}^{'}}{2}\Big(\nabla\hat{\boldsymbol{w}}_{j,h}^{n},\nabla\hat{\boldsymbol{w}}_{j,h}^{n+1}\Big). \tag{2.13}$$

Adding (2.12) and (2.13), using the inequality $\|\boldsymbol{a}\cdot\nabla\boldsymbol{b}\|\le\sqrt{2}\||\boldsymbol{a}|\nabla\boldsymbol{b}\|$ in

$$\begin{aligned}\Big(\hat{\boldsymbol{w}}_{j,h}^{'n}\cdot\nabla\hat{\boldsymbol{v}}_{j,h}^{n},\hat{\boldsymbol{v}}_{j,h}^{n+1}\Big)&=-\Big(\hat{\boldsymbol{w}}_{j,h}^{'n}\cdot\nabla\hat{\boldsymbol{v}}_{j,h}^{n+1},\hat{\boldsymbol{v}}_{j,h}^{n}\Big)\\&=\Big(\hat{\boldsymbol{w}}_{j,h}^{'n}\cdot\nabla\hat{\boldsymbol{v}}_{j,h}^{n+1},\hat{\boldsymbol{v}}_{j,h}^{n+1}-\hat{\boldsymbol{v}}_{j,h}^{n}\Big)\\&\le\|\hat{\boldsymbol{w}}_{j,h}^{'n}\cdot\nabla\hat{\boldsymbol{v}}_{j,h}^{n+1}\|\,\|\hat{\boldsymbol{v}}_{j,h}^{n+1}-\hat{\boldsymbol{v}}_{j,h}^{n}\|\\&\le\sqrt{2}\||\hat{\boldsymbol{w}}_{j,h}^{'n}|\nabla\hat{\boldsymbol{v}}_{j,h}^{n+1}\|\,\|\hat{\boldsymbol{v}}_{j,h}^{n+1}-\hat{\boldsymbol{v}}_{j,h}^{n}\|\\&\le\sqrt{2}\|l_{\hat{\boldsymbol{w}},h}^{n}\nabla\hat{\boldsymbol{v}}_{j,h}^{n+1}\|\,\|\hat{\boldsymbol{v}}_{j,h}^{n+1}-\hat{\boldsymbol{v}}_{j,h}^{n}\|,\end{aligned}$$

and after applying the Cauchy-Schwarz inequality, this reduces to

$$\begin{aligned}
\frac{1}{2\Delta t}\Big(\|\hat{\boldsymbol{v}}_{j,h}^{n+1}\|^2 - \|\tilde{\boldsymbol{v}}_{j,h}^{n}\|^2 + \|\hat{\boldsymbol{v}}_{j,h}^{n+1} - \tilde{\boldsymbol{v}}_{j,h}^{n}\|^2 + \|\hat{\boldsymbol{w}}_{j,h}^{n+1}\|^2 - \|\tilde{\boldsymbol{w}}_{j,h}^{n}\|^2 + \|\hat{\boldsymbol{w}}_{j,h}^{n+1} - \tilde{\boldsymbol{w}}_{j,h}^{n}\|^2\Big) \\
+\frac{\bar{\nu}+\bar{\nu}_m}{2}\Big(\|\nabla\hat{\boldsymbol{v}}_{j,h}^{n+1}\|^2 + \|\nabla\hat{\boldsymbol{w}}_{j,h}^{n+1}\|^2\Big) + \gamma\Big(\|\nabla\cdot\hat{\boldsymbol{v}}_{j,h}^{n+1}\|^2 + \|\nabla\cdot\hat{\boldsymbol{w}}_{j,h}^{n+1}\|^2\Big) \\
+2\mu\Delta t\Big(\|l_{\hat{\boldsymbol{w}},h}^{n}\nabla\hat{\boldsymbol{v}}_{j,h}^{n+1}\|^2 + \|l_{\hat{\boldsymbol{v}},h}^{n}\nabla\hat{\boldsymbol{w}}_{j,h}^{n+1}\|^2\Big) \\
\leq \sqrt{2}\|l_{\hat{\boldsymbol{w}},h}^{n}\nabla\boldsymbol{v}_{j,h}^{n+1}\|\,\|\boldsymbol{v}_{j,h}^{n+1} - \boldsymbol{v}_{j,h}^{n}\| + \sqrt{2}\|l_{v,h}^{n}\nabla\boldsymbol{w}_{j,h}^{n+1}\|\,\|\boldsymbol{w}_{j,h}^{n+1} - \boldsymbol{w}_{j,h}^{n}\| \\
+\|\boldsymbol{f}_{1,j}(t^{n+1})\|\|\hat{\boldsymbol{v}}_{j,h}^{n+1}\| + \|\boldsymbol{f}_{2,j}(t^{n+1})\|\|\hat{\boldsymbol{w}}_{j,h}^{n+1}\| \\
+\frac{|\nu_j - \nu_{m,j}|}{2}\Big(\|\nabla\hat{\boldsymbol{w}}_{j,h}^{n}\|\|\nabla\hat{\boldsymbol{v}}_{j,h}^{n+1}\| + \|\nabla\hat{\boldsymbol{v}}_{j,h}^{n}\|\|\nabla\hat{\boldsymbol{w}}_{j,h}^{n+1}\|\Big) \\
+\frac{|\nu_j^{'} + \nu_{m,j}^{'}|}{2}\Big(\|\nabla\hat{\boldsymbol{v}}_{j,h}^{n}\|\|\nabla\hat{\boldsymbol{v}}_{j,h}^{n+1}\| + \|\nabla\hat{\boldsymbol{w}}_{j,h}^{n}\|\|\nabla\hat{\boldsymbol{w}}_{j,h}^{n+1}\|\Big). \qquad (2.14)
\end{aligned}$$

Using Young's inequality and reducing, we have

$$\begin{aligned}
\frac{1}{2\Delta t}\Big(\|\hat{\boldsymbol{v}}_{j,h}^{n+1}\|^2 - \|\tilde{\boldsymbol{v}}_{j,h}^{n}\|^2 + \|\hat{\boldsymbol{w}}_{j,h}^{n+1}\|^2 - \|\tilde{\boldsymbol{w}}_{j,h}^{n}\|^2\Big) \\
+\frac{1}{4\Delta t}\Big(\|\hat{\boldsymbol{v}}_{j,h}^{n+1} - \tilde{\boldsymbol{v}}_{j,h}^{n}\|^2 + \|\hat{\boldsymbol{w}}_{j,h}^{n+1} - \tilde{\boldsymbol{w}}_{j,h}^{n}\|^2\Big) \\
+\frac{\bar{\nu}+\bar{\nu}_m}{4}\Big(\|\nabla\hat{\boldsymbol{v}}_{j,h}^{n+1}\|^2 + \|\nabla\hat{\boldsymbol{w}}_{j,h}^{n+1}\|^2\Big) + \gamma\Big(\|\nabla\cdot\hat{\boldsymbol{v}}_{j,h}^{n+1}\|^2 + \|\nabla\cdot\hat{\boldsymbol{w}}_{j,h}^{n+1}\|^2\Big) \\
+2(\mu-1)\Delta t\Big(\|l_{\hat{\boldsymbol{w}},h}^{n}\nabla\hat{\boldsymbol{v}}_{j,h}^{n+1}\|^2 + \|l_{\hat{\boldsymbol{v}},h}^{n}\nabla\hat{\boldsymbol{w}}_{j,h}^{n+1}\|^2\Big) \\
\leq \frac{1}{\alpha_j}\Big(\|\boldsymbol{f}_{1,j}(t^{n+1})\|^2 + \|\boldsymbol{f}_{2,j}(t^{n+1})\|^2\Big) \\
+\frac{|\nu_j - \nu_{m,j}| + |\nu_j^{'} + \nu_{m,j}^{'}|}{4}\Big(\|\nabla\hat{\boldsymbol{v}}_{j,h}^{n}\|^2 + \|\nabla\hat{\boldsymbol{w}}_{j,h}^{n}\|^2\|\Big). \qquad (2.15)
\end{aligned}$$

Assuming $\mu > 1$, and dropping non-negative terms from the left-hand-side, this reduces to

$$\begin{aligned}
\frac{1}{2\Delta t}\Big(\|\hat{\boldsymbol{v}}_{j,h}^{n+1}\|^2 - \|\tilde{\boldsymbol{v}}_{j,h}^{n}\|^2 + \|\hat{\boldsymbol{w}}_{j,h}^{n+1}\|^2 - \|\tilde{\boldsymbol{w}}_{j,h}^{n}\|^2\Big) + \frac{\bar{\nu}+\bar{\nu}_m}{4}\Big(\|\nabla\hat{\boldsymbol{v}}_{j,h}^{n+1}\|^2 + \|\nabla\hat{\boldsymbol{w}}_{j,h}^{n+1}\|^2\Big) \\
+\gamma\Big(\|\nabla\cdot\hat{\boldsymbol{v}}_{j,h}^{n+1}\|^2 + \|\nabla\cdot\hat{\boldsymbol{w}}_{j,h}^{n+1}\|^2\Big) \leq \frac{1}{\alpha_j}\Big(\|\boldsymbol{f}_{1,j}(t^{n+1})\|^2 + \|\boldsymbol{f}_{2,j}(t^{n+1})\|^2\Big) \\
+\frac{|\nu_j - \nu_{m,j}| + |\nu_j^{'} + \nu_{m,j}^{'}|}{4}\Big(\|\nabla\hat{\boldsymbol{v}}_{j,h}^{n}\|^2 + \|\nabla\hat{\boldsymbol{w}}_{j,h}^{n}\|^2\|\Big). \qquad (2.16)
\end{aligned}$$

Now choose $\boldsymbol{v}_{j,h} = \tilde{\boldsymbol{v}}_{j,h}^{n+1}$ in (2.2), $q_{j,h} = \hat{q}_{j,h}^{n+1}$ in (2.3) and $\mathbf{s}_{j,h} = \tilde{\boldsymbol{w}}_{j,h}^{n+1}$ in (2.5), $r_{j,h} = \hat{\lambda}_{j,h}^{n+1}$ in (2.6). Then apply Cauchy-Schwarz and Young's inequalities to obtain

$$\begin{aligned}
\|\tilde{\boldsymbol{v}}_{j,h}^{n+1}\|^2 \leq \|\hat{\boldsymbol{v}}_{j,h}^{n+1}\|^2, \\
\|\tilde{\boldsymbol{w}}_{j,h}^{n+1}\|^2 \leq \|\hat{\boldsymbol{w}}_{j,h}^{n+1}\|^2
\end{aligned}$$

for all $n = 0, 1, 2, \cdots, M-1$. Plugging these estimates into (2.16), the result is reduced to

$$\begin{aligned}
&\frac{1}{2\Delta t}\Big(\|\hat{\boldsymbol{v}}_{j,h}^{n+1}\|^2 - \|\hat{\boldsymbol{v}}_{j,h}^{n}\|^2 + \|\hat{\boldsymbol{w}}_{j,h}^{n+1}\|^2 - \|\hat{\boldsymbol{w}}_{j,h}^{n}\|^2\Big) \\
&+\frac{\bar{\nu}+\bar{\nu}_m}{4}\Big(\|\nabla\hat{\boldsymbol{v}}_{j,h}^{n+1}\|^2 - \|\nabla\hat{\boldsymbol{v}}_{j,h}^{n}\|^2 + \|\nabla\hat{\boldsymbol{w}}_{j,h}^{n+1}\|^2 - \|\nabla\hat{\boldsymbol{w}}_{j,h}^{n}\|^2\Big) \\
&+\gamma\Big(\|\nabla\cdot\hat{\boldsymbol{v}}_{j,h}^{n+1}\|^2 + \|\nabla\cdot\hat{\boldsymbol{w}}_{j,h}^{n+1}\|^2\Big) + \frac{\alpha_j}{4}\Big(\|\nabla\hat{\boldsymbol{v}}_{j,h}^{n}\|^2 + \|\nabla\hat{\boldsymbol{w}}_{j,h}^{n}\|^2\|\Big) \\
&\leq \frac{1}{\alpha_j}\Big(\|\boldsymbol{f}_{1,j}(t^{n+1})\|^2 + \|\boldsymbol{f}_{2,j}(t^{n+1})\|^2\Big). \qquad (2.17)
\end{aligned}$$

Multiplying both sides by $2\Delta t$ and summing over the time steps, we have

$$\begin{aligned}
&\|\hat{\boldsymbol{v}}_{j,h}^{M}\|^2 + \|\hat{\boldsymbol{w}}_{j,h}^{M}\|^2 + \frac{\bar{\nu}+\bar{\nu}_m}{2}\Delta t\Big(\|\nabla\hat{\boldsymbol{v}}_{j,h}^{M}\|^2 + \|\nabla\hat{\boldsymbol{w}}_{j,h}^{M}\|^2\Big) + 2\gamma\Delta t\sum_{n=0}^{M-1}\Big(\|\nabla\cdot\hat{\boldsymbol{v}}_{j,h}^{n+1}\|^2 + \|\nabla\cdot\hat{\boldsymbol{w}}_{j,h}^{n+1}\|^2\Big) \\
&+\frac{\alpha_j\Delta t}{2}\sum_{n=0}^{M-1}\Big(\|\nabla\hat{\boldsymbol{v}}_{j,h}^{n}\|^2 + \|\nabla\hat{\boldsymbol{w}}_{j,h}^{n}\|^2\|\Big) \leq \frac{2\Delta t}{\alpha_j}\sum_{n=0}^{M-1}\Big(\|\boldsymbol{f}_{1,j}(t^{n+1})\|^2 + \|\boldsymbol{f}_{2,j}(t^{n+1})\|^2\Big) \\
&+\|\hat{\boldsymbol{v}}_{j,h}^{0}\|^2 + \|\hat{\boldsymbol{w}}_{j,h}^{0}\|^2 + \frac{\bar{\nu}+\bar{\nu}_m}{2}\Delta t\Big(\|\nabla\hat{\boldsymbol{v}}_{j,h}^{0}\|^2 + \|\nabla\hat{\boldsymbol{w}}_{j,h}^{0}\|^2\Big). \qquad (2.18)
\end{aligned}$$

This completes the proof.

□

2.2 Convergence

We now prove that the Algorithm 2 converges to Algorithm 1 as $\gamma \to \infty$. Thus, we need to define the space $\boldsymbol{R}_h := \boldsymbol{V}_h^{\perp} \subset \boldsymbol{X}_h$ to be the orthogonal complement of $\boldsymbol{V}_h$ with respect to the $\boldsymbol{H}^1(\Omega)$ norm.

Lemma 2.2. *Let the finite element pair $(\boldsymbol{X}_h, Q_h) \subset (\boldsymbol{X}, Q)$ satisfy the inf-sup condition* (1.15) *and the divergence-free property, i.e., $\nabla\cdot\boldsymbol{X}_h \subset Q_h$. Then there exists a constant C_R independent of h such that*

$$\|\nabla\boldsymbol{v}_h\| \leq C_R\|\nabla\cdot\boldsymbol{v}_h\|, \quad \forall\boldsymbol{v}_h \in \boldsymbol{R}_h.$$

Assumption 2.1. *We assume there exists a constant C_* which is independent of h, and Δt, such that for sufficiently small h for a fixed mesh and fixed Δt as $\gamma \to \infty$, the solution of the Algorithm 2 satisfies*

$$\max_{1\leq n\leq M}\Big\{\|\hat{\boldsymbol{v}}_{j,h}^{n}\|_\infty, \|\hat{\boldsymbol{w}}_{j,h}^{n}\|_\infty\Big\} \leq C_*, \ \ \textit{for all } \ j = 1, 2, \cdots, J. \qquad (2.19)$$

The Assumption 2.1 is proved later in Lemma 2.4. We define $\alpha_{min} := \min_{1\leq j\leq J}\alpha_j$.

THEOREM 2.3 (Convergence). *Let* $(\boldsymbol{v}_{j,h}^{n+1}, \boldsymbol{w}_{j,h}^{n+1}, q_{j,h}^{n+1})$, *and* $(\hat{\boldsymbol{v}}_{j,h}^{n+1}, \hat{\boldsymbol{w}}_{j,h}^{n+1}, \hat{q}_{j,h}^{n+1})$ *are the solutions to the Algorithm 1, and Algorithm 2, respectively, for* $n = 0, 1, \cdots, M-1$. *We then have*

$$\begin{aligned}
&\Delta t \sum_{n=1}^{M} \Big(\|\nabla <\boldsymbol{v}_h>^n - \nabla <\hat{\boldsymbol{v}}_h>^n \|^2 + \|\nabla <\boldsymbol{w}_h>^n - \nabla <\hat{\boldsymbol{w}}_h>^n \|^2 \Big) \\
&\leq \frac{CC_R^2}{\gamma^2} \left(\frac{1}{\alpha_{min}^3 \Delta t} + \frac{1}{\alpha_{min} \Delta t} + \frac{\Delta t}{\alpha_{min}} + 1 \right) exp\left(\frac{CC_*^2}{\alpha_{min}} + \frac{C\Delta t}{h^3 \alpha_{min}} \right) \\
&\qquad \times \left(\Delta t \sum_{n=0}^{M-1} \sum_{j=1}^{J} \Big(\|q_{j,h}^{n+1} - \hat{q}_{j,h}^{n}\|^2 + \|\lambda_{j,h}^{n+1} - \hat{\lambda}_{j,h}^{n}\|^2 \Big) \right). \qquad (2.20)
\end{aligned}$$

Remark 2.1. *The above theorem states the first order convergence of the penalty-projection algorithm to the Algorithm 1 as* $\gamma \to \infty$ *for a fixed mesh and time-step size.*

Proof: Denote $\boldsymbol{e}_j^{n+1} := \boldsymbol{v}_{j,h}^{n+1} - \hat{\boldsymbol{v}}_{j,h}^{n+1}$, and $\boldsymbol{\epsilon}_j^{n+1} := \boldsymbol{w}_{j,h}^{n+1} - \hat{\boldsymbol{w}}_{j,h}^{n+1}$ and use the following H^1-orthogonal decomposition of the errors:

$$\boldsymbol{e}_j^{n+1} := \boldsymbol{e}_{j,0}^{n+1} + \boldsymbol{e}_{j,\boldsymbol{R}}^{n+1}, \text{ and } \boldsymbol{\epsilon}_j^{n+1} := \boldsymbol{\epsilon}_{j,0}^{n+1} + \boldsymbol{\epsilon}_{j,\boldsymbol{R}}^{n+1},$$

with $\boldsymbol{e}_{j,0}^{n+1}, \boldsymbol{\epsilon}_{j,0}^{n+1} \in \boldsymbol{V}_h$, and $\boldsymbol{e}_{j,\boldsymbol{R}}^{n+1}, \boldsymbol{\epsilon}_{j,\boldsymbol{R}}^{n+1} \in \boldsymbol{R}_h$, for $n = 0, 1, \cdots, M-1$.

Step 1: Estimate of $\boldsymbol{e}_{j,\boldsymbol{R}}^{n+1}$, and $\boldsymbol{\epsilon}_{j,\boldsymbol{R}}^{n+1}$: Subtracting the equation (1.21) from (2.7) and (1.22) from (2.8) produces

$$\begin{aligned}
&\frac{1}{\Delta t}\Big(\boldsymbol{e}_j^{n+1} - \boldsymbol{e}_j^{n}, \boldsymbol{\chi}_{j,h}\Big) + \frac{\bar{\nu} + \bar{\nu}_m}{2} \left(\nabla \boldsymbol{e}_j^{n+1}, \nabla \boldsymbol{\chi}_{j,h}\right) + \gamma\Big(\nabla \cdot \boldsymbol{e}_{j,\boldsymbol{R}}^{n+1}, \nabla \cdot \boldsymbol{\chi}_{j,h}\Big) + b\Big(<\hat{\boldsymbol{w}}_h>^n, \boldsymbol{e}_j^{n+1}, \boldsymbol{\chi}_{j,h}\Big) \\
&\quad + b\Big(<\boldsymbol{\epsilon}>^n, \boldsymbol{v}_{j,h}^{n+1}, \boldsymbol{\chi}_{j,h}\Big) - \Big(q_{j,h}^{n+1} - \hat{q}_{j,h}^{n}, \nabla \cdot \boldsymbol{\chi}_{j,h}\Big) + 2\mu\Delta t\Big((l_{\hat{\boldsymbol{w}},h}^{n})^2 \nabla \boldsymbol{e}_j^{n+1}, \nabla \boldsymbol{\chi}_{j,h}\Big) \\
&\quad + 2\mu\Delta t\Big(\big\{(l_{\boldsymbol{w},h}^{n})^2 - (l_{\hat{\boldsymbol{w}},h}^{n})^2\big\} \nabla \boldsymbol{v}_{j,h}^{n+1}, \nabla \boldsymbol{\chi}_{j,h}\Big) = -b\Big(\hat{\boldsymbol{w}}_{j,h}^{'n}, \boldsymbol{e}_j^{n}, \boldsymbol{\chi}_{j,h}\Big) - b\Big(\boldsymbol{\epsilon}_j^{'n}, \boldsymbol{v}_{j,h}^{n}, \boldsymbol{\chi}_{j,h}\Big) \\
&\quad - \frac{\nu_j - \nu_{m,j}}{2}\Big(\nabla \boldsymbol{\epsilon}_j^{n}, \nabla \boldsymbol{\chi}_{j,h}\Big) - \frac{\nu_j^{'} + \nu_{m,j}^{'}}{2}\Big(\nabla \boldsymbol{e}_j^{n}, \nabla \boldsymbol{\chi}_{j,h}\Big), \qquad (2.21)
\end{aligned}$$

and

$$\begin{aligned}
&\frac{1}{\Delta t}\Big(\boldsymbol{\epsilon}_j^{n+1} - \boldsymbol{\epsilon}_j^{n}, \boldsymbol{l}_{j,h}\Big) + \frac{\bar{\nu} + \bar{\nu}_m}{2} \left(\nabla \boldsymbol{\epsilon}_j^{n+1}, \nabla \boldsymbol{l}_{j,h}\right) + \gamma\Big(\nabla \cdot \boldsymbol{\epsilon}_{j,\boldsymbol{R}}^{n+1}, \nabla \cdot \boldsymbol{l}_{j,h}\Big) + b\Big(<\hat{\boldsymbol{v}}_h>^n, \boldsymbol{\epsilon}_j^{n+1}, \boldsymbol{l}_{j,h}\Big) \\
&\quad + b\Big(<\boldsymbol{e}>^n, \boldsymbol{w}_{j,h}^{n+1}, \boldsymbol{l}_{j,h}\Big) - \Big(\lambda_{j,h}^{n+1} - \hat{\lambda}_{j,h}^{n}, \nabla \cdot \boldsymbol{l}_{j,h}\Big) + 2\mu\Delta t\Big((l_{\hat{\boldsymbol{v}},h}^{n})^2 \nabla \boldsymbol{\epsilon}_j^{n+1}, \nabla \boldsymbol{l}_{j,h}\Big) \\
&\quad + 2\mu\Delta t\Big(\big\{(l_{\boldsymbol{v},h}^{n})^2 - (l_{\hat{\boldsymbol{v}},h}^{n})^2\big\} \nabla \boldsymbol{w}_{j,h}^{n+1}, \nabla \boldsymbol{l}_{j,h}\Big) = -b\Big(\hat{\boldsymbol{v}}_{j,h}^{'n}, \boldsymbol{\epsilon}_j^{n}, \boldsymbol{l}_{j,h}\Big) - b\Big(\boldsymbol{e}_j^{'n}, \boldsymbol{w}_{j,h}^{n}, \boldsymbol{l}_{j,h}\Big) \\
&\quad - \frac{\nu_j - \nu_{m,j}}{2}\Big(\nabla \boldsymbol{e}_j^{n}, \nabla \boldsymbol{l}_{j,h}\Big) - \frac{\nu_j^{'} + \nu_{m,j}^{'}}{2}\Big(\nabla \boldsymbol{\epsilon}_j^{n}, \nabla \boldsymbol{l}_{j,h}\Big). \qquad (2.22)
\end{aligned}$$

Take $\boldsymbol{\chi}_{j,h} = \boldsymbol{e}_j^{n+1}$ in (2.21), and $\boldsymbol{l}_{j,h} = \boldsymbol{\epsilon}_j^{n+1}$ in (2.22), which yield

$$b\Big(<\hat{\boldsymbol{v}}_h>^n, \boldsymbol{\epsilon}_j^{n+1}, \boldsymbol{l}_{j,h}\Big) = 0, \text{ and } b\Big(<\hat{\boldsymbol{w}}_h>^n, \boldsymbol{e}_j^{n+1}, \boldsymbol{\chi}_{j,h}\Big) = 0,$$

and use polarization identity to get

$$\begin{aligned}
&\frac{1}{2\Delta t}\Big(\|\boldsymbol{e}_j^{n+1}\|^2 - \|\boldsymbol{e}_j^n\|^2 + \|\boldsymbol{e}_j^{n+1} - \boldsymbol{e}_j^n\|^2\Big) + \frac{\bar{\nu} + \bar{\nu}_m}{2}\|\nabla \boldsymbol{e}_j^{n+1}\|^2 + \gamma\|\nabla \cdot \boldsymbol{e}_{j,\boldsymbol{R}}^{n+1}\|^2 \\
&+b\Big(<\boldsymbol{\epsilon}>^n, \boldsymbol{v}_{j,h}^{n+1}, \boldsymbol{e}_j^{n+1}\Big) - \Big(q_{j,h}^{n+1} - \hat{q}_{j,h}^n, \nabla \cdot \boldsymbol{e}_{j,\boldsymbol{R}}^{n+1}\Big) + 2\mu\Delta t\|l_{\hat{\boldsymbol{w}},h}^n \nabla \boldsymbol{e}_j^{n+1}\|^2 \\
&+2\mu\Delta t\Big(\big\{(l_{\boldsymbol{w},h}^n)^2 - (l_{\hat{\boldsymbol{w}},h}^n)^2\big\}\nabla \boldsymbol{v}_{j,h}^{n+1}, \nabla \boldsymbol{e}_j^{n+1}\Big) = -b\Big(\hat{\boldsymbol{w}}_{j,h}^{'n}, \boldsymbol{e}_j^n, \boldsymbol{e}_j^{n+1}\Big) \\
&-b\Big(\boldsymbol{\epsilon}_j^{'n}, \boldsymbol{v}_{j,h}^n, \boldsymbol{e}_j^{n+1}\Big) - \frac{\nu_j - \nu_{m,j}}{2}\Big(\nabla \boldsymbol{\epsilon}_j^n, \nabla \boldsymbol{e}_j^{n+1}\Big) - \frac{\nu_j^{'} + \nu_{m,j}^{'}}{2}\Big(\nabla \boldsymbol{e}_j^n, \nabla \boldsymbol{e}_j^{n+1}\Big),
\end{aligned} \tag{2.23}$$

and

$$\begin{aligned}
&\frac{1}{2\Delta t}\Big(\|\boldsymbol{\epsilon}_j^{n+1}\|^2 - \|\boldsymbol{\epsilon}_j^n\|^2 + \|\boldsymbol{\epsilon}_j^{n+1} - \boldsymbol{\epsilon}_j^n\|^2\Big) + \frac{\bar{\nu} + \bar{\nu}_m}{2}\|\nabla \boldsymbol{\epsilon}_j^{n+1}\|^2 + \gamma\|\nabla \cdot \boldsymbol{\epsilon}_{j,\boldsymbol{R}}^{n+1}\|^2 \\
&+b\Big(<\boldsymbol{e}>^n, \boldsymbol{w}_{j,h}^{n+1}, \boldsymbol{\epsilon}_j^{n+1}\Big) - \Big(\lambda_{j,h}^{n+1} - \hat{\lambda}_{j,h}^n, \nabla \cdot \boldsymbol{\epsilon}_{j,\boldsymbol{R}}^{n+1}\Big) + 2\mu\Delta t\|l_{\hat{\boldsymbol{v}},h}^n \nabla \boldsymbol{\epsilon}_j^{n+1}\|^2 \\
&+2\mu\Delta t\Big(\big\{(l_{\boldsymbol{v},h}^n)^2 - (l_{\hat{\boldsymbol{v}},h}^n)^2\big\}\nabla \boldsymbol{w}_{j,h}^{n+1}, \nabla \boldsymbol{\epsilon}_j^{n+1}\Big) = -b\Big(\hat{\boldsymbol{v}}_{j,h}^{'n}, \boldsymbol{\epsilon}_j^n, \boldsymbol{\epsilon}_j^{n+1}\Big) \\
&-b\Big(\boldsymbol{e}_j^{'n}, \boldsymbol{w}_{j,h}^n, \boldsymbol{\epsilon}_j^{n+1}\Big) - \frac{\nu_j - \nu_{m,j}}{2}\Big(\nabla \boldsymbol{e}_j^n, \nabla \boldsymbol{\epsilon}_j^{n+1}\Big) - \frac{\nu_j^{'} + \nu_{m,j}^{'}}{2}\Big(\nabla \boldsymbol{\epsilon}_j^n, \nabla \boldsymbol{\epsilon}_j^{n+1}\Big).
\end{aligned} \tag{2.24}$$

Now, we find the bound of the terms in (2.23) first. Rearranging and applying Cauchy-Schwarz and Young's inequalities in the following nonlinear term yields

$$\begin{aligned}
-b\Big(\hat{\boldsymbol{w}}_{j,h}^{'n}, \boldsymbol{e}_j^n, \boldsymbol{e}_j^{n+1}\Big) &= -b\Big(\hat{\boldsymbol{w}}_{j,h}^{'n}, \boldsymbol{e}_j^{n+1}, \boldsymbol{e}_j^{n+1} - \boldsymbol{e}_j^n\Big) \\
&\leq \|\hat{\boldsymbol{w}}_{j,h}^{'n} \cdot \nabla \boldsymbol{e}_j^{n+1}\|\|\boldsymbol{e}_j^{n+1} - \boldsymbol{e}_j^n\| \\
&\leq \sqrt{2}\|l_{\hat{\boldsymbol{w}},h}^n \nabla \boldsymbol{e}_j^{n+1}\|\|\boldsymbol{e}_j^{n+1} - \boldsymbol{e}_j^n\| \\
&\leq 2\Delta t\|l_{\hat{\boldsymbol{w}},h}^n \nabla \boldsymbol{e}_j^{n+1}\|^2 + \frac{1}{4\Delta t}\|\boldsymbol{e}_j^{n+1} - \boldsymbol{e}_j^n\|^2.
\end{aligned}$$

Applying Cauchy-Schwarz and Young's inequalities, we have

$$\begin{aligned}
\frac{|\nu_j - \nu_{m,j}|}{2}\Big|\Big(\nabla \boldsymbol{\epsilon}_j^n, \nabla \boldsymbol{e}_j^{n+1}\Big)\Big| &\leq \frac{|\nu_j - \nu_{m,j}|}{4}\Big(\|\nabla \boldsymbol{\epsilon}_j^n\|^2 + \|\nabla \boldsymbol{e}_j^{n+1}\|^2\Big), \\
\frac{|\nu_j^{'} + \nu_{m,j}^{'}|}{2}\Big|\Big(\nabla \boldsymbol{e}_j^n, \nabla \boldsymbol{e}_j^{n+1}\Big)\Big| &\leq \frac{|\nu_j^{'} + \nu_{m,j}^{'}|}{4}\Big(\|\nabla \boldsymbol{e}_j^n\|^2 + \|\nabla \boldsymbol{e}_j^{n+1}\|^2\Big), \\
\Big|\Big(q_{j,h}^{n+1} - \hat{q}_{j,h}^n, \nabla \cdot \boldsymbol{e}_{j,\boldsymbol{R}}^{n+1}\Big)\Big| &\leq \frac{1}{2\gamma}\|q_{j,h}^{n+1} - \hat{q}_{j,h}^n\|^2 + \frac{\gamma}{2}\|\nabla \cdot \boldsymbol{e}_{j,\boldsymbol{R}}^{n+1}\|^2.
\end{aligned}$$

Using Hölder's inequality, estimate in Lemma 1.1, Sobolev embedding theorem, Poincaré, and Young's inequalities provides

$$\begin{aligned}
\Big|b\Big(<\boldsymbol{\epsilon}>^n, \boldsymbol{v}_{j,h}^{n+1}, \boldsymbol{e}_j^{n+1}\Big)\Big| &\leq \|<\boldsymbol{\epsilon}>^n\|\|\nabla \boldsymbol{v}_{j,h}^{n+1}\|_{L^3}\|\boldsymbol{e}_j^{n+1}\|_{L^6} \\
&\leq CC_*\|<\boldsymbol{\epsilon}>^n\|\|\nabla \boldsymbol{e}_j^{n+1}\| \\
&\leq \frac{\alpha_j}{12}\|\nabla \boldsymbol{e}_j^{n+1}\|^2 + \frac{CC_*^2}{\alpha_j}\|<\boldsymbol{\epsilon}>^n\|^2, \\
\Big|b\Big(\boldsymbol{\epsilon}_j^{'n}, \boldsymbol{v}_{j,h}^{n}, \boldsymbol{e}_j^{n+1}\Big)\Big| &\leq \|\boldsymbol{\epsilon}_j^{'n}\|\|\nabla \boldsymbol{v}_{j,h}^{n}\|_{L^3}\|\boldsymbol{e}_j^{n+1}\|_{L^6} \\
&\leq CC_*\|\boldsymbol{\epsilon}_j^{'n}\|\|\nabla \boldsymbol{e}_j^{n+1}\| \\
&\leq \frac{\alpha_j}{12}\|\nabla \boldsymbol{e}_j^{n+1}\|^2 + \frac{CC_*^2}{\alpha_j}\|\boldsymbol{\epsilon}_j^{'n}\|^2.
\end{aligned}$$

For the third non-linear term, we apply Hölder's and triangle inequalities, stability estimate of Algorithm 1, uniform boundedness in Lemma 1.1 and in Assumption 2.1, Agmon's [38], discrete inverse, and Young's inequalities, to get

$$\begin{aligned}
&2\mu\Delta t\Big(\big\{(l_{\boldsymbol{w},h}^n)^2-(l_{\hat{\boldsymbol{w}},h}^n)^2\big\}\nabla \boldsymbol{v}_{j,h}^{n+1}, \nabla \boldsymbol{e}_j^{n+1}\Big) \\
&\quad\leq 2\mu\Delta t\|(l_{\boldsymbol{w},h}^n)^2 - (l_{\hat{\boldsymbol{w}},h}^n)^2\|_\infty\|\nabla \boldsymbol{v}_{j,h}^{n+1}\|\|\nabla \boldsymbol{e}_j^{n+1}\| \\
&\quad= 2\mu\Delta t\|\sum_{i=1}^{J}\Big(|\boldsymbol{w}_{i,h}^{'n}|^2 - |\hat{\boldsymbol{w}}_{i,h}^{'n}|^2\Big)\|_\infty\|\nabla \boldsymbol{v}_{j,h}^{n+1}\|\|\nabla \boldsymbol{e}_j^{n+1}\| \\
&\quad\leq 2\mu\Delta t\sum_{i=1}^{J}\|(\boldsymbol{w}_{i,h}^{'n} - \hat{\boldsymbol{w}}_{i,h}^{'n})\cdot(\boldsymbol{w}_{i,h}^{'n} + \hat{\boldsymbol{w}}_{i,h}^{'n})\|_\infty\|\nabla \boldsymbol{v}_{j,h}^{n+1}\|\|\nabla \boldsymbol{e}_j^{n+1}\| \\
&\quad\leq 2\mu\Delta t\sum_{i=1}^{J}\|\boldsymbol{w}_{i,h}^{'n} - \hat{\boldsymbol{w}}_{i,h}^{'n}\|_\infty\|\boldsymbol{w}_{i,h}^{'n} + \hat{\boldsymbol{w}}_{i,h}^{'n}\|_\infty\|\nabla \boldsymbol{v}_{j,h}^{n+1}\|\|\nabla \boldsymbol{e}_j^{n+1}\| \\
&\quad\leq C\Delta t^{\frac{1}{2}}\sum_{i=1}^{J}\|\boldsymbol{\epsilon}_i^{'n}\|_\infty\Big(\|\boldsymbol{w}_{i,h}^{'n}\|_\infty + \|\hat{\boldsymbol{w}}_{i,h}^{'n}\|_\infty\Big)\|\nabla \boldsymbol{e}_j^{n+1}\| \\
&\quad\leq C\Delta t^{\frac{1}{2}}\sum_{i=1}^{J}\|\boldsymbol{\epsilon}_i^{n}\|_\infty\|\nabla \boldsymbol{e}_j^{n+1}\| \leq C\Delta t^{\frac{1}{2}}h^{-\frac{3}{2}}\sum_{i=1}^{J}\|\boldsymbol{\epsilon}_i^{n}\|\|\nabla \boldsymbol{e}_j^{n+1}\| \\
&\quad\leq \frac{\alpha_j}{12}\|\nabla \boldsymbol{e}_j^{n+1}\|^2 + \frac{C\Delta t}{h^3\alpha_j}\sum_{i=1}^{J}\|\boldsymbol{\epsilon}_i^{n}\|^2. \qquad (2.25)
\end{aligned}$$

Using the above estimates in (2.23), choosing $\mu > \max\{1, \frac{1}{2\Delta t}\}$, dropping non-negative terms and reducing produces

$$\begin{aligned}
&\frac{1}{2\Delta t}\Big(\|\boldsymbol{e}_j^{n+1}\|^2 - \|\boldsymbol{e}_j^{n}\|^2\Big) + \frac{\bar{\nu}+\bar{\nu}_m}{4}\|\nabla \boldsymbol{e}_j^{n+1}\|^2 + \frac{\gamma}{2}\|\nabla\cdot \boldsymbol{e}_{j,\boldsymbol{R}}^{n+1}\|^2 \\
&\le \frac{|\nu_j - \nu_{m,j}|}{4}\|\nabla \boldsymbol{\epsilon}_j^{n}\|^2 + \frac{|\nu_j^{'} + \nu_{m,j}^{'}|}{4}\|\nabla \boldsymbol{e}_j^{n}\|^2 + \frac{1}{2\gamma}\|q_{j,h}^{n+1} - \hat{q}_{j,h}^{n}\|^2 \\
&\quad + \frac{CC_*^2}{\alpha_j}\Big(\|<\boldsymbol{\epsilon}>^n\|^2 + \|\boldsymbol{\epsilon}_j^{'n}\|^2\Big) + \frac{C\Delta t}{h^3\alpha_j}\sum_{i=1}^{J}\|\boldsymbol{\epsilon}_i^n\|^2. \qquad (2.26)
\end{aligned}$$

Now, apply similar estimates to the right hand side terms of (2.24) to produce

$$\begin{aligned}
&\frac{1}{2\Delta t}\Big(\|\boldsymbol{\epsilon}_j^{n+1}\|^2 - \|\boldsymbol{\epsilon}_j^{n}\|^2\Big) + \frac{\bar{\nu}+\bar{\nu}_m}{4}\|\nabla \boldsymbol{\epsilon}_j^{n+1}\|^2 + \frac{\gamma}{2}\|\nabla\cdot \boldsymbol{\epsilon}_{j,\boldsymbol{R}}^{n+1}\|^2 \\
&\le \frac{|\nu_j - \nu_{m,j}|}{4}\|\nabla \boldsymbol{e}_j^{n}\|^2 + \frac{|\nu_j^{'} + \nu_{m,j}^{'}|}{4}\|\nabla \boldsymbol{\epsilon}_j^{n}\|^2 + \frac{1}{2\gamma}\|\lambda_{j,h}^{n+1} - \hat{\lambda}_{j,h}^{n}\|^2 \\
&\quad + \frac{CC_*^2}{\alpha_j}\Big(\|<\boldsymbol{e}>^n\|^2 + \|\boldsymbol{e}_j^{'n}\|^2\Big) + \frac{C\Delta t}{h^3\alpha_j}\sum_{i=1}^{J}\|\boldsymbol{e}_i^n\|^2. \qquad (2.27)
\end{aligned}$$

Add (2.26) and (2.27), and rearrange

$$\begin{aligned}
&\frac{1}{2\Delta t}\Big(\|\boldsymbol{e}_j^{n+1}\|^2 - \|\boldsymbol{e}_j^{n}\|^2 + \|\boldsymbol{\epsilon}_j^{n+1}\|^2 - \|\boldsymbol{\epsilon}_j^{n}\|^2\Big) \\
&+ \frac{\bar{\nu}+\bar{\nu}_m}{4}\Big(\|\nabla \boldsymbol{e}_j^{n+1}\|^2 - \|\nabla \boldsymbol{e}_j^{n}\|^2 + \|\nabla \boldsymbol{\epsilon}_j^{n+1}\|^2 - \|\nabla \boldsymbol{\epsilon}_j^{n}\|^2\Big) + \frac{\alpha_j}{4}\Big(\|\nabla \boldsymbol{e}_j^{n}\|^2 + \|\nabla \boldsymbol{\epsilon}_j^{n}\|^2\Big) \\
&+ \frac{\gamma}{2}\Big(\|\nabla\cdot \boldsymbol{e}_{j,\boldsymbol{R}}^{n+1}\|^2 + \|\nabla\cdot \boldsymbol{\epsilon}_{j,\boldsymbol{R}}^{n+1}\|^2\Big) \le \frac{1}{2\gamma}\Big(\|q_{j,h}^{n+1} - \hat{q}_{j,h}^{n}\|^2 + \|\lambda_{j,h}^{n+1} - \hat{\lambda}_{j,h}^{n}\|^2\Big) \\
&+ \frac{CC_*^2}{\alpha_j}\Big(\|<\boldsymbol{e}>^n\|^2 + \|\boldsymbol{e}_j^{'n}\|^2 + \|<\boldsymbol{\epsilon}>^n\|^2 + \|\boldsymbol{\epsilon}_j^{'n}\|^2\Big) + \frac{C\Delta t}{h^3\alpha_j}\sum_{i=1}^{J}\Big(\|\boldsymbol{e}_i^n\|^2 + \|\boldsymbol{\epsilon}_i^n\|^2\Big). \qquad (2.28)
\end{aligned}$$

Now multiply both sides by $2\Delta t$, and sum over the time steps $n = 0, 1, \cdots, M-1$ to get

$$\begin{aligned}
&\|\boldsymbol{e}_j^{M}\|^2 + \|\boldsymbol{\epsilon}_j^{M}\|^2 + \frac{\bar{\nu}+\bar{\nu}_m}{2}\Delta t\Big(\|\nabla \boldsymbol{e}_j^{M}\|^2 + \|\nabla \boldsymbol{\epsilon}_j^{M}\|^2\Big) + \frac{\alpha_j}{2}\Delta t\sum_{n=0}^{M-1}\Big(\|\nabla \boldsymbol{e}_j^{n}\|^2 + \|\nabla \boldsymbol{\epsilon}_j^{n}\|^2\Big) \\
&+ \Delta t\sum_{n=0}^{M-1}\gamma\Big(\|\nabla\cdot \boldsymbol{e}_{j,\boldsymbol{R}}^{n+1}\|^2 + \|\nabla\cdot \boldsymbol{\epsilon}_{j,\boldsymbol{R}}^{n+1}\|^2\Big) \le \frac{\Delta t}{\gamma}\sum_{n=0}^{M-1}\Big(\|q_{j,h}^{n+1} - \hat{q}_{j,h}^{n}\|^2 + \|\lambda_{j,h}^{n+1} - \hat{\lambda}_{j,h}^{n}\|^2\Big) \\
&+ \frac{CC_*^2}{\alpha_j}\Delta t\sum_{n=0}^{M-1}\Big(\|<\boldsymbol{e}>^n\|^2 + \|\boldsymbol{e}_j^{'n}\|^2 + \|<\boldsymbol{\epsilon}>^n\|^2 + \|\boldsymbol{\epsilon}_j^{'n}\|^2\Big) + \frac{C\Delta t^2}{h^3\alpha_j}\sum_{n=1}^{M-1}\sum_{i=1}^{J}\Big(\|\boldsymbol{e}_i^n\|^2 + \|\boldsymbol{\epsilon}_i^n\|^2\Big). \qquad (2.29)
\end{aligned}$$

Using triangle, Cauchy-Schwarz, and Young's inequalities to get

$$\|\boldsymbol{e}_j^M\|^2+\|\boldsymbol{\epsilon}_j^M\|^2+\frac{\alpha_j\Delta t}{2}\sum_{n=1}^{M}\Big(\|\nabla\boldsymbol{e}_j^n\|^2+\|\nabla\boldsymbol{\epsilon}_j^n\|^2\Big)+\Delta t\sum_{n=1}^{M}\gamma\Big(\|\nabla\cdot\boldsymbol{e}_{j,\boldsymbol{R}}^n\|^2+\|\nabla\cdot\boldsymbol{\epsilon}_{j,\boldsymbol{R}}^n\|^2\Big)$$
$$\leq\frac{\Delta t}{\gamma}\sum_{n=0}^{M-1}\Big(\|q_{j,h}^{n+1}-\hat{q}_{j,h}^n\|^2+\|\lambda_{j,h}^{n+1}-\hat{\lambda}_{j,h}^n\|^2\Big)+\left(\frac{CC_*^2}{\alpha_j}\Delta t+\frac{C\Delta t^2}{h^3\alpha_j}\right)\sum_{n=1}^{M-1}\sum_{j=1}^{J}\Big(\|\boldsymbol{e}_j^n\|^2+\|\boldsymbol{\epsilon}_j^n\|^2\Big). \quad (2.30)$$

Summing over $j=1,2,\cdots,J$, we have

$$\sum_{j=1}^{J}\|\boldsymbol{e}_j^M\|^2+\sum_{j=1}^{J}\|\boldsymbol{\epsilon}_j^M\|^2+\frac{\alpha_{min}\Delta t}{2}\sum_{n=1}^{M}\sum_{j=1}^{J}\Big(\|\nabla\boldsymbol{e}_j^n\|^2+\|\nabla\boldsymbol{\epsilon}_j^n\|^2\Big)$$
$$+\gamma\Delta t\sum_{n=1}^{M}\sum_{j=1}^{J}\Big(\|\nabla\cdot\boldsymbol{e}_{j,\boldsymbol{R}}^n\|^2+\|\nabla\cdot\boldsymbol{\epsilon}_{j,\boldsymbol{R}}^n\|^2\Big)\leq\frac{\Delta t}{\gamma}\sum_{n=0}^{M-1}\sum_{j=1}^{J}\Big(\|q_{j,h}^{n+1}-\hat{q}_{j,h}^n\|^2+\|\lambda_{j,h}^{n+1}-\hat{\lambda}_{j,h}^n\|^2\Big)$$
$$+\Delta t\sum_{n=1}^{M-1}\left(\frac{CC_*^2}{\alpha_{min}}+\frac{C\Delta t}{h^3\alpha_{min}}\right)\sum_{j=1}^{J}\Big(\|\boldsymbol{e}_j^n\|^2+\|\boldsymbol{\epsilon}_j^n\|^2\Big). \quad (2.31)$$

Apply discrete Grönwall inequality given in Lemma 1.1 to get

$$\sum_{j=1}^{J}\|\boldsymbol{e}_j^M\|^2+\sum_{j=1}^{J}\|\boldsymbol{\epsilon}_j^M\|^2+\frac{\alpha_{min}\Delta t}{2}\sum_{n=1}^{M}\sum_{j=1}^{J}\Big(\|\nabla\boldsymbol{e}_j^n\|^2+\|\nabla\boldsymbol{\epsilon}_j^n\|^2\Big)+\gamma\Delta t\sum_{n=1}^{M}\sum_{j=1}^{J}\Big(\|\nabla\cdot\boldsymbol{e}_{j,\boldsymbol{R}}^n\|^2+\|\nabla\cdot\boldsymbol{\epsilon}_{j,\boldsymbol{R}}^n\|^2\Big)$$
$$\leq\frac{1}{\gamma}exp\left(CT\left(\frac{C_*^2}{\alpha_{min}}+\frac{\Delta t}{h^3\alpha_{min}}\right)\right)\left(\Delta t\sum_{n=0}^{M-1}\sum_{j=1}^{J}\Big(\|q_{j,h}^{n+1}-\hat{q}_{j,h}^n\|^2+\|\lambda_{j,h}^{n+1}-\hat{\lambda}_{j,h}^n\|^2\Big)\right). \quad (2.32)$$

Using Lemma 2.2 with (2.32) yields the following bound

$$\Delta t\sum_{n=1}^{M}\sum_{j=1}^{J}\Big(\|\nabla\boldsymbol{e}_{j,\boldsymbol{R}}^n\|^2+\|\nabla\boldsymbol{\epsilon}_{j,\boldsymbol{R}}^n\|^2\Big)\leq C_R^2\Delta t\sum_{n=1}^{M}\sum_{j=1}^{J}\Big(\|\nabla\cdot\boldsymbol{e}_{j,\boldsymbol{R}}^n\|^2+\|\nabla\cdot\boldsymbol{\epsilon}_{j,\boldsymbol{R}}^n\|^2\Big)$$
$$\leq\frac{C_R^2}{\gamma^2}exp\left(\frac{CC_*^2}{\alpha_{min}}+\frac{C\Delta t}{h^3\alpha_{min}}\right)\left(\Delta t\sum_{n=0}^{M-1}\sum_{j=1}^{J}\Big(\|q_{j,h}^{n+1}-\hat{q}_{j,h}^n\|^2+\|\lambda_{j,h}^{n+1}-\hat{\lambda}_{j,h}^n\|^2\Big)\right). \quad (2.33)$$

Step 2: Estimate of $\boldsymbol{e}_{j,0}^n$, and $\boldsymbol{\epsilon}_{j,0}^n$: To find a bound on $\Delta t\sum_{n=1}^{M}\sum_{j=1}^{J}\Big(\|\nabla\boldsymbol{e}_{j,0}^n\|^2+\|\nabla\boldsymbol{\epsilon}_{j,0}^n\|^2\Big)$, take $\boldsymbol{\chi}_{j,h}=\boldsymbol{e}_{j,0}^{n+1}$ in (2.21), and $\boldsymbol{l}_{j,h}=\boldsymbol{\epsilon}_{j,0}^{n+1}$ in (2.22), which yield

$$\frac{1}{\Delta t}\Big(\boldsymbol{e}_j^{n+1}-\boldsymbol{e}_j^{n},\boldsymbol{e}_{j,0}^{n+1}\Big)+\frac{\bar{\nu}+\bar{\nu}_m}{2}\|\nabla\boldsymbol{e}_{j,0}^{n+1}\|^2=-b\Big(<\hat{\boldsymbol{w}}_h>^n,\boldsymbol{e}_{j,\boldsymbol{R}}^{n+1},\boldsymbol{e}_{j,0}^{n+1}\Big)$$
$$-b\Big(<\boldsymbol{\epsilon}>^n,\boldsymbol{v}_{j,h}^{n+1},\boldsymbol{e}_{j,0}^{n+1}\Big)-2\mu\Delta t\Big((l_{\hat{\boldsymbol{w}},h}^n)^2\nabla\boldsymbol{e}_j^{n+1},\nabla\boldsymbol{e}_{j,0}^{n+1}\Big)$$
$$-2\mu\Delta t\Big(\big\{(l_{\boldsymbol{w},h}^n)^2-(l_{\hat{\boldsymbol{w}},h}^n)^2\big\}\nabla\boldsymbol{v}_{j,h}^{n+1},\nabla\boldsymbol{e}_{j,0}^{n+1}\Big)-b\Big(\hat{\boldsymbol{w}}_{j,h}^{'n},\boldsymbol{e}_j^n,\boldsymbol{e}_{j,0}^{n+1}\Big)$$
$$-b\Big(\boldsymbol{\epsilon}_j^{'n},\boldsymbol{v}_{j,h}^n,\boldsymbol{e}_{j,0}^{n+1}\Big)-\frac{\nu_j-\nu_{m,j}}{2}\Big(\nabla\boldsymbol{\epsilon}_{j,0}^n,\nabla\boldsymbol{e}_{j,0}^{n+1}\Big)-\frac{\nu_j^{'}+\nu_{m,j}^{'}}{2}\Big(\nabla\boldsymbol{e}_{j,0}^n,\nabla\boldsymbol{e}_{j,0}^{n+1}\Big),\tag{2.34}$$

and

$$\frac{1}{\Delta t}\Big(\boldsymbol{\epsilon}_j^{n+1}-\boldsymbol{\epsilon}_j^{n},\boldsymbol{\epsilon}_{j,0}^{n+1}\Big)+\frac{\bar{\nu}+\bar{\nu}_m}{2}\|\nabla\boldsymbol{\epsilon}_{j,0}^{n+1}\|^2=-b\Big(<\hat{\boldsymbol{v}}_h>^n,\boldsymbol{\epsilon}_{j,\boldsymbol{R}}^{n+1},\boldsymbol{\epsilon}_{j,0}^{n+1}\Big)$$
$$-b\Big(<\boldsymbol{e}>^n,\boldsymbol{w}_{j,h}^{n+1},\boldsymbol{\epsilon}_{j,0}^{n+1}\Big)-2\mu\Delta t\Big((l_{\hat{\boldsymbol{v}},h}^n)^2\nabla\boldsymbol{\epsilon}_j^{n+1},\nabla\boldsymbol{\epsilon}_{j,0}^{n+1}\Big)$$
$$-2\mu\Delta t\Big(\big\{(l_{\boldsymbol{v},h}^n)^2-(l_{\hat{\boldsymbol{v}},h}^n)^2\big\}\nabla\boldsymbol{w}_{j,h}^{n+1},\nabla\boldsymbol{\epsilon}_{j,0}^{n+1}\Big)-b\Big(\hat{\boldsymbol{v}}_{j,h}^{'n},\boldsymbol{\epsilon}_j^n,\boldsymbol{\epsilon}_{j,0}^{n+1}\Big)$$
$$-b\Big(\boldsymbol{e}_j^{'n},\boldsymbol{w}_{j,h}^n,\boldsymbol{\epsilon}_{j,0}^{n+1}\Big)-\frac{\nu_j-\nu_{m,j}}{2}\Big(\nabla\boldsymbol{e}_{j,0}^n,\nabla\boldsymbol{\epsilon}_{j,0}^{n+1}\Big)-\frac{\nu_j^{'}+\nu_{m,j}^{'}}{2}\Big(\nabla\boldsymbol{\epsilon}_{j,0}^n,\nabla\boldsymbol{\epsilon}_{j,0}^{n+1}\Big).\tag{2.35}$$

Apply the non-linear bound given in (1.14), and Hölder's inequality for the first, and second non-linear terms of (2.34), respectively, to obtain

$$\frac{1}{\Delta t}\Big(\boldsymbol{e}_j^{n+1}-\boldsymbol{e}_j^{n},\boldsymbol{e}_{j,0}^{n+1}\Big)+\frac{\bar{\nu}+\bar{\nu}_m}{2}\|\nabla\boldsymbol{e}_{j,0}^{n+1}\|^2+2\mu\Delta t\|l_{\hat{\boldsymbol{w}},h}^n\nabla\boldsymbol{e}_{j,0}^{n+1}\|^2$$
$$\leq C\|\nabla<\hat{\boldsymbol{w}}_h>^n\|\|\nabla\boldsymbol{e}_{j,\boldsymbol{R}}^{n+1}\|\|\nabla\boldsymbol{e}_{j,0}^{n+1}\|+C\|<\boldsymbol{\epsilon}>^n\|\|\nabla\boldsymbol{v}_{j,h}^{n+1}\|_{L^3}\|\nabla\boldsymbol{e}_{j,0}^{n+1}\|$$
$$-2\mu\Delta t\Big((l_{\hat{\boldsymbol{w}},h}^n)^2\nabla\boldsymbol{e}_{j,\boldsymbol{R}}^{n+1},\nabla\boldsymbol{e}_{j,0}^{n+1}\Big)-2\mu\Delta t\Big(\big\{(l_{\boldsymbol{w},h}^n)^2-(l_{\hat{\boldsymbol{w}},h}^n)^2\big\}\nabla\boldsymbol{v}_{j,h}^{n+1},\nabla\boldsymbol{e}_{j,0}^{n+1}\Big)$$
$$-b\Big(\hat{\boldsymbol{w}}_{j,h}^{'n},\boldsymbol{e}_j^n,\boldsymbol{e}_{j,0}^{n+1}\Big)-b\Big(\boldsymbol{\epsilon}_j^{'n},\boldsymbol{v}_{j,h}^n,\boldsymbol{e}_{j,0}^{n+1}\Big)-\frac{\nu_j-\nu_{m,j}}{2}\Big(\nabla\boldsymbol{\epsilon}_{j,0}^n,\nabla\boldsymbol{e}_{j,0}^{n+1}\Big)$$
$$-\frac{\nu_j^{'}+\nu_{m,j}^{'}}{2}\Big(\nabla\boldsymbol{e}_{j,0}^n,\nabla\boldsymbol{e}_{j,0}^{n+1}\Big).\tag{2.36}$$

Using Cauchy-Schwarz and Young's inequalities yields

$$\begin{aligned}-b\Big(\hat{\boldsymbol{w}}_{j,h}^{'n},\boldsymbol{e}_j^n,\boldsymbol{e}_{j,0}^{n+1}\Big)&=b\Big(\hat{\boldsymbol{w}}_{j,h}^{'n},\boldsymbol{e}_{j,0}^{n+1},\boldsymbol{e}_j^n\Big)\\&\leq\|\hat{\boldsymbol{w}}_{j,h}^{'n}\cdot\nabla\boldsymbol{e}_{j,0}^{n+1}\|\|\boldsymbol{e}_j^n\|\\&\leq\sqrt{2}\||\hat{\boldsymbol{w}}_{j,h}^{'n}|\nabla\boldsymbol{e}_{j,0}^{n+1}\|\|\boldsymbol{e}_j^n\|\\&\leq\sqrt{2}\|l_{\hat{\boldsymbol{w}},h}^n\nabla\boldsymbol{e}_{j,0}^{n+1}\|\|\boldsymbol{e}_j^n\|\\&\leq\|l_{\hat{\boldsymbol{w}},h}^n\nabla\boldsymbol{e}_{j,0}^{n+1}\|^2+\frac{1}{2}\|\boldsymbol{e}_j^n\|^2.\end{aligned}$$

Using the above bound, triangle inequality, stability estimate, Assumption 2.1, and finally rearranging,

we have

$$\begin{aligned}
&\frac{1}{\Delta t}\Big(\boldsymbol{e}_j^{n+1}-\boldsymbol{e}_j^{n},\boldsymbol{e}_{j,0}^{n+1}\Big)+\frac{\bar{\nu}+\bar{\nu}_m}{2}\|\nabla\boldsymbol{e}_{j,0}^{n+1}\|^2+(2\mu\Delta t-1)\,\|l_{\hat{\boldsymbol{w}},h}^{n}\nabla\boldsymbol{e}_{j,0}^{n+1}\|^2\\
\leq\frac{C}{(\bar{\nu}+\bar{\nu}_m)^{\frac{1}{2}}\Delta t^{\frac{1}{2}}}\|\nabla\boldsymbol{e}_{j,\boldsymbol{R}}^{n+1}\|\|\nabla\boldsymbol{e}_{j,0}^{n+1}\|+CC_*\|<\boldsymbol{\epsilon}>^n\|\|\nabla\boldsymbol{e}_{j,0}^{n+1}\|+2\mu\Delta t\Big|\Big((l_{\hat{\boldsymbol{w}},h}^{n})^2\nabla\boldsymbol{e}_{j,\boldsymbol{R}}^{n+1},\nabla\boldsymbol{e}_{j,0}^{n+1}\Big)\Big|\\
+2\mu\Delta t\Big|\Big(\{(l_{\boldsymbol{w},h}^{n})^2-(l_{\hat{\boldsymbol{w}},h}^{n})^2\}\nabla\boldsymbol{v}_{j,h}^{n+1},\nabla\boldsymbol{e}_{j,0}^{n+1}\Big)\Big|+\frac{1}{2}\|\boldsymbol{e}_j^{n}\|^2+\Big|b\Big(\boldsymbol{\epsilon}_j^{'n},\boldsymbol{v}_{j,h}^{n},\boldsymbol{e}_{j,0}^{n+1}\Big)\Big|\\
+\frac{|\nu_j-\nu_{m,j}|}{2}\Big|\Big(\nabla\boldsymbol{\epsilon}_{j,0}^{n},\nabla\boldsymbol{e}_{j,0}^{n+1}\Big)\Big|+\frac{|\nu_j^{'}+\nu_{m,j}^{'}|}{2}\Big|\Big(\nabla\boldsymbol{e}_{j,0}^{n},\nabla\boldsymbol{e}_{j,0}^{n+1}\Big)\Big|.
\end{aligned}\tag{2.37}$$

To evaluate the discrete time-derivative term, we use polarization identity, Cauchy-Schwarz, Young's and Poincaré's inequalities

$$\begin{aligned}
\frac{1}{\Delta t}\Big(\boldsymbol{e}_j^{n+1}-\boldsymbol{e}_j^{n},\boldsymbol{e}_{j,0}^{n+1}\Big)&=\frac{1}{\Delta t}\Big(\boldsymbol{e}_j^{n+1}-\boldsymbol{e}_j^{n},\boldsymbol{e}_j^{n+1}-\boldsymbol{e}_{j,\boldsymbol{R}}^{n+1}\Big)\\
&=\frac{1}{2\Delta t}\Big(\|\boldsymbol{e}_j^{n+1}-\boldsymbol{e}_j^{n}\|^2+\|\boldsymbol{e}_j^{n+1}\|^2-\|\boldsymbol{e}_j^{n}\|^2\Big)-\frac{1}{\Delta t}\Big(\boldsymbol{e}_j^{n+1}-\boldsymbol{e}_j^{n},\boldsymbol{e}_{j,\boldsymbol{R}}^{n+1}\Big)\\
&\geq\frac{1}{2\Delta t}\Big(\|\boldsymbol{e}_j^{n+1}\|^2-\|\boldsymbol{e}_j^{n}\|^2\Big)-\frac{C}{\Delta t}\|\nabla\boldsymbol{e}_{j,\boldsymbol{R}}^{n+1}\|^2.
\end{aligned}$$

Plugging the above estimate into (2.37) and using Cauchy-Schwarz's, and Young's inequalities, yields

$$\begin{aligned}
&\frac{1}{2\Delta t}\Big(\|\boldsymbol{e}_j^{n+1}\|^2-\|\boldsymbol{e}_j^{n}\|^2\Big)+\frac{\bar{\nu}+\bar{\nu}_m}{2}\|\nabla\boldsymbol{e}_{j,0}^{n+1}\|^2+(2\mu\Delta t-1)\,\|l_{\hat{\boldsymbol{w}},h}^{n}\nabla\boldsymbol{e}_{j,0}^{n+1}\|^2\\
&\leq\frac{C}{\Delta t}\left(\frac{1}{\alpha_j^2}+1\right)\|\nabla\boldsymbol{e}_{j,\boldsymbol{R}}^{n+1}\|^2+\frac{CC_*^2}{\alpha_j}\|<\boldsymbol{\epsilon}>^n\|^2+2\mu\Delta t\Big|\Big((l_{\hat{\boldsymbol{w}},h}^{n})^2\nabla\boldsymbol{e}_{j,\boldsymbol{R}}^{n+1},\nabla\boldsymbol{e}_{j,0}^{n+1}\Big)\Big|\\
&+2\mu\Delta t\Big|\Big(\{(l_{\boldsymbol{w},h}^{n})^2-(l_{\hat{\boldsymbol{w}},h}^{n})^2\}\nabla\boldsymbol{v}_{j,h}^{n+1},\nabla\boldsymbol{e}_{j,0}^{n+1}\Big)\Big|+\frac{\alpha_j}{12}\|\nabla\boldsymbol{e}_{j,0}^{n+1}\|^2+\frac{1}{2}\|\boldsymbol{e}_j^{n}\|^2+\Big|b\Big(\boldsymbol{\epsilon}_j^{'n},\boldsymbol{v}_{j,h}^{n},\boldsymbol{e}_{j,0}^{n+1}\Big)\Big|\\
&+\frac{|\nu_j-\nu_{m,j}|}{4}\Big(\|\nabla\boldsymbol{\epsilon}_{j,0}^{n}\|^2+\|\nabla\boldsymbol{e}_{j,0}^{n+1}\|^2\Big)+\frac{|\nu_j^{'}+\nu_{m,j}^{'}|}{4}\Big(\|\nabla\boldsymbol{e}_{j,0}^{n}\|^2+\|\nabla\boldsymbol{e}_{j,0}^{n+1}\|^2\Big).
\end{aligned}\tag{2.38}$$

We now find the bounds for the non-linear terms. For the first non-linear term, we use Cauchy-Schwarz, and Young's inequalities, uniform boundedness in Assumption 2.1, and the stability estimate to obtain

$$\begin{aligned}
2\mu\Delta t\Big|\Big((l_{\hat{\boldsymbol{w}},h}^{n})^2\nabla\boldsymbol{e}_{j,\boldsymbol{R}}^{n+1},\nabla\boldsymbol{e}_{j,0}^{n+1}\Big)\Big|&\leq 2\mu\Delta t\|l_{\hat{\boldsymbol{w}},h}^{n}\nabla\boldsymbol{e}_{j,\boldsymbol{R}}^{n+1}\|\|l_{\hat{\boldsymbol{w}},h}^{n}\nabla\boldsymbol{e}_{j,0}^{n+1}\|\\
&\leq\mu\Delta t\|l_{\hat{\boldsymbol{w}},h}^{n}\nabla\boldsymbol{e}_{j,\boldsymbol{R}}^{n+1}\|^2+\mu\Delta t\|l_{\hat{\boldsymbol{w}},h}^{n}\nabla\boldsymbol{e}_{j,0}^{n+1}\|^2\\
&\leq\mu\Delta t\|l_{\hat{\boldsymbol{w}},h}^{n}\|_\infty^2\|\nabla\boldsymbol{e}_{j,\boldsymbol{R}}^{n+1}\|^2+\mu\Delta t\|l_{\hat{\boldsymbol{w}},h}^{n}\nabla\boldsymbol{e}_{j,0}^{n+1}\|^2\\
&\leq C\Delta t\|\nabla\boldsymbol{e}_{j,\boldsymbol{R}}^{n+1}\|^2+\mu\Delta t\|l_{\hat{\boldsymbol{w}},h}^{n}\nabla\boldsymbol{e}_{j,0}^{n+1}\|^2.
\end{aligned}$$

For the second non-linear term, we follow the same treatment as in (2.25), and get

$$2\mu\Delta t\Big(\big\{(l^n_{\boldsymbol{w},h})^2-(l^n_{\dot{\boldsymbol{w}},h})^2\big\}\nabla \boldsymbol{v}^{n+1}_{j,h},\nabla \boldsymbol{e}^{n+1}_{j,0}\Big)\leq \frac{\alpha_j}{12}\|\nabla \boldsymbol{e}^{n+1}_{j,0}\|^2+\frac{C\Delta t}{h^3\alpha_j}\sum_{i=1}^{J}\|\boldsymbol{\epsilon}^n_i\|^2.$$

For the last non-linear term, we apply Hölder's inequality, estimate in Lemma 1.1, Sobolev embedding theorem, Poincaré and Young's inequalities to get

$$\begin{aligned}|b\Big(\boldsymbol{\epsilon}^{'n}_j,\boldsymbol{v}^n_{j,h},\boldsymbol{e}^{n+1}_{j,0}\Big)| &\leq \|\boldsymbol{\epsilon}^{'n}_j\|\|\nabla \boldsymbol{v}^n_{j,h}\|_{L^3}\|\boldsymbol{e}^{n+1}_{j,0}\|_{L^6}\\ &\leq CC_*\|\boldsymbol{\epsilon}^{'n}_j\|\|\nabla \boldsymbol{e}^{n+1}_{j,0}\|\\ &\leq \frac{\alpha_j}{12}\|\nabla \boldsymbol{e}^{n+1}_{j,0}\|^2+\frac{CC^2_*}{\alpha_j}\|\boldsymbol{\epsilon}^{'n}_j\|^2.\end{aligned}$$

Use the above estimates, assume $\mu>\max\{1,\frac{1}{2\Delta t}\}$ to drop non-negative terms from left, and reducing, the equation (2.38) becomes

$$\begin{aligned}&\frac{1}{2\Delta t}\Big(\|\boldsymbol{e}^{n+1}_j\|^2-\|\boldsymbol{e}^n_j\|^2\Big)+\frac{\bar{\nu}+\bar{\nu}_m}{4}\|\nabla \boldsymbol{e}^{n+1}_{j,0}\|^2\\ &\leq \frac{C}{\Delta t}\left(\frac{1}{\alpha_j^2}+1+\Delta t^2\right)\|\nabla \boldsymbol{e}^{n+1}_{j,\boldsymbol{R}}\|^2+\frac{CC^2_*}{\alpha_j}\Big(\|<\boldsymbol{\epsilon}>^n\|^2+\|\boldsymbol{\epsilon}^{'n}_j\|^2\Big)\\ &+\frac{C\Delta t}{h^3\alpha_j}\sum_{i=1}^{J}\|\boldsymbol{\epsilon}^n_i\|^2+\frac{1}{2}\|\boldsymbol{e}^n_j\|^2+\frac{|\nu_j-\nu_{m,j}|}{4}\|\nabla \boldsymbol{\epsilon}^n_{j,0}\|^2+\frac{|\nu^{'}_j+\nu^{'}_{m,j}|}{4}\|\nabla \boldsymbol{e}^n_{j,0}\|^2.\end{aligned}\tag{2.39}$$

Apply similar techniques to (2.35), yields

$$\begin{aligned}&\frac{1}{2\Delta t}\Big(\|\boldsymbol{\epsilon}^{n+1}_j\|^2-\|\boldsymbol{\epsilon}^n_j\|^2\Big)+\frac{\bar{\nu}+\bar{\nu}_m}{4}\|\nabla \boldsymbol{\epsilon}^{n+1}_{j,0}\|^2\\ &\leq \frac{C}{\Delta t}\left(\frac{1}{\alpha_j^2}+1+\Delta t^2\right)\|\nabla \boldsymbol{\epsilon}^{n+1}_{j,\boldsymbol{R}}\|^2+\frac{CC^2_*}{\alpha_j}\Big(\|<\boldsymbol{e}>^n\|^2+\|\boldsymbol{e}^{'n}_j\|^2\Big)\\ &+\frac{C\Delta t}{h^3\alpha_j}\sum_{i=1}^{J}\|\boldsymbol{e}^n_i\|^2+\frac{1}{2}\|\boldsymbol{\epsilon}^n_j\|^2+\frac{|\nu_j-\nu_{m,j}|}{4}\|\nabla \boldsymbol{e}^n_{j,0}\|^2+\frac{|\nu^{'}_j+\nu^{'}_{m,j}|}{4}\|\nabla \boldsymbol{\epsilon}^n_{j,0}\|^2.\end{aligned}\tag{2.40}$$

Add equations (2.39), and (2.40), and use triangle inequality, to get

$$\begin{aligned}&\frac{1}{2\Delta t}\Big(\|\boldsymbol{e}^{n+1}_j\|^2-\|\boldsymbol{e}^n_j\|^2+\|\boldsymbol{\epsilon}^{n+1}_j\|^2-\|\boldsymbol{\epsilon}^n_j\|^2\Big)+\frac{\bar{\nu}+\bar{\nu}_m}{4}\Big(\|\nabla \boldsymbol{e}^{n+1}_{j,0}\|^2+\|\nabla \boldsymbol{\epsilon}^{n+1}_{j,0}\|^2\Big)\\ &\leq \frac{C}{\Delta t}\left(\frac{1}{\alpha_j^2}+1+\Delta t^2\right)\Big(\|\nabla \boldsymbol{e}^{n+1}_{j,\boldsymbol{R}}\|^2+\|\nabla \boldsymbol{\epsilon}^{n+1}_{j,\boldsymbol{R}}\|^2\Big)+\left(\frac{CC^2_*}{\alpha_j}+\frac{C\Delta t}{h^3\alpha_j}+\frac{1}{2}\right)\sum_{j=1}^{J}\Big(\|\boldsymbol{e}^n_j\|^2+\|\boldsymbol{\epsilon}^n_j\|^2\Big)\\ &+\frac{|\nu_j-\nu_{m,j}|+|\nu^{'}_j+\nu^{'}_{m,j}|}{4}\Big(\|\nabla \boldsymbol{e}^n_{j,0}\|^2+\|\nabla \boldsymbol{\epsilon}^n_{j,0}\|^2\Big).\end{aligned}\tag{2.41}$$

Rearranging

$$\begin{aligned}
&\frac{1}{2\Delta t}\Big(\|\boldsymbol{e}_j^{n+1}\|^2-\|\boldsymbol{e}_j^{n}\|^2+\|\boldsymbol{\epsilon}_j^{n+1}\|^2-\|\boldsymbol{\epsilon}_j^{n}\|^2\Big)\\
&+\frac{\bar{\nu}+\bar{\nu}_m}{4}\Big(\|\nabla\boldsymbol{e}_{j,0}^{n+1}\|^2-\|\nabla\boldsymbol{e}_{j,0}^{n}\|^2+\|\nabla\boldsymbol{\epsilon}_{j,0}^{n+1}\|^2-\|\nabla\boldsymbol{\epsilon}_{j,0}^{n}\|^2\Big)\\
+\frac{\alpha_j}{4}\Big(\|\nabla\boldsymbol{e}_{j,0}^{n}\|^2+\|\nabla\boldsymbol{\epsilon}_{j,0}^{n}\|^2\Big)&\leq\frac{C}{\Delta t}\left(\frac{1}{\alpha_j^2}+1+\Delta t^2\right)\Big(\|\nabla\boldsymbol{e}_{j,\boldsymbol{R}}^{n+1}\|^2+\|\nabla\boldsymbol{\epsilon}_{j,\boldsymbol{R}}^{n+1}\|^2\Big)\\
&+\left(\frac{CC_*^2}{\alpha_j}+\frac{C\Delta t}{h^3\alpha_j}+\frac{1}{2}\right)\sum_{j=1}^{J}\Big(\|\boldsymbol{e}_j^{n}\|^2+\|\boldsymbol{\epsilon}_j^{n}\|^2\Big).
\end{aligned}\tag{2.42}$$

Multiply both sides by $2\Delta t$, and summing over the time-step $n=0,1,\cdots,M-1$, results in

$$\begin{aligned}
\|\boldsymbol{e}_j^{M}\|^2+\|\boldsymbol{\epsilon}_j^{M}\|^2+\frac{\bar{\nu}+\bar{\nu}_m}{2}\Delta t\Big(\|\nabla\boldsymbol{e}_{j,0}^{M}\|^2+\|\nabla\boldsymbol{\epsilon}_{j,0}^{M}\|^2\Big)+\frac{\alpha_j}{2}\Delta t\sum_{n=1}^{M-1}\Big(\|\nabla\boldsymbol{e}_{j,0}^{n}\|^2+\|\nabla\boldsymbol{\epsilon}_{j,0}^{n}\|^2\Big)\\
\leq C\left(\frac{1}{\alpha_j^2}+1+\Delta t^2\right)\sum_{n=1}^{M}\Big(\|\nabla\boldsymbol{e}_{j,\boldsymbol{R}}^{n}\|^2+\|\nabla\boldsymbol{\epsilon}_{j,\boldsymbol{R}}^{n}\|^2\Big)\\
+\Delta t\left(\frac{CC_*^2}{\alpha_j}+\frac{C\Delta t}{h^3\alpha_j}+1\right)\sum_{n=1}^{M-1}\sum_{j=1}^{J}\Big(\|\boldsymbol{e}_j^{n}\|^2+\|\boldsymbol{\epsilon}_j^{n}\|^2\Big).
\end{aligned}\tag{2.43}$$

Now, simplifying, and summing over $j=1,2,\cdots,J$, we have

$$\begin{aligned}
\sum_{j=1}^{J}\Big(\|\boldsymbol{e}_j^{M}\|^2+\|\boldsymbol{\epsilon}_j^{M}\|^2\Big)+\Delta t\sum_{n=1}^{M}\frac{\alpha_{min}}{2}\sum_{j=1}^{J}\Big(\|\nabla\boldsymbol{e}_{j,0}^{n}\|^2+\|\nabla\boldsymbol{\epsilon}_{j,0}^{n}\|^2\Big)\\
\leq\sum_{n=1}^{M}C\left(\frac{1}{\alpha_{min}^2}+1+\Delta t^2\right)\sum_{j=1}^{J}\Big(\|\nabla\boldsymbol{e}_{j,\boldsymbol{R}}^{n}\|^2+\|\nabla\boldsymbol{\epsilon}_{j,\boldsymbol{R}}^{n}\|^2\Big)\\
+\Delta t\sum_{n=1}^{M-1}\left(\frac{CC_*^2}{\alpha_{min}}+\frac{C\Delta t}{h^3\alpha_{min}}+J\right)\sum_{j=1}^{J}\Big(\|\boldsymbol{e}_j^{n}\|^2+\|\boldsymbol{\epsilon}_j^{n}\|^2\Big).
\end{aligned}\tag{2.44}$$

Apply the version of the discrete Grönwall inequality given in Lemma 1.1

$$\begin{aligned}
&\sum_{j=1}^{J}\Big(\|\boldsymbol{e}_j^{M}\|^2+\|\boldsymbol{\epsilon}_j^{M}\|^2\Big)+\frac{\alpha_{min}}{2}\Delta t\sum_{n=1}^{M}\sum_{j=1}^{J}\Big(\|\nabla\boldsymbol{e}_{j,0}^{n}\|^2+\|\nabla\boldsymbol{\epsilon}_{j,0}^{n}\|^2\Big)\\
\leq exp\left(\frac{CC_*^2}{\alpha_{min}}+\frac{C\Delta t}{h^3\alpha_{min}}+JT\right)&\left[C\left(\frac{1}{\alpha_{min}^2}+1+\Delta t^2\right)\sum_{n=1}^{M}\sum_{j=1}^{J}\Big(\|\nabla\boldsymbol{e}_{j,\boldsymbol{R}}^{n}\|^2+\|\nabla\boldsymbol{\epsilon}_{j,\boldsymbol{R}}^{n}\|^2\Big)\right],
\end{aligned}\tag{2.45}$$

and use the estimate (2.33) in (2.45), to get

$$\begin{aligned}
\Delta t\sum_{n=1}^{M}\sum_{j=1}^{J}\Big(\|\nabla\boldsymbol{e}_{j,0}^{n}\|^2+\|\nabla\boldsymbol{\epsilon}_{j,0}^{n}\|^2\Big)&\leq\frac{CC_R^2}{\gamma^2\alpha_{min}}exp\left(\frac{CC_*^2}{\alpha_{min}}+\frac{C\Delta t}{h^3\alpha_{min}}\right)\\
\times\left[\left(\frac{1}{\alpha_{min}^2}+1+\Delta t^2\right)\sum_{n=0}^{M-1}\sum_{j=1}^{J}\Big(\|q_{j,h}^{n+1}-\hat{q}_{j,h}^{n}\|^2+\|\lambda_{j,h}^{n+1}-\hat{\lambda}_{j,h}^{n}\|^2\Big)\right].
\end{aligned}\tag{2.46}$$

Using triangle and Young's inequalities

$$\Delta t\sum_{n=1}^{M}\left(\|\nabla<\boldsymbol{e}_0>^n\|^2+\|\nabla<\boldsymbol{\epsilon}_0>^n\|^2\right)\leq\frac{2\Delta t}{J^2}\sum_{n=1}^{M}\sum_{j=1}^{J}\left(\|\nabla\boldsymbol{e}_{j,0}^n\|^2+\|\nabla\boldsymbol{\epsilon}_{j,0}^n\|^2\right)$$
$$\leq\frac{CC_R^2}{\gamma^2\alpha_{min}}exp\left(\frac{CC_*^2}{\alpha_{min}}+\frac{C\Delta t}{h^3\alpha_{min}}\right)$$
$$\times\left[\left(\frac{1}{\alpha_{min}^2}+1+\Delta t^2\right)\sum_{n=0}^{M-1}\sum_{j=1}^{J}\left(\|q_{j,h}^{n+1}-\hat{q}_{j,h}^n\|^2+\|\lambda_{j,h}^{n+1}-\hat{\lambda}_{j,h}^n\|^2\right)\right],\tag{2.47}$$

and

$$\Delta t\sum_{n=1}^{M}\left(\|\nabla<\boldsymbol{e}_{\boldsymbol{R}}>^n\|^2+\|\nabla<\boldsymbol{\epsilon}_{\boldsymbol{R}}>^n\|^2\right)\leq\frac{2\Delta t}{J^2}\sum_{n=1}^{M}\sum_{j=1}^{J}\left(\|\nabla\boldsymbol{e}_{j,\boldsymbol{R}}^n\|^2+\|\nabla\boldsymbol{\epsilon}_{j,\boldsymbol{R}}^n\|^2\right)$$
$$\leq\frac{CC_R^2}{\gamma^2}exp\left(\frac{CC_*^2}{\alpha_{min}}+\frac{C\Delta t}{h^3\alpha_{min}}\right)\left(\Delta t\sum_{n=0}^{M-1}\sum_{j=1}^{J}\left(\|q_{j,h}^{n+1}-\hat{q}_{j,h}^n\|^2+\|\lambda_{j,h}^{n+1}-\hat{\lambda}_{j,h}^n\|^2\right)\right).\tag{2.48}$$

Finally, apply triangle and Young's inequalities on

$$\|\nabla<\boldsymbol{v}_h>^n-\nabla<\hat{\boldsymbol{v}}_h>^n\|^2+\|\nabla<\boldsymbol{w}_h>^n-\nabla<\hat{\boldsymbol{w}}_h>^n\|^2$$

to obtain the desire result.

□

We prove the following Lemma by strong mathematical induction.

Lemma 2.4. *If $\gamma\to\infty$ then there exists a constant C_* which is independent of h, and Δt, such that for sufficiently small h for a fixed mesh and fixed Δt, the solution of the Algorithm 2 satisfies*

$$\max_{0\leq n\leq M}\left\{\|\hat{\boldsymbol{v}}_{j,h}^n\|_\infty,\|\hat{\boldsymbol{w}}_{j,h}^n\|_\infty\right\}\leq C_*,\ \ \textit{for all}\ \ j=1,2,\cdots,J.\tag{2.49}$$

Proof: Basic step: $\hat{\boldsymbol{v}}_{j,h}^0=I_h(\boldsymbol{v}_j^{true}(0,\boldsymbol{x}))$, where I_h is an appropriate interpolation operator. Because of the regularity assumption of $\boldsymbol{v}_j^{true}(0,\boldsymbol{x})$, we have $\|\hat{\boldsymbol{v}}_{j,h}^0\|_\infty\leq C_*$, for some constant $C_*>0$.
Inductive step: Assume for some $L\in\mathbb{N}$ and $L<M$, $\|\hat{\boldsymbol{v}}_{j,h}^n\|_\infty\leq C_*$ holds true for $n=0,1,\cdots,L$. Then, using triangle inequality and Lemma 1.1, we have

$$\|\hat{\boldsymbol{v}}_{j,h}^{L+1}\|_\infty\leq\|\hat{\boldsymbol{v}}_{j,h}^{L+1}-\boldsymbol{v}_{j,h}^{L+1}\|_\infty+C_*.$$

Using Agmon's inequality [38], and discrete inverse inequality, yields

$$\|\hat{\boldsymbol{v}}_{j,h}^{L+1}\|_\infty\leq Ch^{-\frac{3}{2}}\|\hat{\boldsymbol{v}}_{j,h}^{L+1}-\boldsymbol{v}_{j,h}^{L+1}\|+C_*.\tag{2.50}$$

Next, using equation (2.32)

$$\|\hat{\boldsymbol{v}}_{j,h}^{L+1}\|_\infty \leq C_* + \frac{C}{h^{\frac{3}{2}}\gamma^{\frac{1}{2}}} exp\left(CT\left(\frac{C_*^2}{\alpha_{min}} + \frac{\Delta t}{h^3\alpha_{min}}\right)\right)\left(\Delta t\sum_{n=0}^{L}\sum_{j=1}^{J}\left(\|q_{j,h}^{n+1} - \hat{q}_{j,h}^{n}\|^2 + \|\lambda_{j,h}^{n+1} - \hat{\lambda}_{j,h}^{n}\|^2\right)\right)^{\frac{1}{2}}. \quad (2.51)$$

For a fixed mesh, and timestep size, as $\gamma \to \infty$, yields $\|\hat{\boldsymbol{v}}_{j,h}^{L+1}\|_\infty \leq C_*$. Hence, by the principle of strong mathematical induction, $\|\hat{\boldsymbol{v}}_{j,h}^{n}\|_\infty \leq C_*$ holds true for $0 \leq n \leq M$.

Similarly, we can prove the uniform boundedness of $\hat{\boldsymbol{w}}_{j,h}^{n}$.

□

2.3 Numerical Experiments

To test the proposed algorithm and the associated theories, in this section, we present results of numerical experiments. We use $J = 20$ realizations, with an index of $j = 1, 2, \cdots, J$ in all experiments through out this thesis.

For MHD simulations, it is crucial to enforce the solenoidal constraint $\nabla \cdot \boldsymbol{B}_{j,h} = 0$ strongly, otherwise, it can produce large errors in the solution [9, 32]. Thus, it is popular to use pointwise divergence-free element such as (P_2, P_1^{disc}) Scott-Vogelius (SV) elements on barycenter refined regular triangular meshes to enforce the divergence constraints [1, 19, 25, 36, 37]. However, using the SV element requires higher degrees of freedom which increases the computational complexity. To overcome this issue, the proposed Algorithms have a feature to use grad-div stabilization parameter which allows us to use weakly divergence-free element without reducing the accuracy of the solutions [10, 15] with the appropriate choice of the parameter [21]. Thus, we will use stable weakly divergence-free Taylor-hood (TH) element (P_2, P_1) for the velocity-pressure and magnetic field-magnetic pressure pairs on regular unstructured triangular mesh with grad-div stabilization parameter $\gamma = 10^5$. To estimate the viscosity parameters ν, and ν_m, we draw an independent sample of size $J = 20$ from a uniform distribution for each parameter.

2.3.1 Convergence Rate Verification

We will begin this experiment with the following manufactured analytical functions,

$$\boldsymbol{v} = \begin{pmatrix} \cos y + (1+e^t)\sin y \\ \sin x + (1+e^t)\cos x \end{pmatrix},\ \boldsymbol{w} = \begin{pmatrix} \cos y - (1+e^t)\sin y \\ \sin x - (1+e^t)\cos x \end{pmatrix},\ p = \sin(x+y)(1+e^t),\ \text{and}\ \lambda = 0. \quad (2.52)$$

For clarity, $\nabla \cdot \boldsymbol{v} = \nabla \cdot \boldsymbol{w} = 0$. Next, by introducing a perturbation parameter ϵ we introduce noise in the above analytical functions as below to create manufactured solutions of (1.11)-(1.13)

$$\boldsymbol{v}_j(\boldsymbol{x},t) := (1+k_j\epsilon)\,\boldsymbol{v},\ \boldsymbol{w}_j(\boldsymbol{x},t) := (1+k_j\epsilon)\,\boldsymbol{w},\ p_j := (1+k_j\epsilon)p,\ \text{and}\ \lambda_j := 0, \quad (2.53)$$

where $k_j = (-1)^{j+1}\lceil j/2 \rceil/5$, and $j = 1, 2, \cdots, 20$. We consider the kinematic viscosity ν and magnetic diffusivity ν_m are continuous random variables with uniform distribution. In this experiment, we consider $\nu \sim \mathcal{U}(0.0009, 0.0011)$ with $E[\nu] = 0.001$, $\nu \sim \mathcal{U}(0.009, 0.011)$ with $E[\nu] = 0.01$, and $\nu_m \sim \mathcal{U}(0.0009, 0.0011)$ with $E[\nu_m] = 0.001$. For each of the cases, we collect a i.i.d sample size of 20 which leads us to have two two-dimensional random samples. For a fixed j together with pair $(\nu_j, \nu_{m,j})$, and the analytical solution in (2.53), we compute the forcing functions as follows:

$$\begin{aligned} \boldsymbol{f}_{1,j} &= \boldsymbol{v}_{j,t} + \boldsymbol{w}_j \cdot \nabla \boldsymbol{v}_j - \frac{\nu_j + \nu_{m,j}}{2}\Delta \boldsymbol{v}_j - \frac{\nu_j - \nu_{m,j}}{2}\Delta \boldsymbol{w}_j + \nabla q_j, \\ \boldsymbol{f}_{2,j} &= \boldsymbol{w}_{j,t} + \boldsymbol{v}_j \cdot \nabla \boldsymbol{w}_j - \frac{\nu_j + \nu_{m,j}}{2}\Delta \boldsymbol{w}_j - \frac{\nu_j - \nu_{m,j}}{2}\Delta \boldsymbol{v}_j + \nabla r_j. \end{aligned}$$

We consider a domain $\Omega = (0,1)^2$, boundary conditions $\boldsymbol{v}_{j,h}|_{\partial\Omega} = \boldsymbol{v}_j$, and $\boldsymbol{w}_{j,h}|_{\partial\Omega} = \boldsymbol{w}_j$, and use $\boldsymbol{v}^0_{j,h} = \boldsymbol{v}_j(\boldsymbol{x},0)$, and $\boldsymbol{w}^0_{j,h} = \boldsymbol{w}_j(\boldsymbol{x},0)$ as the first timestep initial condition and use them to generate a second initial condition $\boldsymbol{v}^1_{j,h}$, and $\boldsymbol{w}^1_{j,h}$ for $t = \Delta t$. Using the Algorithm 1, we compute the ensemble average solution $(<\boldsymbol{v}_h>^n, <\boldsymbol{w}_h>^n)$ at $t = t^n$ compare with the true ensemble average solution $(<\boldsymbol{v}(t^n)>, <\boldsymbol{w}(t^n)>)$. For all j, we run the simulations and compute the ensemble average of the solutions, use it for further simulations.

For $\boldsymbol{z} = \boldsymbol{v}$ or $\boldsymbol{w}$, we define the error as $<\boldsymbol{e_z}> := <\boldsymbol{z}> - <\boldsymbol{z}_h>$ and compute

$$\|<\boldsymbol{e_z}>\|_{2,1} := \|<\boldsymbol{e_z}>\|_{L^2(0,T;H^1(\Omega)^d)}.$$

To receive the temporal convergence, we use a fixed mesh width of $h = 1/64$, end time $T = 1$, vary timestep size as $\Delta t = T/4, T/8, T/16, T/32$, and $T/64$, on the other hand, to get the spatial convergence, we use a small end time $T = 0.001$, a fixed timestep size $\Delta t = T/8$, vary mesh width as $h = 1/4, 1/8, 1/16, 1/32$, and $1/64$. For both cases, we run the simulations using the proposed Algorithm 1 varying the perturbation parameter ϵ (which introduce noise in the initial, and boundary conditions

and forcing functions), and the two two-dimensional random samples $\{(\nu_j, \nu_{m,j}) \in [0.0009, 0.0011] \times [0.0009, 0.0011]\}$ and $\{(\nu_j, \nu_{m,j}) \in [0.009, 0.011] \times [0.0009, 0.0011]\}$, where $j = 1, 2, \cdots, 20$.

Then, we record the errors, compute the convergence rates, and present them in Tables (2.1) to (2.6). In Tables (2.1) to (2.3), we observe the second order temporal convergence which is an excellent agreement with the theoretical claim, and in Tables (2.4) to (2.6) we observe a second order spatial convergence which is also consistent with the theory as we have used (P_2, P_1) element.

We append Tables 2.1 to 2.6 to provide the temporal and spatial convergence at various ϵ values.

Table 2.1: SPP-Scheme: Temporal errors and convergence rates for $\boldsymbol{v}$ and $\boldsymbol{w}$ with $\epsilon = 0.0$. The left-hand side tables are utilizing a $\gamma = 10^6$ while the right-hand side tables are utilizing a $\gamma = 1000$.

Temporal convergence (fixed $h = 1/64$, $T = 1$) with $j = 1, 2, \cdots, 20$								
$\epsilon = 0.0$	$\{(\nu_j, \nu_{m,j}) \in [0.0009, 0.0011] \times [0.0009, 0.0011]\}$				$\{(\nu_j, \nu_{m,j}) \in [0.009, 0.011] \times [0.0009, 0.0011]\}$			
Δt	$\|<\boldsymbol{e_v}>\|_{2,1}$	rate	$\|<\boldsymbol{e_w}>\|_{2,1}$	rate	$\|<\boldsymbol{e_v}>\|_{2,1}$	rate	$\|<\boldsymbol{e_w}>\|_{2,1}$	rate
$\frac{T}{4}$	9.9868e-01		7.7220e-01		5.2665e-01		4.5646e-01	
$\frac{T}{8}$	4.8885e-01	1.03	3.7913e-01	1.03	3.0570e-01	0.78	2.7844e-01	0.71
$\frac{T}{16}$	2.4218e-01	1.01	1.8806e-01	1.01	1.7439e-01	0.81	1.6337e-01	0.77
$\frac{T}{32}$	1.2062e-01	1.01	9.3749e-02	1.00	9.4094e-02	0.89	8.9479e-02	0.87
$\frac{T}{64}$	6.0175e-02	1.00	4.6772e-02	1.00	4.7543e-02	0.98	4.5659e-02	0.97

Table 2.2: SPP-Scheme: Temporal errors and convergence rates for $\boldsymbol{v}$ and $\boldsymbol{w}$ with $\epsilon = 0.001$. The left-hand side tables are utilizing a $\gamma = 10^6$ while the right-hand side tables are utilizing a $\gamma = 1000$.

Temporal convergence (fixed $h = 1/64$, $T = 1$) with $j = 1, 2, \cdots, 20$								
$\epsilon = 0.001$	$\{(\nu_j, \nu_{m,j}) \in [0.0009, 0.0011] \times [0.0009, 0.0011]\}$				$\{(\nu_j, \nu_{m,j}) \in [0.009, 0.011] \times [0.0009, 0.0011]\}$			
Δt	$\|<\boldsymbol{e_v}>\|_{2,1}$	rate	$\|<\boldsymbol{e_w}>\|_{2,1}$	rate	$\|<\boldsymbol{e_v}>\|_{2,1}$	rate	$\|<\boldsymbol{e_w}>\|_{2,1}$	rate
$\frac{T}{4}$	9.9696e-01		7.6768e-01		5.2627e-01		4.5578e-01	
$\frac{T}{8}$	4.8837e-01	1.03	3.7790e-01	1.02	3.0550e-01	0.78	2.7814e-01	0.71
$\frac{T}{16}$	2.4206e-01	1.01	1.8773e-01	1.01	1.7429e-01	0.81	1.6324e-01	0.77
$\frac{T}{32}$	1.2058e-01	1.01	9.3659e-02	1.00	9.4045e-02	0.89	8.9417e-02	0.87
$\frac{T}{64}$	6.0164e-02	1.00	4.6742e-02	1.00	4.7513e-02	0.99	4.5624e-02	0.97

Table 2.3: SPP-Scheme: Temporal errors and convergence rates for $\boldsymbol{v}$ and $\boldsymbol{w}$ with $\epsilon = 0.01$. The left-hand side tables are utilizing a $\gamma = 5 * 10^6$ while the right-hand side tables are utilizing a $\gamma = 500$.

Temporal convergence (fixed $h = 1/64$, $T = 1$) with $j = 1, 2, \cdots, 20$								
$\epsilon = 0.01$	$\{(\nu_j, \nu_{m,j}) \in [0.0009, 0.0011] \times [0.0009, 0.0011]\}$				$\{(\nu_j, \nu_{m,j}) \in [0.009, 0.011] \times [0.0009, 0.0011]\}$			
Δt	$\|<\boldsymbol{e_v}>\|_{2,1}$	rate	$\|<\boldsymbol{e_w}>\|_{2,1}$	rate	$\|<\boldsymbol{e_v}>\|_{2,1}$	rate	$\|<\boldsymbol{e_w}>\|_{2,1}$	rate
$\frac{T}{4}$	8.7552e-01		5.5278e-01		4.9256e-01		4.0207e-01	
$\frac{T}{8}$	4.5127e-01	0.96	3.0317e-01	0.87	2.8613e-01	0.78	2.5118e-01	0.68
$\frac{T}{16}$	2.3237e-01	0.96	1.6389e-01	0.89	1.6344e-01	0.81	1.4997e-01	0.74
$\frac{T}{32}$	1.1917e-01	0.96	8.6968e-02	0.91	8.7809e-02	0.90	8.2699e-02	0.86
$\frac{T}{64}$	6.1127e-02	0.96	4.5461e-02	0.94	4.3426e-02	1.02	4.1739e-02	0.99

Table 2.4: SPP-Scheme: Spatial errors and convergence rates for $\boldsymbol{v}$ and $\boldsymbol{w}$ with $\epsilon = 0.0$, and $\gamma = 10^6$.

Spatial convergence (fixed $T = 0.001$, $\Delta t = T/8$) with $j = 1, 2, \cdots, 20$								
$\epsilon = 0.0$	$\{(\nu_j, \nu_{m,j}) \in [0.0009, 0.0011] \times [0.0009, 0.0011]\}$				$\{(\nu_j, \nu_{m,j}) \in [0.009, 0.011] \times [0.0009, 0.0011]\}$			
h	$\|<\boldsymbol{e_v}>\|_{2,1}$	rate	$\|<\boldsymbol{e_w}>\|_{2,1}$	rate	$\|<\boldsymbol{e_v}>\|_{2,1}$	rate	$\|<\boldsymbol{e_w}>\|_{2,1}$	rate
$\frac{1}{4}$	1.1422e-04		2.1889e-04		1.1422e-04		2.1889e-04	
$\frac{1}{8}$	2.8712e-05	1.99	5.4683e-05	2.00	2.8712e-05	1.99	5.4683e-05	2.00
$\frac{1}{16}$	7.1879e-06	2.00	1.3669e-05	2.00	7.1879e-06	2.00	1.3669e-05	2.00
$\frac{1}{32}$	1.7989e-06	2.00	3.4177e-06	2.00	1.7988e-06	2.00	3.4176e-06	2.00
$\frac{1}{64}$	4.6009e-07	1.97	8.5915e-07	1.99	4.5706e-07	1.98	8.5798e-07	1.99

Table 2.5: SPP-Scheme: Spatial errors and convergence rates for $\boldsymbol{v}$ and $\boldsymbol{w}$ with $\epsilon = 0.001$, and $\gamma = 10^6$.

Spatial convergence (fixed $T = 0.001$, $\Delta t = T/8$) with $j = 1, 2, \cdots, 20$								
$\epsilon = 0.001$	$\{(\nu_j, \nu_{m,j}) \in [0.0009, 0.0011] \times [0.0009, 0.0011]\}$				$\{(\nu_j, \nu_{m,j}) \in [0.009, 0.011] \times [0.0009, 0.0011]\}$			
h	$\|<\boldsymbol{e_v}>\|_{2,1}$	rate	$\|<\boldsymbol{e_w}>\|_{2,1}$	rate	$\|<\boldsymbol{e_v}>\|_{2,1}$	rate	$\|<\boldsymbol{e_w}>\|_{2,1}$	rate
$\frac{1}{4}$	1.1422e-04		2.1889e-04		1.1422e-04		2.1889e-04	
$\frac{1}{8}$	2.8712e-05	1.99	5.4683e-05	2.00	2.8712e-05	1.99	5.4683e-05	2.00
$\frac{1}{16}$	7.1879e-06	2.00	1.3669e-05	2.00	7.1879e-06	2.00	1.3669e-05	2.00
$\frac{1}{32}$	1.7989e-06	2.00	3.4177e-06	2.00	1.7988e-06	2.00	3.4176e-06	2.00
$\frac{1}{64}$	4.6012e-07	1.97	8.5920e-07	1.99	4.5695e-07	1.98	8.5796e-07	1.99

Table 2.6: SPP-Scheme: Spatial errors and convergence rates for $\boldsymbol{v}$ and $\boldsymbol{w}$ with $\epsilon = 0.01$, and $\gamma = 10^6$.

Spatial convergence (fixed $T = 0.001$, $\Delta t = T/8$) with $j = 1, 2, \cdots, 20$								
$\epsilon = 0.01$	$\{(\nu_j, \nu_{m,j}) \in [0.0009, 0.0011] \times [0.0009, 0.0011]\}$				$\{(\nu_j, \nu_{m,j}) \in [0.009, 0.011] \times [0.0009, 0.0011]\}$			
h	$\|<\boldsymbol{e_v}>\|_{2,1}$	rate	$\|<\boldsymbol{e_w}>\|_{2,1}$	rate	$\|<\boldsymbol{e_v}>\|_{2,1}$	rate	$\|<\boldsymbol{e_w}>\|_{2,1}$	rate
$\frac{1}{4}$	1.1422e-04		2.1889e-04		1.1422e-04		2.1889e-04	
$\frac{1}{8}$	2.8712e-05	1.99	5.4683e-05	2.00	2.8712e-05	1.99	5.4683e-05	2.00
$\frac{1}{16}$	7.1882e-06	2.00	1.3669e-05	2.00	7.1882e-06	2.00	1.3669e-05	2.00
$\frac{1}{32}$	1.8012e-06	2.00	3.4189e-06	2.00	1.8010e-06	2.00	3.4188e-06	2.00
$\frac{1}{64}$	4.7631e-07	1.92	8.6788e-07	1.98	4.7252e-07	1.93	8.6622e-07	1.98

2.3.2 Channel Flow over a Step Problem

We will now demonstrate Algorithm 2 within a two dimensional channel flow past a unit step under the influence of a magnetic field within figures (2.1) to (2.2). The domain of the flow is a 30×10 rectangular channel over a 1×1 step on the lower wall, five units away from the inflow. We implement boundary conditions for $\boldsymbol{u}$ and $\boldsymbol{B}$ corresponding to the no slip velocity conditions. Figures(2.1)-(2.2) will run utilizing a $T = 40$ with a timestep of $\Delta t = 0.05$. The simulations will be utilizing a constant coupling parameter $s = 0.001$, stabilization parameter $\gamma = 100000$, mean kinematic viscosity $E[\nu] = 0.001$ for a random sample with distribution $\nu \sim \mathcal{U}(0.0009, 0.0011)$, and mean magnetic diffusivity $E[\nu_m] = 0.01$ for a random sample with the distribution $\nu_m \sim \mathcal{U}(0.009, 0.011)$. The solutions from Algorithm 1 will be denoted as "Usual MHD". The no slip boundary condition is prescribed for the velocity and $B =< 0, 1 >^T$ is enforced for the magnetic field on the walls. At the inflow, we set $u =< y(10 - y)/25, 0 >^T$ and $B =< 0, 1 >^T$, and the outflow condition uses a channel extension of 10 units, and at the end of the extension, we set outflow velocity and magnetic field equal to their counterpart in the inflow. For our simulation we will be utilizing a $u_0 :=< y(10 - y)/25, 0 >^T$ and $B_0 :=< 0, 1 >^T$ as initial conditions. A triangular unstructured mesh of the domain that provides a total of $419,058$ degrees of freedom (dof) is considered, where velocity dof $= 186,134$, magnetic field dof $= 186,134$, pressure dof $= 23,395$, and magnetic pressure dof $= 23,395$.

Following a similar idea from [33], we will be considering outflow boundary conditions $\partial\Omega = \Gamma_1 \cup \Gamma_2$ with velocity boundary conditions $\boldsymbol{u}|_{\Gamma_1} = 0$ and $(-\nu\nabla\boldsymbol{u} + pI) \cdot n|_{\Gamma_2} = 0$. We will change the definition of the velocity space such that:

$$\boldsymbol{X}_h = \{\boldsymbol{v}_h \in \boldsymbol{\mathcal{P}}_k(\mathcal{T}_h) \cap \boldsymbol{H}^1(\Omega),\ \boldsymbol{v}_h|_{\Gamma_1} = 0\},$$

We will also implement the natural boundary condition $\big((-\nu\nabla\boldsymbol{u}_h^{n+1} - \gamma(\nabla \cdot \boldsymbol{u}_h^{n+1})I) \cdot n\big)|_{\Gamma_2} = 0$ in step 1 and step 3 by dropping the resulting integral within the formulation. We will also implement the Dirichlet condition $p_h^{n+1}|_{\Gamma_2} = 0$ in step 2 and step 4, and change this velocity space to:

$$\boldsymbol{Y}_h = \{\boldsymbol{v}_h \in \boldsymbol{\mathcal{P}}_k(\mathcal{T}_h) \cap \boldsymbol{H}^1(\Omega),\ \boldsymbol{v}_h \cdot n|_{\Gamma_1} = 0\}.$$

Fig. 2.1: A comparison for the velocity ensemble average solutions between the SPP-FEM algorithm (left hand side), and the preliminary BE-MHD algorithm (right hand side). Both algorithms are shown at $T = 40$ with an $E[\nu_j] = 0.001$ and $E[\nu_{m,j}] = 0.01$ for MHD channel flow over a step.

SPP-FEM

BE-MHD

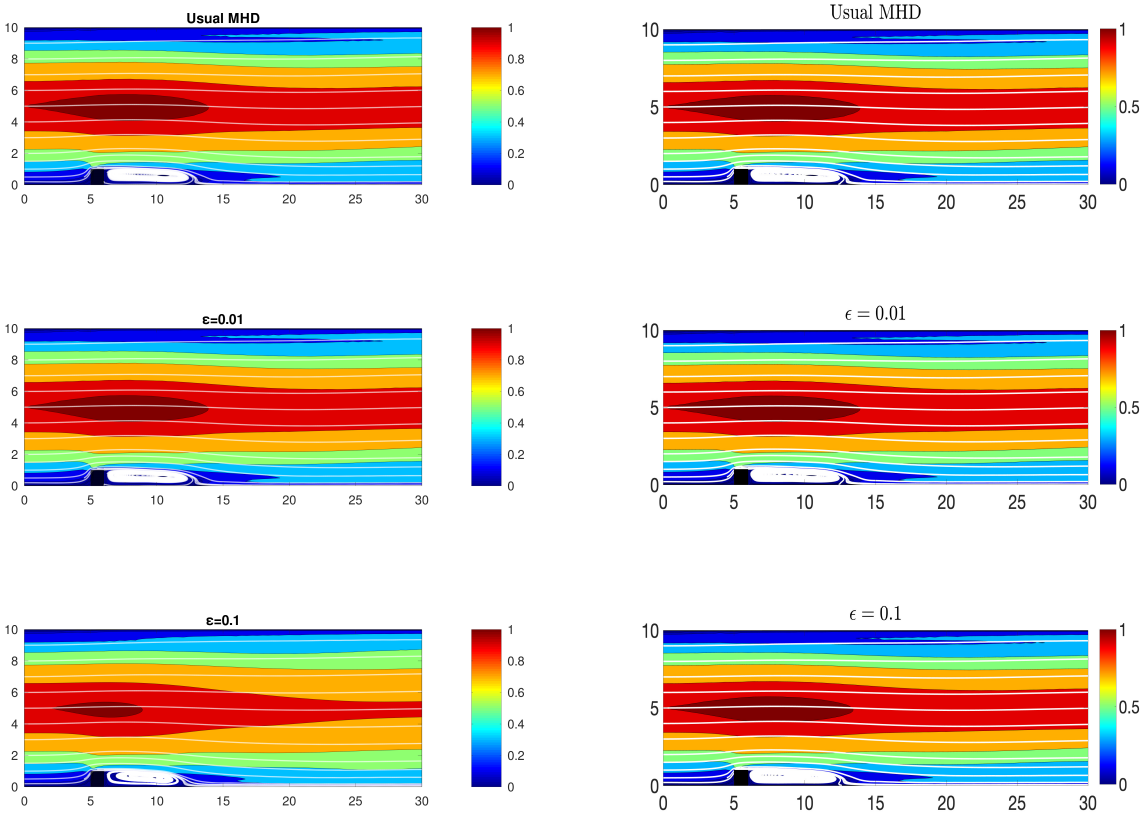

Fig. 2.2: A comparison for the magnetic field ensemble average solutions between the SPP-FEM algorithm (left hand side), and the preliminary BE-MHD algorithm (right hand side). Both algorithms are shown at $T = 40$ with an $E[\nu_j] = 0.001$ and $E[\nu_{m,j}] = 0.01$ for MHD channel flow over a step.

SPP-FEM

BE-MHD

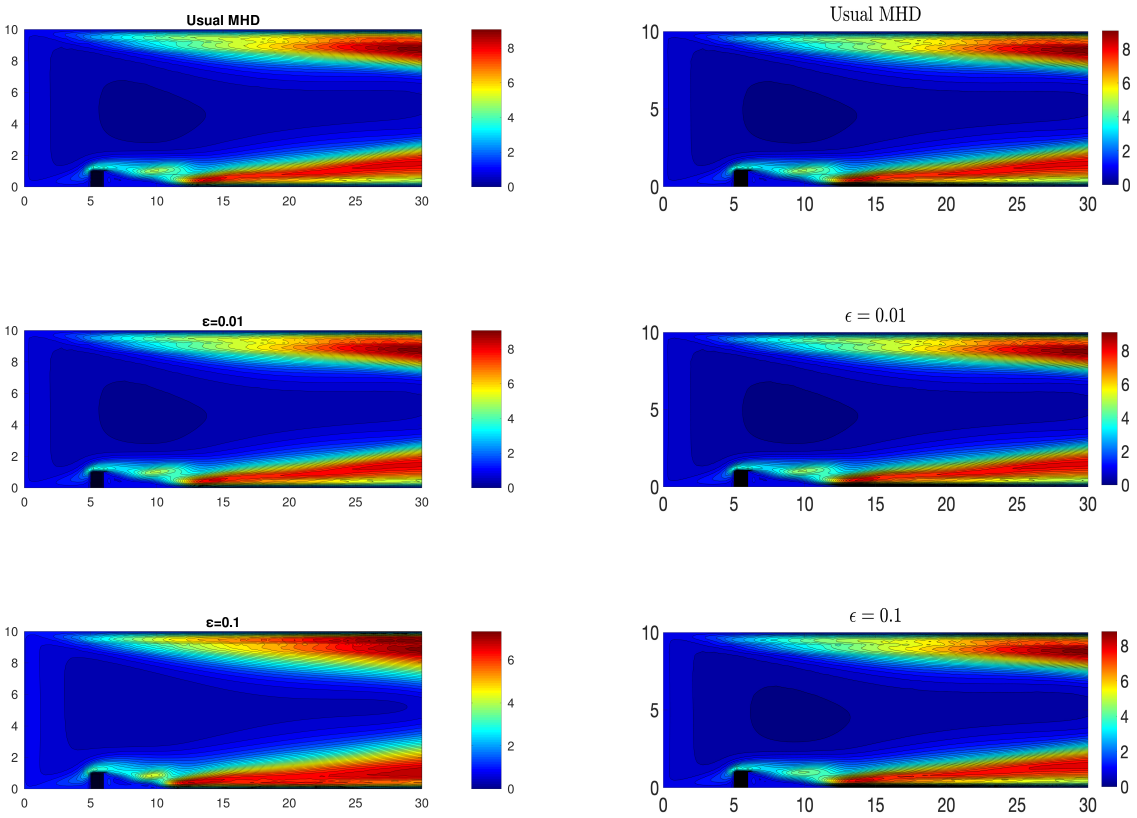

2.3.3 Lid-driven Cavity

We now consider a 2D benchmark regularized lid-driven cavity problem [4, 16, 27] with a domain $\Omega = (-1, 1)^2$. No-slip boundary conditions are applied to all sides excluding the lid of the cavity located at the top of the simulation. We will impose

$$\boldsymbol{u}_j = \left(1 + \frac{(-1)^{j+1}\lceil j/2 \rceil}{5}\epsilon\right)\begin{pmatrix}(1-x^2)^2\\0\end{pmatrix}.$$

For the magnetic field boundary conditions, we assign

$$\boldsymbol{B}_j = \left(1 + \frac{(-1)^{j+1}\lceil j/2 \rceil}{5}\epsilon\right)\begin{pmatrix}0\\1\end{pmatrix}.$$

on all sides. The generated computational mesh of the domain provides a total of 729,840 degrees of freedom (dof), where velocity dof $= 324,266$, magnetic field dof $= 324,266$, pressure dof $= 40,654$, and magnetic pressure dof $= 40,654$. With the absence of any magnetic field or external sources at the beginning of the simulation, the flow initiates in a state of rest.

To study the long-time unsteady flow behavior, we first validate our computation with available data from literature [16]. To initiate the process, we commence by conducting a simulation without the magnetic field (by setting $s = 0$ in the model) while maintaining the Reynolds number $Re = 15000$. This implies that there are no perturbations in the viscosities, and the initial and boundary conditions remain unchanged. The maximum velocity of the lid is 1 and the characteristic length is 2, therefore we must define the viscosity $\nu = 2/Re$. We run the simulation with time-step size $\Delta t = 5$ until the simulation finishes at $T = 600$. The Fig.2.3 illustrates the presence of a prominent primary vortex located at the center of the cavity. Additionally, there are two smaller vortices observed near the bottom corners, as well as a minuscule vortex situated at the upper left corner.

All simulations ran will utilize a chosen coupling parameter s with a fixed $\epsilon = 0.01$ and can be seen in Figures 2.4 to 2.5.

Fig. 2.3: A regularized lid driven cavity problem showing the velocity strength with streamlines over speed contours for $Re = 15000$ using coupling parameter $s = 0.0$.

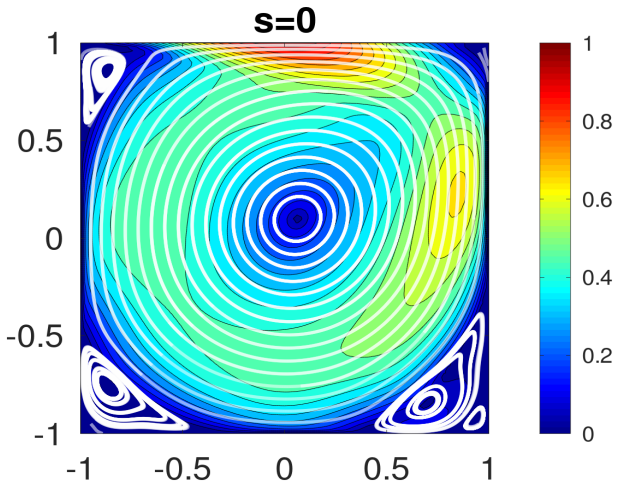

Fig. 2.4: A regularized lid driven cavity problem showing the velocity strength with streamlines over speed contours for random $Re \in [13636.36, 16666.67]$ at $T = 600$ using various coupling parameter s values.

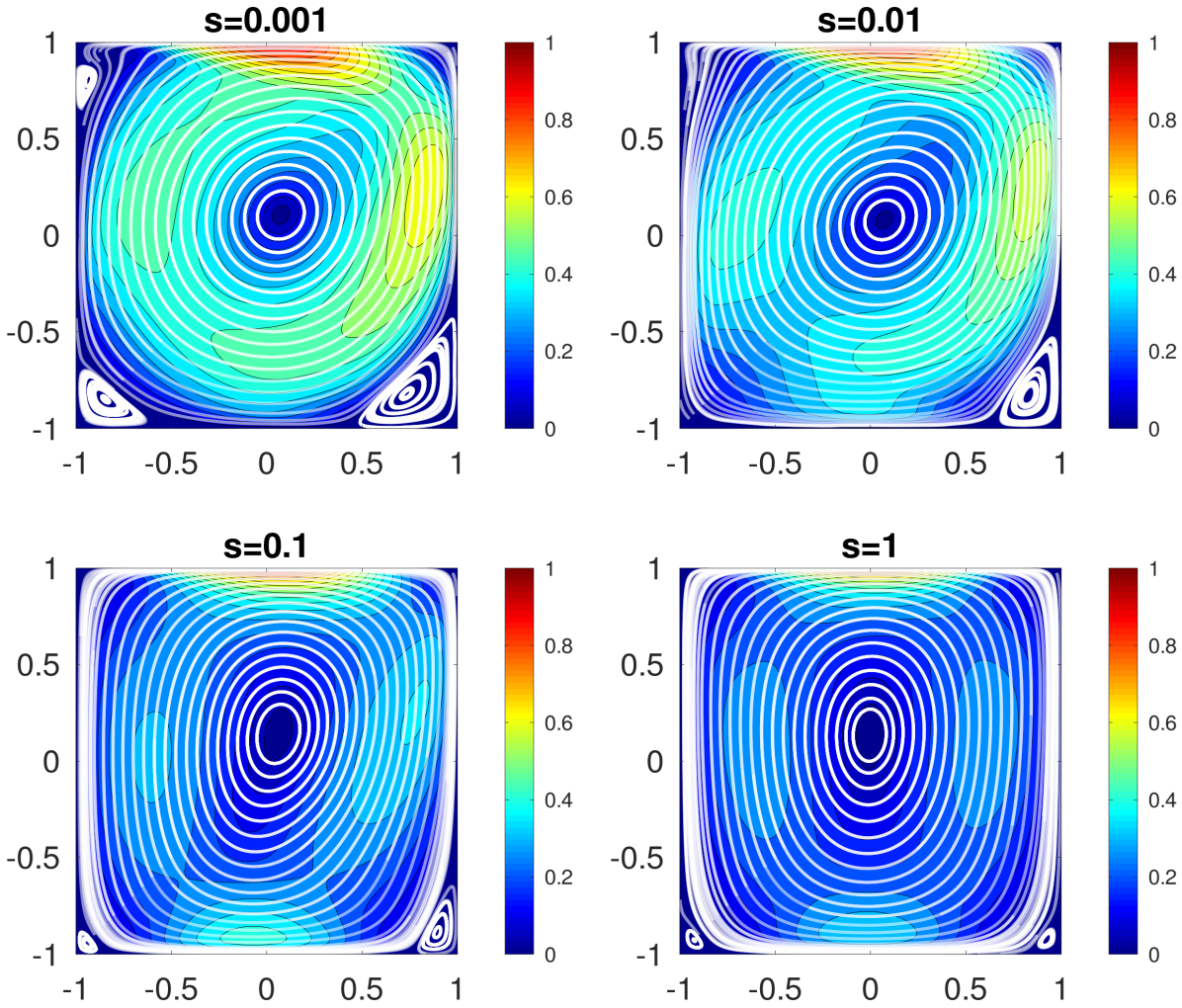

Fig. 2.5: A regularized lid driven cavity problem showing the magnetic field solution with streamlines over speed contours for random $Re \in [13636.36, 16666.67]$ at $T = 600$ using various s values.

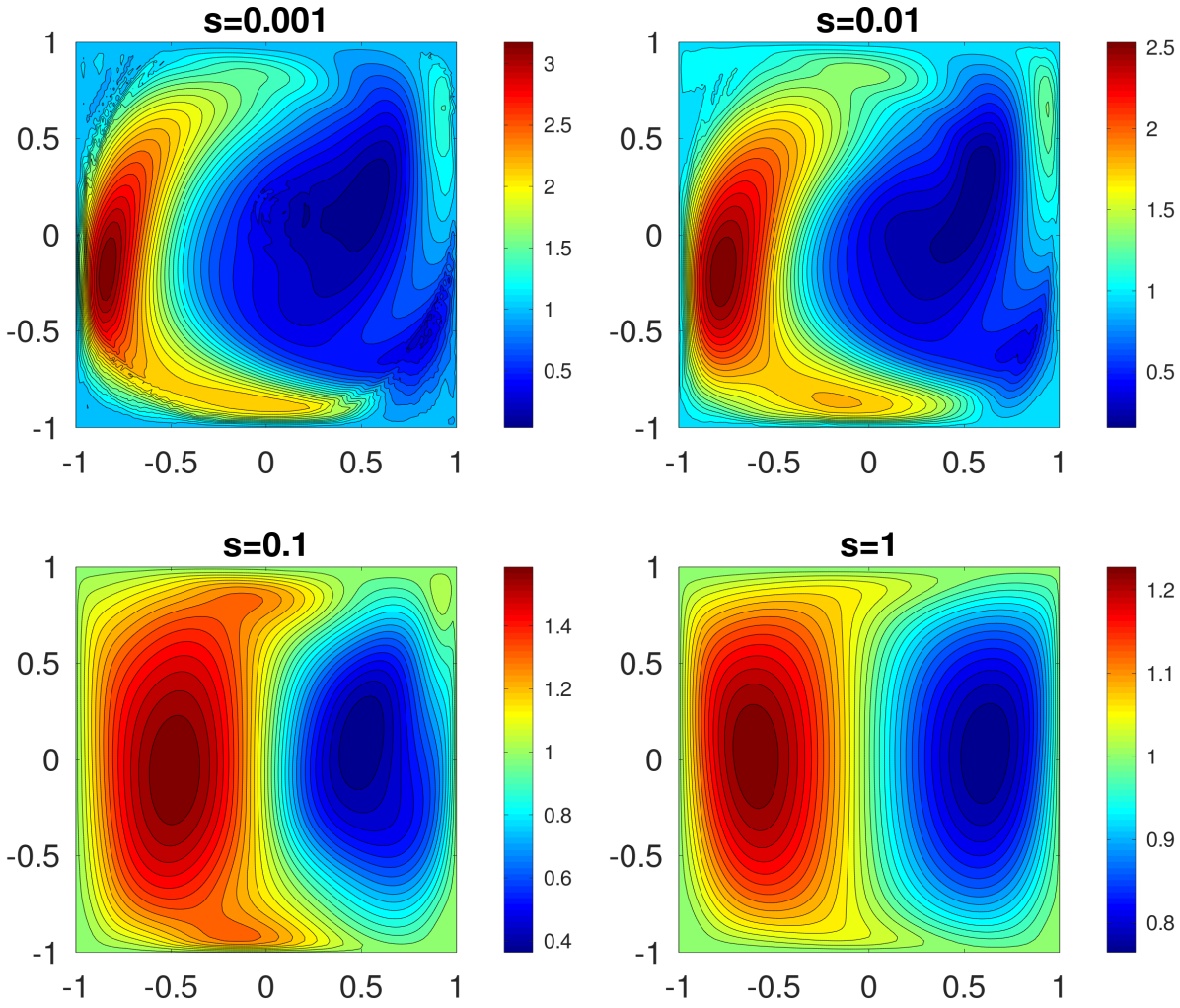

3 Implicit-Explicit Second Order Time-stepping Ensemble Scheme

We suppress the spatial discretization momentarily to keep the focus on the main idea. We consider a uniform time-step size Δt and let $t^n = n\Delta t$ for $n = 0, 1, \cdots$, then computing the J solutions independently, it takes the following form:

Step 1: For $j = 1, \cdots, J$,

$$\begin{aligned}\frac{3\boldsymbol{v}_{j,h}^{n+1}}{2\Delta t} + <\boldsymbol{w}>^n \cdot\nabla\boldsymbol{v}_{j,h}^{n+1} - \frac{\bar{\nu}+\bar{\nu}_m}{2}\Delta\boldsymbol{v}_{j,h}^{n+1} + \gamma\nabla(\nabla\cdot\boldsymbol{v}_{j,h}^{n+1}) + \nabla q_{j,h}^{n+1} = \boldsymbol{f}_{1,j}(t^{n+1})\\ + \frac{4\boldsymbol{v}_{j,h}^{n} - \boldsymbol{v}_{j,h}^{n-1}}{2\Delta t} - \boldsymbol{w}_{j,h}^{'n}\cdot\nabla(2\boldsymbol{v}_{j,h}^{n} - \boldsymbol{v}_{j,h}^{n-1}) + \frac{\nu_{j,h}^{'} + \nu_{m,j}^{'}}{2}\Delta(2\boldsymbol{v}_{j,h}^{n} - \boldsymbol{v}_{j,h}^{n-1})\\ + (1-\theta)\frac{\nu_{j,h}-\nu_{m,j}}{2}\Delta\boldsymbol{w}_{j,h}^{n} + \theta\frac{\nu_{j,h}-\nu_{m,j}}{2}\Delta(2\boldsymbol{w}_{j,h}^{n} - \boldsymbol{w}_{j,h}^{n-1}),\end{aligned} \tag{3.1}$$

$$\nabla\cdot\boldsymbol{v}_{j,h}^{n+1} = 0. \tag{3.2}$$

Step 2: For $j = 1, \cdots, J$,

$$\begin{aligned}\frac{3\boldsymbol{w}_{j,h}^{n+1}}{2\Delta t} + <\boldsymbol{v}>^n \cdot\nabla\boldsymbol{w}_{j,h}^{n+1} - \frac{\bar{\nu}+\bar{\nu}_m}{2}\Delta\boldsymbol{w}_{j,h}^{n+1} + \gamma\nabla(\nabla\cdot\boldsymbol{w}_{j,h}^{n+1}) + \nabla r_{j,h}^{n+1} = \boldsymbol{f}_{2,j}(t^{n+1})\\ + \frac{4\boldsymbol{w}_{j,h}^{n} - \boldsymbol{w}_{j,h}^{n-1}}{2\Delta t} - \boldsymbol{v}_{j,h}^{'n}\cdot\nabla(2\boldsymbol{w}_{j,h}^{n} - \boldsymbol{w}_{j,h}^{n-1}) + \frac{\nu_{j,h}^{'} + \nu_{m,j}^{'}}{2}\Delta(2\boldsymbol{w}_{j,h}^{n} - \boldsymbol{w}_{j,h}^{n-1})\\ + (1-\theta)\frac{\nu_{j,h}-\nu_{m,j}}{2}\Delta\boldsymbol{v}_{j,h}^{n} + \theta\frac{\nu_{j,h}-\nu_{m,j}}{2}\Delta(2\boldsymbol{v}_{j,h}^{n} - \boldsymbol{v}_{j,h}^{n-1}),\end{aligned} \tag{3.3}$$

$$\nabla\cdot\boldsymbol{w}_{j,h}^{n+1} = 0. \tag{3.4}$$

Here, $\boldsymbol{v}_{j,h}^n, \boldsymbol{w}_{j,h}^n, q_{j,h}^n$, and $r_{j,h}^n$ denote approximations of $\boldsymbol{v}_j(\cdot,t^n), \boldsymbol{w}_j(\cdot,t^n), q_j(\cdot,t^n)$, and $r_j(\cdot,t^n)$, respectively. The ensemble average and fluctuation about the ensemble average are defined as follows:

$$\left.\begin{aligned} <\boldsymbol{z}>^n &:= \frac{1}{J}\sum_{j=1}^{J}(2\boldsymbol{z}_j^n - \boldsymbol{z}_j^{n-1}), \quad \boldsymbol{z}_j^{'n} := 2\boldsymbol{z}_j^n - \boldsymbol{z}_j^{n-1} - <\boldsymbol{z}>^n,\\ \bar{\nu} &:= \frac{1}{J}\sum_{j=1}^{J}\nu_j, \quad \nu_j^{'} := \nu_j - \bar{\nu},\\ \bar{\nu}_m &:= \frac{1}{J}\sum_{j=1}^{J}\nu_{m,j}, \quad \nu_{m,j}^{'} := \nu_{m,j} - \bar{\nu}_m. \end{aligned}\right\} \tag{3.5}$$

We observe, at time $t = t^{n+1}$, the sub-problem (3.1)-(3.2) has unknowns $\boldsymbol{v}_{j,h}^{n+1}$, and $q_{j,h}^{n+1}$ and on the other hand, the sub-problem (3.3)-(3.4) has unknowns $\boldsymbol{w}_{j,h}^{n+1}$, and $r_{j,h}^{n+1}$. Thus, the two sub-problems are decoupled and can be solved simultaneously. Moreover, the coefficient of each unknown in the two sub-problems does not depend on j, which allows having the same system matrix for all of the

j realizations at each time-step after the finite element assembly. Consequently, we only need to solve a single linear system with J different right-hand-side vectors at each time-step. Therefore, in contrast to solving J different simulations independently, we only need a single LU decomposition or its variant if a direct solver is possible to use and a single preconditioner is needed to build if a block-iterative solver is used. This allows us to reduce a massive computational complexity for simulating convective-dominated MHD ensemble flow problems with low variability.

3.1 Fully Discrete θ-Scheme

Using a finite element spatial discretization, we investigate the proposed decoupled ensemble scheme (3.1)-(3.4) in a fully discrete setting. Following the definitions in (3.5), we define the discrete ensemble average solutions as

$$<\boldsymbol{v}_h>^n := \frac{1}{J}\sum_{j=1}^{J}(2\boldsymbol{v}_{j,h}^n - \boldsymbol{v}_{j,h}^{n-1}), \quad <\boldsymbol{w}_h>^n := \frac{1}{J}\sum_{j=1}^{J}(2\boldsymbol{w}_{j,h}^n - \boldsymbol{w}_{j,h}^{n-1}).$$

The fully discrete, and decoupled time-stepping scheme for computing MHD flow ensembles is defined below.

Algorithm 3: Fully discrete and decoupled second order timestepping ensemble scheme

Given time-step $\Delta t > 0$, end time $T > 0$, grad-div parameter $\gamma > 0$, initial conditions $\boldsymbol{v}_j^0, \boldsymbol{w}_j^0, \boldsymbol{v}_j^1, \boldsymbol{w}_j^1 \in \boldsymbol{H}^2 \cup \boldsymbol{V}$ and $\boldsymbol{f}_{1,j}, \boldsymbol{f}_{2,j} \in L^2\left(0, T; \boldsymbol{H}^{-1}(\Omega)\right)$ for $j = 1, 2, \cdots, J$. We set $M = T/\Delta t$ and for $n = 1, \cdots, M-1$, to compute: Find $\boldsymbol{v}_{j,h}^{n+1} \in \boldsymbol{V}_h$ satisfying, for all $\boldsymbol{\chi}_{j,h} \in \boldsymbol{V}_h$:

$$\begin{aligned}
&\left(\frac{3\boldsymbol{v}_{j,h}^{n+1} - 4\boldsymbol{v}_{j,h}^{n} + \boldsymbol{v}_{j,h}^{n-1}}{2\Delta t}, \boldsymbol{\chi}_{j,h}\right) + b^*\left(< \boldsymbol{w}_h >^n, \boldsymbol{v}_{j,h}^{n+1}, \boldsymbol{\chi}_{j,h}\right) + b^*\left(\boldsymbol{w}_{j,h}^{'n}, 2\boldsymbol{v}_{j,h}^{n} - \boldsymbol{v}_{j,h}^{n-1}, \boldsymbol{\chi}_{j,h}\right) \\
&+ \frac{\bar{\nu} + \bar{\nu}_m}{2}\left(\nabla \boldsymbol{v}_{j,h}^{n+1}, \nabla \boldsymbol{\chi}_{j,h}\right) + \frac{\nu_j^{'} + \nu_{m,j}^{'}}{2}\left(\nabla(2\boldsymbol{v}_{j,h}^{n} - \boldsymbol{v}_{j,h}^{n-1}), \nabla \boldsymbol{\chi}_{j,h}\right) \\
&+ (1-\theta)\frac{\nu_j - \nu_{m,j}}{2}\left(\nabla \boldsymbol{w}_{j,h}^{n}, \nabla \boldsymbol{\chi}_{j,h}\right) + \theta\frac{\nu_j - \nu_{m,j}}{2}\left(\nabla(2\boldsymbol{w}_{j,h}^{n} - \boldsymbol{w}_{j,h}^{n-1}), \nabla \boldsymbol{\chi}_{j,h}\right) \\
&+ \gamma\left(\nabla \cdot \boldsymbol{v}_{j,h}^{n+1}, \nabla \cdot \boldsymbol{\chi}_{j,h}\right) = \left(\boldsymbol{f}_{1,j}(t^{n+1}), \boldsymbol{\chi}_{j,h}\right). \qquad (3.6)
\end{aligned}$$

Find $\boldsymbol{w}_{j,h}^{n+1} \in \boldsymbol{V}_h$ satisfying, for all $\boldsymbol{l}_{j,h} \in \boldsymbol{V}_h$:

$$\begin{aligned}
&\left(\frac{3\boldsymbol{w}_{j,h}^{n+1} - 4\boldsymbol{w}_{j,h}^{n} + \boldsymbol{w}_{j,h}^{n-1}}{2\Delta t}, \boldsymbol{l}_{j,h}\right) + b^*\left(< \boldsymbol{v}_h >^n, \boldsymbol{w}_{j,h}^{n+1}, \boldsymbol{l}_{j,h}\right) + b^*\left(\boldsymbol{v}_{j,h}^{'n}, 2\boldsymbol{w}_{j,h}^{n} - \boldsymbol{w}_{j,h}^{n-1}, \boldsymbol{l}_{j,h}\right) \\
&+ \frac{\bar{\nu} + \bar{\nu}_m}{2}\left(\nabla \boldsymbol{w}_{j,h}^{n+1}, \nabla \boldsymbol{l}_{j,h}\right) + \frac{\nu_j^{'} + \nu_{m,j}^{'}}{2}\left(\nabla(2\boldsymbol{w}_{j,h}^{n} - \boldsymbol{w}_{j,h}^{n-1}), \nabla \boldsymbol{l}_{j,h}\right) \\
&+ (1-\theta)\frac{\nu_j - \nu_{m,j}}{2}\left(\nabla \boldsymbol{v}_{j,h}^{n}, \nabla \boldsymbol{l}_{j,h}\right) + \theta\frac{\nu_j - \nu_{m,j}}{2}\left(\nabla(2\boldsymbol{v}_{j,h}^{n} - \boldsymbol{v}_{j,h}^{n-1}), \nabla \boldsymbol{l}_{j,h}\right) \\
&+ \gamma\left(\nabla \cdot \boldsymbol{w}_{j,h}^{n+1}, \nabla \cdot \boldsymbol{l}_{j,h}\right) = \left(\boldsymbol{f}_{2,j}(t^{n+1}), \boldsymbol{l}_{j,h}\right). \qquad (3.7)
\end{aligned}$$

3.2 Stability Analysis

We now prove stability and well-posedness for the Algorithm 3. To simplify the notation, denote $\alpha_j := \bar{\nu} + \bar{\nu}_m - |\nu_j - \nu_{m,j}|(1+2\theta) - 3|\nu_j^{'} + \nu_{m,j}^{'}| > 0$, for $j = 1, 2, \cdots, J$, which will allow us to choose the biggest possible θ on

$$\frac{\theta}{1+\theta} < \frac{\bar{\nu}}{\bar{\nu}_m} < \frac{1+\theta}{\theta}.$$

Theorem 3.1. *Suppose* $\boldsymbol{f}_{1,j}, \boldsymbol{f}_{2,j} \in L^2\left(0,T;\boldsymbol{H}^{-1}(\Omega)^d\right)$, *and* $\boldsymbol{v}_{j,h}^0$, $\boldsymbol{w}_{j,h}^0 \in \boldsymbol{H}^1(\Omega)d$, *then the solutions to the Algorithm 3 are stable: For* $\Delta t \leq \frac{\alpha_{min}h^2}{C \max\limits_{1\leq j\leq J}\left\{\|\nabla \boldsymbol{v}_{j,h}'^n\|^2, \|\nabla \boldsymbol{w}_{j,h}'^n\|^2\right\}}$, *if* $\alpha_j > 0$

$$
\begin{aligned}
&\|\boldsymbol{v}_{j,h}^M\|^2 + \|2\boldsymbol{v}_{j,h}^M - \boldsymbol{v}_{j,h}^{M-1}\|^2 + \|\boldsymbol{w}_{j,h}^M\|^2 + \|2\boldsymbol{w}_{j,h}^M - \boldsymbol{w}_{j,h}^{M-1}\|^2 \\
&+ \alpha_j \Delta t \sum_{n=2}^{M}\left(\|\nabla \boldsymbol{v}_{j,h}^n\|^2 + \|\nabla \boldsymbol{w}_{j,h}^n\|^2\right) + 4\gamma\Delta t \sum_{n=2}^{M}\left(\|\nabla\cdot \boldsymbol{v}_{j,h}^n\|^2 + \|\nabla\cdot \boldsymbol{w}_{j,h}^n\|^2\right) \\
&\leq \|\boldsymbol{v}_{j,h}^0\|^2 + \|\boldsymbol{w}_{j,h}^0\|^2 + \|2\boldsymbol{v}_{j,h}^1 - \boldsymbol{v}_{j,h}^0\|^2 + \|2\boldsymbol{w}_{j,h}^1 - \boldsymbol{w}_{j,h}^0\|^2 \\
&+ (\bar{\nu} + \bar{\nu}_m)\Delta t\Big(\|\nabla \boldsymbol{v}_{j,h}^1\|^2 + \|\nabla \boldsymbol{w}_{j,h}^1\|^2 + \|\nabla \boldsymbol{v}_{j,h}^0\|^2 + \|\nabla \boldsymbol{w}_{j,h}^0\|^2\Big) \\
&+ \frac{8\Delta t}{\alpha_j}\sum_{n=1}^{M-1}\left(\|\boldsymbol{f}_{1,j}(t^{n+1})\|_{-1}^2 + \|\boldsymbol{f}_{2,j}(t^{n+1})\|_{-1}^2\right).
\end{aligned} \tag{3.8}
$$

Proof: The proof can be considered as 3 steps: In order to get the solution norms, we choose the test functions in the first step, in the second step we find the upper bounds of the terms on the right-hand-side, and then finally we combine the estimates, reduces terms and completes the proof as follows:

First, choose test functions to get solution norms. Choose $\boldsymbol{\chi}_{j,h} = \boldsymbol{v}_{j,h}^{n+1}$ in (3.6), and $\boldsymbol{l}_{j,h} = \boldsymbol{w}_{j,h}^{n+1}$ in (3.7), respectively to obtain

$$
\begin{aligned}
&\left(\frac{3\boldsymbol{v}_{j,h}^{n+1} - 4\boldsymbol{v}_{j,h}^n + \boldsymbol{v}_{j,h}^{n-1}}{2\Delta t}, \boldsymbol{v}_{j,h}^{n+1}\right) + b^*\left(\boldsymbol{w}_{j,h}'^n, 2\boldsymbol{v}_{j,h}^n - \boldsymbol{v}_{j,h}^{n-1}, \boldsymbol{v}_{j,h}^{n+1}\right) + \frac{\bar{\nu}+\bar{\nu}_m}{2}\|\nabla \boldsymbol{v}_{j,h}^{n+1}\|^2 \\
&+ \gamma\|\nabla\cdot \boldsymbol{v}_{j,h}^{n+1}\|^2 = \left(\boldsymbol{f}_{1,j}(t^{n+1}), \boldsymbol{v}_{j,h}^{n+1}\right) - \frac{\nu_j^{'} + \nu_{m,j}^{'}}{2}\left(\nabla(2\boldsymbol{v}_{j,h}^n - \boldsymbol{v}_{j,h}^{n-1}), \nabla \boldsymbol{v}_{j,h}^{n+1}\right) \\
&- (1-\theta)\frac{\nu_j - \nu_{m,j}}{2}\left(\nabla \boldsymbol{w}_{j,h}^n, \nabla \boldsymbol{v}_{j,h}^{n+1}\right) - \theta\frac{\nu_j - \nu_{m,j}}{2}\left(\nabla(2\boldsymbol{w}_{j,h}^n - \boldsymbol{w}_{j,h}^{n-1}), \nabla \boldsymbol{v}_{j,h}^{n+1}\right),
\end{aligned} \tag{3.9}
$$

and

$$
\begin{aligned}
&\left(\frac{3\boldsymbol{w}_{j,h}^{n+1} - 4\boldsymbol{w}_{j,h}^n + \boldsymbol{w}_{j,h}^{n-1}}{2\Delta t}, \boldsymbol{w}_{j,h}^{n+1}\right) + b^*\left(\boldsymbol{v}_{j,h}'^n, 2\boldsymbol{w}_{j,h}^n - \boldsymbol{w}_{j,h}^{n-1}, \boldsymbol{w}_{j,h}^{n+1}\right) + \frac{\bar{\nu}+\bar{\nu}_m}{2}\|\nabla \boldsymbol{w}_{j,h}^{n+1}\|^2 \\
&+ \gamma\|\nabla\cdot \boldsymbol{w}_{j,h}^{n+1}\|^2 = \left(\boldsymbol{f}_{2,j}(t^{n+1}), \boldsymbol{w}_{j,h}^{n+1}\right) - \frac{\nu_j^{'} + \nu_{m,j}^{'}}{2}\left(\nabla(2\boldsymbol{w}_{j,h}^n - \boldsymbol{w}_{j,h}^{n-1}), \nabla \boldsymbol{w}_{j,h}^{n+1}\right) \\
&- (1-\theta)\frac{\nu_j - \nu_{m,j}}{2}\left(\nabla \boldsymbol{v}_{j,h}^n, \nabla \boldsymbol{w}_{j,h}^{n+1}\right) - \theta\frac{\nu_j - \nu_{m,j}}{2}\left(\nabla(2\boldsymbol{v}_{j,h}^n - \boldsymbol{v}_{j,h}^{n-1}), \nabla \boldsymbol{w}_{j,h}^{n+1}\right).
\end{aligned} \tag{3.10}
$$

Using the following identity

$$
(3a - 4b + c, a) = \frac{a^2 + (2a-b)^2}{2} - \frac{b^2 + (2b-c)^2}{2} + \frac{(a-2b+c)^2}{2}, \tag{3.11}
$$

we write

$$\begin{aligned}\frac{1}{4\Delta t}\Big(\|\boldsymbol{v}_{j,h}^{n+1}\|^2-\|\boldsymbol{v}_{j,h}^{n}\|^2+\|2\boldsymbol{v}_{j,h}^{n+1}-\boldsymbol{v}_{j,h}^{n}\|^2-\|2\boldsymbol{v}_{j,h}^{n}-\boldsymbol{v}_{j,h}^{n-1}\|^2+\|\boldsymbol{v}_{j,h}^{n+1}-2\boldsymbol{v}_{j,h}^{n}+\boldsymbol{v}_{j,h}^{n-1}\|^2\Big)\\ +b^*\left(\boldsymbol{w}_{j,h}^{'n},2\boldsymbol{v}_{j,h}^{n}-\boldsymbol{v}_{j,h}^{n-1},\boldsymbol{v}_{j,h}^{n+1}\right)+\frac{\bar{\nu}+\bar{\nu}_m}{2}\|\nabla\boldsymbol{v}_{j,h}^{n+1}\|^2+\gamma\|\nabla\cdot\boldsymbol{v}_{j,h}^{n+1}\|^2\\ =(\boldsymbol{f}_{1,j}(t^{n+1}),v_{j,h}^{n+1})-\frac{\nu_j-\nu_{m,j}}{2}\big((1+\theta)\nabla\boldsymbol{w}_{j,h}^{n}-\theta\nabla\boldsymbol{w}_{j,h}^{n-1},\nabla\boldsymbol{v}_{j,h}^{n+1}\big)\\ -\frac{\nu_j^{'}+\nu_{m,j}^{'}}{2}\left(\nabla(2\boldsymbol{v}_{j,h}^{n}-\boldsymbol{v}_{j,h}^{n-1}),\nabla\boldsymbol{v}_{j,h}^{n+1}\right),\end{aligned}\tag{3.12}$$

and

$$\begin{aligned}\frac{1}{4\Delta t}\Big(\|\boldsymbol{w}_{j,h}^{n+1}\|^2-\|\boldsymbol{w}_{j,h}^{n}\|^2+\|2\boldsymbol{w}_{j,h}^{n+1}-\boldsymbol{w}_{j,h}^{n}\|^2-\|2\boldsymbol{w}_{j,h}^{n}-\boldsymbol{w}_{j,h}^{n-1}\|^2+\|\boldsymbol{w}_{j,h}^{n+1}-2\boldsymbol{w}_{j,h}^{n}+\boldsymbol{w}_{j,h}^{n-1}\|^2\Big)\\ +b^*\left(\boldsymbol{v}_{j,h}^{'n},2\boldsymbol{w}_{j,h}^{n}-\boldsymbol{w}_{j,h}^{n-1},\boldsymbol{w}_{j,h}^{n+1}\right)+\frac{\bar{\nu}+\bar{\nu}_m}{2}\|\nabla\boldsymbol{w}_{j,h}^{n+1}\|^2+\gamma\|\nabla\cdot\boldsymbol{w}_{j,h}^{n+1}\|^2\\ =(\boldsymbol{f}_{2,j}(t^{n+1}),w_{j,h}^{n+1})-\frac{\nu_j-\nu_{m,j}}{2}\big((1+\theta)\nabla\boldsymbol{v}_{j,h}^{n}-\theta\nabla\boldsymbol{v}_{j,h}^{n-1},\nabla\boldsymbol{w}_{j,h}^{n+1}\big)\\ -\frac{\nu_j^{'}+\nu_{m,j}^{'}}{2}\left(\nabla(2\boldsymbol{w}_{j,h}^{n}-\boldsymbol{w}_{j,h}^{n-1}),\nabla\boldsymbol{w}_{j,h}^{n+1}\right).\end{aligned}\tag{3.13}$$

Next, following the property $b^*(\boldsymbol{u},\boldsymbol{v},\boldsymbol{w})=-b^*(\boldsymbol{u},\boldsymbol{w},\boldsymbol{v})$, using the bound in (1.14) and discrete inverse inequality, we have

$$\begin{aligned}b^*\Big(\boldsymbol{w}_{j,h}^{'n},2\boldsymbol{v}_{j,h}^{n}-\boldsymbol{v}_{j,h}^{n-1},\boldsymbol{v}_{j,h}^{n+1}\Big)&=b^*\left(\boldsymbol{w}_{j,h}^{'n},\boldsymbol{v}_{j,h}^{n+1},\boldsymbol{v}_{j,h}^{n+1}-2\boldsymbol{v}_{j,h}^{n}+\boldsymbol{v}_{j,h}^{n-1}\right)\\ &\le C\|\nabla\boldsymbol{w}_{j,h}^{'n}\|\|\nabla\boldsymbol{v}_{j,h}^{n+1}\|\|\nabla\left(\boldsymbol{v}_{j,h}^{n+1}-2\boldsymbol{v}_{j,h}^{n}+\boldsymbol{v}_{j,h}^{n-1}\right)\|\\ &\le\frac{C}{h}\|\nabla\boldsymbol{w}_{j,h}^{'n}\|\|\nabla\boldsymbol{v}_{j,h}^{n+1}\|\|\boldsymbol{v}_{j,h}^{n+1}-2\boldsymbol{v}_{j,h}^{n}+\boldsymbol{v}_{j,h}^{n-1}\|.\end{aligned}\tag{3.14}$$

Using the above bound, adding equations (3.12) and (3.13), applying the Cauchy-Schwarz and Young's inequalities to the $\nu_j-\nu_{m,j}$, and $\nu_j^{'}+\nu_{m,j}^{'}$ terms, and rearranging, this yields

$$\begin{aligned}
&\frac{1}{4\Delta t}\Big(\|\boldsymbol{v}_{j,h}^{n+1}\|^2-\|\boldsymbol{v}_{j,h}^{n}\|^2+\|2\boldsymbol{v}_{j,h}^{n+1}-\boldsymbol{v}_{j,h}^{n}\|^2-\|2\boldsymbol{v}_{j,h}^{n}-\boldsymbol{v}_{j,h}^{n-1}\|^2+\|\boldsymbol{v}_{j,h}^{n+1}-2\boldsymbol{v}_{j,h}^{n}+\boldsymbol{v}_{j,h}^{n-1}\|^2\\
&+\|\boldsymbol{w}_{j,h}^{n+1}\|^2-\|\boldsymbol{w}_{j,h}^{n}\|^2+\|2\boldsymbol{w}_{j,h}^{n+1}-\boldsymbol{w}_{j,h}^{n}\|^2-\|2\boldsymbol{w}_{j,h}^{n}-\boldsymbol{w}_{j,h}^{n-1}\|^2+\|\boldsymbol{w}_{j,h}^{n+1}-2\boldsymbol{w}_{j,h}^{n}+\boldsymbol{w}_{j,h}^{n-1}\|^2\Big)\\
&+\frac{\bar{\nu}+\bar{\nu}_m}{2}\left(\|\nabla\boldsymbol{v}_{j,h}^{n+1}\|^2+\|\nabla\boldsymbol{w}_{j,h}^{n+1}\|^2\right)+\gamma\left(\|\nabla\cdot\boldsymbol{v}_{j,h}^{n+1}\|^2+\|\nabla\cdot\boldsymbol{w}_{j,h}^{n+1}\|^2\right)\\
&\leq\frac{|\nu_j-\nu_{m,j}|\,(1+2\theta)+3|\nu_j^{'}+\nu_{m,j}^{'}|}{4}\left(\|\nabla\boldsymbol{v}_{j,h}^{n+1}\|^2+\|\nabla\boldsymbol{w}_{j,h}^{n+1}\|^2\right)\\
&+\frac{|\nu_j-\nu_{m,j}|\,(1+\theta)+2|\nu_j^{'}+\nu_{m,j}^{'}|}{4}\left(\|\nabla\boldsymbol{v}_{j,h}^{n}\|^2+\|\nabla\boldsymbol{w}_{j,h}^{n}\|^2\right)\\
&+\frac{|\nu_j-\nu_{m,j}|\,\theta+|\nu_j^{'}+\nu_{m,j}^{'}|}{4}\left(\|\nabla\boldsymbol{v}_{j,h}^{n-1}\|^2+\|\nabla\boldsymbol{w}_{j,h}^{n-1}\|^2\right)\\
&+\frac{C}{h}\|\nabla\boldsymbol{w}_{j,h}^{'n}\|\|\nabla\boldsymbol{v}_{j,h}^{n+1}\|\|\boldsymbol{v}_{j,h}^{n+1}-2\boldsymbol{v}_{j,h}^{n}+\boldsymbol{v}_{j,h}^{n-1}\|\\
&+\frac{C}{h}\|\nabla\boldsymbol{v}_{j,h}^{'n}\|\|\nabla\boldsymbol{w}_{j,h}^{n+1}\|\|\boldsymbol{w}_{j,h}^{n+1}-2\boldsymbol{w}_{j,h}^{n}+\boldsymbol{w}_{j,h}^{n-1}\|\\
&+\|\boldsymbol{f}_{1,j}(t^{n+1})\|_{-1}\|\nabla\boldsymbol{v}_{j,h}^{n+1}\|+\|\boldsymbol{f}_{2,j}(t^{n+1})\|_{-1}\|\nabla\boldsymbol{w}_{j,h}^{n+1}\|. \qquad (3.15)
\end{aligned}$$

Next, we apply Young's inequality using $\alpha_j/8$ with the forcing terms, and non-linear terms, noting that $\alpha_j>0$ by the assumed choice of θ, and hiding terms on the left, and rearranging, we have

$$\begin{aligned}
&\frac{1}{4\Delta t}\Big(\|\boldsymbol{v}_{j,h}^{n+1}\|^2-\|\boldsymbol{v}_{j,h}^{n}\|^2+\|2\boldsymbol{v}_{j,h}^{n+1}-\boldsymbol{v}_{j,h}^{n}\|^2-\|2\boldsymbol{v}_{j,h}^{n}-\boldsymbol{v}_{j,h}^{n-1}\|^2\\
&+\|\boldsymbol{w}_{j,h}^{n+1}\|^2-\|\boldsymbol{w}_{j,h}^{n}\|^2+\|2\boldsymbol{w}_{j,h}^{n+1}-\boldsymbol{w}_{j,h}^{n}\|^2-\|2\boldsymbol{w}_{j,h}^{n}-\boldsymbol{w}_{j,h}^{n-1}\|^2\Big)\\
&+\frac{\bar{\nu}+\bar{\nu}_m}{4}\left(\|\nabla\boldsymbol{v}_{j,h}^{n+1}\|^2+\|\nabla\boldsymbol{w}_{j,h}^{n+1}\|^2\right)+\gamma\left(\|\nabla\cdot\boldsymbol{v}_{j,h}^{n+1}\|^2+\|\nabla\cdot\boldsymbol{w}_{j,h}^{n+1}\|^2\right)\\
&+\left(\frac{1}{4\Delta t}-\frac{C}{\alpha_j h^2}\|\nabla\boldsymbol{w}_{j,h}^{'n}\|^2\right)\|\boldsymbol{v}_{j,h}^{n+1}-2\boldsymbol{v}_{j,h}^{n}+\boldsymbol{v}_{j,h}^{n-1}\|^2\\
&+\left(\frac{1}{4\Delta t}-\frac{C}{\alpha_j h^2}\|\nabla\boldsymbol{v}_{j,h}^{'n}\|^2\right)\|\boldsymbol{w}_{j,h}^{n+1}-2\boldsymbol{w}_{j,h}^{n}+\boldsymbol{w}_{j,h}^{n-1}\|^2\\
&\leq\frac{|\nu_j-\nu_{m,j}|\,(1+\theta)+2|\nu_j^{'}+\nu_{m,j}^{'}|}{4}\left(\|\nabla\boldsymbol{v}_{j,h}^{n}\|^2+\|\nabla\boldsymbol{w}_{j,h}^{n}\|^2\right)\\
&+\frac{|\nu_j-\nu_{m,j}|\,\theta+|\nu_j^{'}+\nu_{m,j}^{'}|}{4}\left(\|\nabla\boldsymbol{v}_{j,h}^{n-1}\|^2+\|\nabla\boldsymbol{w}_{j,h}^{n-1}\|^2\right)\\
&+\frac{2}{\alpha_j}\|\boldsymbol{f}_{1,j}(t^{n+1})\|_{-1}^2+\frac{2}{\alpha_j}\|\boldsymbol{f}_{2,j}(t^{n+1})\|_{-1}^2. \qquad (3.16)
\end{aligned}$$

Now we choose $\Delta t\leq\frac{\alpha_{\min}h^2}{C\max\limits_{1\leq j\leq J}\left\{\|\nabla\boldsymbol{v}_{j,h}^{'n}\|^2,\|\nabla\boldsymbol{w}_{j,h}^{'n}\|^2\right\}}$, drop non-negative terms from left, and rearrange, we have

$$
\begin{aligned}
&\frac{1}{4\Delta t}\Big(\|\boldsymbol{v}_{j,h}^{n+1}\|^2-\|\boldsymbol{v}_{j,h}^{n}\|^2+\|2\boldsymbol{v}_{j,h}^{n+1}-\boldsymbol{v}_{j,h}^{n}\|^2-\|2\boldsymbol{v}_{j,h}^{n}-\boldsymbol{v}_{j,h}^{n-1}\|^2\\
&+\|\boldsymbol{w}_{j,h}^{n+1}\|^2-\|\boldsymbol{w}_{j,h}^{n}\|^2+\|2\boldsymbol{w}_{j,h}^{n+1}-\boldsymbol{w}_{j,h}^{n}\|^2-\|2\boldsymbol{w}_{j,h}^{n}-\boldsymbol{w}_{j,h}^{n-1}\|^2\Big)\\
&+\frac{\bar{\nu}+\bar{\nu}_m}{4}\Big(\|\nabla\boldsymbol{v}_{j,h}^{n+1}\|^2-\|\nabla\boldsymbol{v}_{j,h}^{n}\|^2+\|\nabla\boldsymbol{w}_{j,h}^{n+1}\|^2-\|\nabla\boldsymbol{w}_{j,h}^{n}\|^2\Big)\\
&+\frac{\bar{\nu}+\bar{\nu}_m-|\nu_j-\nu_{m,j}|\,(1+\theta)-2|\nu_j^{'}+\nu_{m,j}^{'}|}{4}\Big(\|\nabla\boldsymbol{v}_{j,h}^{n}\|^2-\|\nabla\boldsymbol{v}_{j,h}^{n-1}\|^2+\|\nabla\boldsymbol{w}_{j,h}^{n}\|^2-\|\nabla\boldsymbol{w}_{j,h}^{n-1}\|^2\Big)\\
&+\frac{\bar{\nu}+\bar{\nu}_m-|\nu_j-\nu_{m,j}|\,(1+2\theta)-3|\nu_j^{'}+\nu_{m,j}^{'}|}{4}\Big(\|\nabla\boldsymbol{v}_{j,h}^{n-1}\|^2+\|\nabla\boldsymbol{w}_{j,h}^{n-1}\|^2\Big)\\
&+\gamma\Big(\|\nabla\cdot\boldsymbol{v}_{j,h}^{n+1}\|^2+\|\nabla\cdot\boldsymbol{w}_{j,h}^{n+1}\|^2\Big)\le\frac{2}{\alpha_j}\|\boldsymbol{f}_{1,j}(t^{n+1})\|_{-1}^2+\frac{2}{\alpha_j}\|\boldsymbol{f}_{2,j}(t^{n+1})\|_{-1}^2. \qquad (3.17)
\end{aligned}
$$

Multiplying both sides by $4\Delta t$, and summing over time-steps $n=1,\cdots,M-1$, dropping non-negative terms from the left hand side completes the proof.

□

3.3 Convergence

In this section, we will prove the error estimate of Algorithm 3.

Theorem 3.2. *Consider $m=\max\{2,k+1\}$, and $j=1,2,\cdots,J$, assume $(\boldsymbol{v}_j,\boldsymbol{w}_j,q_j)$ solves (1.11)-(1.13) and satisfies*

$$
\begin{aligned}
&\boldsymbol{v}_j,\boldsymbol{w}_j\in L^\infty\big(0,T;\boldsymbol{H}^m(\Omega)^d\big),\ \ q_j,r_j\in L^2\big(0,T,L^2(\Omega)^d\big),\\
&\boldsymbol{v}_{j,t},\boldsymbol{v}_{j,t}\in L^\infty\big(0,T,\boldsymbol{H}^1(\Omega)^d\big),\boldsymbol{v}_{j,tt},\boldsymbol{v}_{j,tt}\in L^\infty\big(0,T,\boldsymbol{H}^1(\Omega)^d\big),\boldsymbol{v}_{j,ttt},\boldsymbol{v}_{j,ttt}\in L^\infty\big(0,T,\boldsymbol{L}^2(\Omega)^d\big).
\end{aligned}
$$

Then the solution $(\boldsymbol{v}_{j,h},\boldsymbol{w}_{j,h})$ to Algorithm 3 converges to the true solution: For any

$$
\Delta t\le\frac{\alpha_{\min}h^2}{C\max\limits_{1\le j\le J}\Big\{\|\nabla\boldsymbol{v}_{j,h}^{'n}\|^2,\|\nabla\boldsymbol{w}_{j,h}^{'n}\|^2\Big\}},
$$

one has

$$
\begin{aligned}
&\|<\boldsymbol{v}>(T)-<\boldsymbol{v}_h>^M\|+\|<\boldsymbol{w}>(T)-<\boldsymbol{w}_h>^M\|\\
&+(\Delta t)^{\frac{1}{2}}\sum_{n=2}^{M}\Big\{\|\nabla\big(<\boldsymbol{v}>(t^n)-<\boldsymbol{v}_h>^n\big)\|^2+\|\nabla\big(<\boldsymbol{w}>(t^n)-<\boldsymbol{w}_h>^n\big)\|^2\Big\}^{\frac{1}{2}}\\
&\le C\Big(h^k+(\Delta t)^2+(1-\theta)\Delta t\sqrt{\frac{1}{J}\sum_{j=1}^{J}(\nu_j-\nu_{m,j})^2}\Big). \qquad (3.18)
\end{aligned}
$$

Proof: At first we build an error equation. Testing (1.11), and (1.12) with $\boldsymbol{\chi}_{j,h} \in \boldsymbol{V}_h$, and $\boldsymbol{l}_{j,h} \in \boldsymbol{V}_h$, respectively at the time level t^{n+1}, the continuous variational formulations can be written

$$\begin{aligned}
&\left(\frac{3\boldsymbol{v}_j(t^{n+1}) - 4\boldsymbol{v}_j(t^n) + \boldsymbol{v}_j(t^{n-1})}{2\Delta t}, \boldsymbol{\chi}_{j,h}\right) + b^*\big(\boldsymbol{w}_j(t^{n+1}), \boldsymbol{v}_j(t^{n+1}), \boldsymbol{\chi}_{j,h}\big) \\
&+\frac{\bar{\nu} + \bar{\nu}_m}{2}\big(\nabla \boldsymbol{v}_j(t^{n+1}), \nabla \boldsymbol{\chi}_{j,h}\big) + \frac{\nu_j^{'} + \nu_{m,j}^{'}}{2}\big(\nabla(2\boldsymbol{v}_j(t^n) - \boldsymbol{v}_j(t^{n-1})), \nabla \boldsymbol{\chi}_{j,h}\big) \\
&+\frac{\nu_j - \nu_{m,j}}{2}\big((1+\theta)\nabla \boldsymbol{w}_j(t^n) - \theta \nabla \boldsymbol{w}_j(t^{n-1}), \boldsymbol{\chi}_{j,h}\big) \\
&-\big(q_j(t^{n+1}), \nabla \cdot \boldsymbol{\chi}_{j,h}\big) + \gamma\big(\nabla \cdot \boldsymbol{v}_j(t^{n+1}), \nabla \cdot \boldsymbol{\chi}_{j,h}\big) = \big(\boldsymbol{f}_{1,j}(t^{n+1}), \boldsymbol{\chi}_{j,h}\big) \\
&-\frac{\nu_j^{'} + \nu_{m,j}^{'}}{2}\Big(\nabla\big(\boldsymbol{v}_j(t^{n+1}) - 2\boldsymbol{v}_j(t^n) + \boldsymbol{v}_j(t^{n-1})\big), \nabla \boldsymbol{\chi}_{j,h}\Big) \\
&-\frac{\nu_j - \nu_{m,j}}{2}\big(\nabla(\boldsymbol{w}_j(t^{n+1}) - (1+\theta)\boldsymbol{w}_j(t^n) + \theta \boldsymbol{w}_j(t^{n-1})), \boldsymbol{\chi}_{j,h}\big) \\
&-\left(\boldsymbol{v}_{j,t}(t^{n+1}) - \frac{3\boldsymbol{v}_j(t^{n+1}) - 4\boldsymbol{v}_j(t^n) + \boldsymbol{v}_j(t^{n-1})}{2\Delta t}, \boldsymbol{\chi}_{j,h}\right),
\end{aligned} \tag{3.19}$$

and

$$\begin{aligned}
&\left(\frac{3\boldsymbol{w}_j(t^{n+1}) - 4\boldsymbol{w}_j(t^n) + \boldsymbol{w}_j(t^{n-1})}{2\Delta t}, \boldsymbol{l}_{j,h}\right) + b^*\big(\boldsymbol{v}_j(t^{n+1}), \boldsymbol{w}_j(t^{n+1}), \boldsymbol{l}_{j,h}\big) \\
&+\frac{\bar{\nu} + \bar{\nu}_m}{2}\big(\nabla \boldsymbol{w}_j(t^{n+1}), \nabla \boldsymbol{l}_{j,h}\big) + \frac{\nu_j^{'} + \nu_{m,j}^{'}}{2}\big(\nabla(2\boldsymbol{w}_j(t^n) - \boldsymbol{w}_j(t^{n-1})), \nabla \boldsymbol{l}_{j,h}\big) \\
&+\frac{\nu_j - \nu_{m,j}}{2}\big((1+\theta)\nabla \boldsymbol{v}_j(t^n) - \theta \nabla \boldsymbol{v}_j(t^{n-1}), \boldsymbol{l}_{j,h}\big) \\
&-\big(r_j(t^{n+1}), \nabla \cdot \boldsymbol{l}_{j,h}\big) + \gamma\big(\nabla \cdot \boldsymbol{w}_j(t^{n+1}), \nabla \cdot \boldsymbol{l}_{j,h}\big) = \big(\boldsymbol{f}_{2,j}(t^{n+1}), \boldsymbol{l}_{j,h}\big) \\
&-\frac{\nu_j^{'} + \nu_{m,j}^{'}}{2}\Big(\nabla\big(\boldsymbol{w}_j(t^{n+1}) - 2\boldsymbol{w}_j(t^n) + \boldsymbol{w}_j(t^{n-1})\big), \nabla \boldsymbol{l}_{j,h}\Big) \\
&-\frac{\nu_j - \nu_{m,j}}{2}\big(\nabla(\boldsymbol{v}_j(t^{n+1}) - (1+\theta)\boldsymbol{v}_j(t^n) + \theta \boldsymbol{v}_j(t^{n-1})), \boldsymbol{l}_{j,h}\big) \\
&-\left(\boldsymbol{w}_{j,t}(t^{n+1}) - \frac{3\boldsymbol{w}_j(t^{n+1}) - 4\boldsymbol{w}_j(t^n) + \boldsymbol{w}_j(t^{n-1})}{2\Delta t}, \boldsymbol{l}_{j,h}\right).
\end{aligned} \tag{3.20}$$

Note that $\big(\nabla \cdot \boldsymbol{v}_j(t^{n+1}), \nabla \cdot \boldsymbol{\chi}_{j,h}\big) = \big(\nabla \cdot \boldsymbol{w}_j(t^{n+1}), \nabla \cdot \boldsymbol{l}_{j,h}\big) = 0$. Denote $\boldsymbol{e}_{\boldsymbol{v},j}^n := \boldsymbol{v}_j(t^n) - \boldsymbol{v}_{j,h}^n$, and $\boldsymbol{e}_{\boldsymbol{w},j}^n := \boldsymbol{w}_j(t^n) - \boldsymbol{w}_{j,h}^n$. Subtracting (3.6) and (3.7) from equation (3.19) and (3.20), respectively it yields

$$\begin{aligned}
&\left(\frac{3\boldsymbol{e}_{\boldsymbol{v},j}^{n+1} - 4\boldsymbol{e}_{\boldsymbol{v},j}^n + \boldsymbol{e}_{\boldsymbol{v},j}^{n-1}}{2\Delta t}, \boldsymbol{\chi}_{j,h}\right) + \frac{\bar{\nu} + \bar{\nu}_m}{2}(\nabla \boldsymbol{e}_{\boldsymbol{v},j}^{n+1}, \nabla \boldsymbol{\chi}_{j,h}) + \frac{\nu_j^{'} + \nu_{m,j}^{'}}{2}\Big(\nabla\big(2\boldsymbol{e}_{\boldsymbol{v},j}^n - \boldsymbol{e}_{\boldsymbol{v},j}^{n-1}\big), \nabla \boldsymbol{\chi}_{j,h}\Big) \\
&+\frac{\nu_j - \nu_{m,j}}{2}\big((1+\theta)\nabla \boldsymbol{e}_{\boldsymbol{w},j}^n - \theta \nabla \boldsymbol{e}_{\boldsymbol{w},j}^{n-1}, \nabla \boldsymbol{\chi}_{j,h}\big) + b^*\big(2\boldsymbol{e}_{\boldsymbol{w},j}^n - \boldsymbol{e}_{\boldsymbol{w},j}^{n-1}, \boldsymbol{v}_j(t^{n+1}), \boldsymbol{\chi}_{j,h}\big) \\
&+b^*\big(2\boldsymbol{w}_{j,h}^n - \boldsymbol{w}_{j,h}^{n-1}, \boldsymbol{e}_{\boldsymbol{v},j}^{n+1}, \boldsymbol{\chi}_{j,h}\big) - b^*\big(\boldsymbol{w}_{j,h}^{'n}, \boldsymbol{e}_{\boldsymbol{v},j}^{n+1} - 2\boldsymbol{e}_{\boldsymbol{v},j}^n + \boldsymbol{e}_{\boldsymbol{v},j}^{n-1}, \boldsymbol{\chi}_{j,h}\big) \\
&-\big(q_j(t^{n+1}), \nabla \cdot \boldsymbol{\chi}_{j,h}\big) + \gamma\big(\nabla \cdot \boldsymbol{e}_{\boldsymbol{v},j}^{n+1}, \nabla \cdot \boldsymbol{\chi}_{j,h}\big) = -G_1(t, \boldsymbol{v}_j, \boldsymbol{w}_j, \boldsymbol{\chi}_{j,h}),
\end{aligned} \tag{3.21}$$

and

$$\begin{aligned}
&\Big(\frac{3\boldsymbol{e}_{\boldsymbol{w},j}^{n+1}-4\boldsymbol{e}_{\boldsymbol{w},j}^{n}+\boldsymbol{e}_{\boldsymbol{w},j}^{n-1}}{2\Delta t},\boldsymbol{l}_{j,h}\Big)+\frac{\bar{\nu}+\bar{\nu}_m}{2}(\nabla e_{\boldsymbol{w},j}^{n+1},\nabla\boldsymbol{l}_{j,h})+\frac{\nu_j^{'}+\nu_{m,j}^{'}}{2}\Big(\nabla\big(2\boldsymbol{e}_{\boldsymbol{w},j}^{n}-\boldsymbol{e}_{\boldsymbol{w},j}^{n-1}\big),\nabla\boldsymbol{l}_{j,h}\Big)\\
&+\frac{\nu_j-\nu_{m,j}}{2}\big((1+\theta)\nabla e_{\boldsymbol{v},j}^{n}-\theta\nabla e_{\boldsymbol{v},j}^{n-1},\nabla\boldsymbol{l}_{j,h}\big)+b^*\big(2\boldsymbol{e}_{\boldsymbol{w},j}^{n}-\boldsymbol{e}_{\boldsymbol{v},j}^{n-1},\boldsymbol{w}_j(t^{n+1}),\boldsymbol{l}_{j,h}\big)\\
&+b^*\big(2\boldsymbol{v}_{j,h}^{n}-\boldsymbol{v}_{j,h}^{n-1},\boldsymbol{e}_{\boldsymbol{w},j}^{n+1},\boldsymbol{l}_{j,h}\big)-b^*(\boldsymbol{v}_{j,h}^{'n},\boldsymbol{e}_{\boldsymbol{w},j}^{n+1}-2\boldsymbol{e}_{\boldsymbol{w},j}^{n}+\boldsymbol{e}_{\boldsymbol{w},j}^{n-1},\boldsymbol{l}_{j,h})\\
&-\big(r_j(t^{n+1}),\nabla\cdot\boldsymbol{l}_{j,h}\big)+\gamma\big(\nabla\cdot\boldsymbol{e}_{\boldsymbol{w},j}^{n+1},\nabla\cdot\boldsymbol{l}_{j,h}\big)=-G_2(t,\boldsymbol{v}_j,\boldsymbol{w}_j,\boldsymbol{l}_{j,h}),
\end{aligned}\tag{3.22}$$

where

$$\begin{aligned}
G_1(t,\boldsymbol{v}_j,\boldsymbol{w}_j,\boldsymbol{\chi}_{j,h}) &:= b^*\big(\boldsymbol{w}_j(t^{n+1})-2\boldsymbol{w}_j(t^n)+\boldsymbol{w}_j(t^{n-1}),\boldsymbol{v}_j(t^{n+1}),\boldsymbol{\chi}_{j,h}\big)\\
&+b^*\big(\boldsymbol{w}_{j,h}^{'n},\boldsymbol{v}_j(t^{n+1})-2\boldsymbol{v}_j(t^n)+\boldsymbol{v}_j(t^{n-1}),\boldsymbol{\chi}_{j,h}\big)\\
&+\frac{\nu_j^{'}+\nu_{m,j}^{'}}{2}\Big(\nabla\big(\boldsymbol{v}_j(t^{n+1})-2\boldsymbol{v}_j(t^n)+\boldsymbol{v}_j(t^{n-1})\big),\nabla\boldsymbol{\chi}_{j,h}\Big)\\
&+\frac{\nu_j-\nu_{m,j}}{2}\big(\nabla(\boldsymbol{w}_j(t^{n+1})-(1+\theta)\boldsymbol{w}_j(t^n)+\theta\boldsymbol{w}_j(t^{n-1})),\nabla\boldsymbol{\chi}_{j,h}\big)\\
&+\Big(\boldsymbol{v}_{j,t}(t^{n+1})-\frac{3\boldsymbol{v}_j(t^{n+1})-4\boldsymbol{v}_j(t^n)+\boldsymbol{v}_j(t^{n-1})}{2\Delta t},\boldsymbol{\chi}_{j,h}\Big),
\end{aligned}$$

and

$$\begin{aligned}
G_2(t,\boldsymbol{v}_j,\boldsymbol{w}_j,\boldsymbol{l}_{j,h}) &:= b^*\big(\boldsymbol{v}_j(t^{n+1})-2\boldsymbol{v}_j(t^n)+\boldsymbol{v}_j(t^{n-1}),\boldsymbol{w}_j(t^{n+1}),\boldsymbol{l}_{j,h}\big)\\
&+b^*\big(\boldsymbol{v}_{j,h}^{'n},\boldsymbol{w}_j(t^{n+1})-2\boldsymbol{w}_j(t^n)+\boldsymbol{w}_j(t^{n-1}),\boldsymbol{l}_{j,h}\big)\\
&+\frac{\nu_j^{'}+\nu_{m,j}^{'}}{2}\Big(\nabla\big(\boldsymbol{w}_j(t^{n+1})-2\boldsymbol{w}_j(t^n)+\boldsymbol{w}_j(t^{n-1})\big),\nabla\boldsymbol{l}_{j,h}\Big)\\
&+\frac{\nu_j-\nu_{m,j}}{2}\big(\nabla(\boldsymbol{v}_j(t^{n+1})-(1+\theta)\boldsymbol{v}_j(t^n)+\theta\boldsymbol{v}_j(t^{n-1})),\nabla\boldsymbol{l}_{j,h}\big)\\
&+\Big(\boldsymbol{w}_{j,t}(t^{n+1})-\frac{3\boldsymbol{w}_j(t^{n+1})-4\boldsymbol{w}_j(t^n)+\boldsymbol{w}_j(t^{n-1})}{2\Delta t},\boldsymbol{l}_{j,h}\Big).
\end{aligned}$$

Now we decompose the errors as

$$\begin{aligned}
\boldsymbol{e}_{\boldsymbol{v},j}^{n} &:= \boldsymbol{v}_j(t^n)-\boldsymbol{v}_{j,h}^{n}=(\boldsymbol{v}_j(t^n)-\tilde{\boldsymbol{v}}_j^{n})-(\boldsymbol{v}_{j,h}^{n}-\tilde{\boldsymbol{v}}_j^{n}):=\boldsymbol{\eta}_{\boldsymbol{v},j}^{n}-\boldsymbol{\varphi}_{j,h}^{n},\\
\boldsymbol{e}_{\boldsymbol{w},j}^{n} &:= \boldsymbol{w}_j(t^n)-\boldsymbol{w}_{j,h}^{n}=(\boldsymbol{w}_j(t^n)-\tilde{\boldsymbol{w}}_j^{n})-(\boldsymbol{w}_{j,h}^{n}-\tilde{\boldsymbol{w}}_j^{n}):=\boldsymbol{\eta}_{\boldsymbol{w},j}^{n}-\boldsymbol{\psi}_{j,h}^{n},
\end{aligned}$$

where $\tilde{\boldsymbol{v}}_j^{n}:=P_{\boldsymbol{V}_h}^{L^2}(\boldsymbol{v}_j(t^n))\in\boldsymbol{V}_h$ and $\tilde{\boldsymbol{w}}_j^{n}:=P_{\boldsymbol{V}_h}^{L^2}(\boldsymbol{w}_j(t^n))\in\boldsymbol{V}_h$ are the L^2 projections of $\boldsymbol{v}_j(t^n)$ and $\boldsymbol{w}_j(t^n)$ into $\boldsymbol{V}_h$, respectively. Note that $(\boldsymbol{\eta}_{\boldsymbol{v},j}^{n},\boldsymbol{v}_{j,h})=(\boldsymbol{\eta}_{\boldsymbol{w},j}^{n},\boldsymbol{v}_{j,h})=0\ \ \forall\boldsymbol{v}_{j,h}\in\boldsymbol{V}_h$. Rewriting, we have

for $\boldsymbol{\chi}_{j,h}, \boldsymbol{l}_{j,h} \in \boldsymbol{V}_h$

$$
\begin{aligned}
&\Big(\frac{3\boldsymbol{\varphi}_{j,h}^{n+1} - 4\boldsymbol{\varphi}_{j,h}^{n} + \boldsymbol{\varphi}_{j,h}^{n-1}}{2\Delta t}, \boldsymbol{\chi}_{j,h}\Big) + \frac{\bar{\nu} + \bar{\nu}_m}{2}(\nabla\boldsymbol{\varphi}_{j,h}^{n+1}, \nabla\boldsymbol{\chi}_{j,h}) + \frac{\nu_j^{'} + \nu_{m,j}^{'}}{2}\big(\nabla(2\boldsymbol{\varphi}_{j,h}^{n} - \boldsymbol{\varphi}_{j,h}^{n-1}), \nabla\boldsymbol{\chi}_{j,h}\big) \\
&+ \frac{\nu_j - \nu_{m,j}}{2}\big((1+\theta)\nabla\boldsymbol{\psi}_{j,h}^{n} - \theta\nabla\boldsymbol{\psi}_{j,h}^{n-1}, \nabla\boldsymbol{\chi}_{j,h}\big) + b^*\big(2\boldsymbol{\psi}_{j,h}^{n} - \boldsymbol{\psi}_{j,h}^{n-1}, \boldsymbol{v}_j(t^{n+1}), \boldsymbol{\chi}_{j,h}\big) \\
&+ b^*(2\boldsymbol{w}_{j,h}^{n} - \boldsymbol{w}_{j,h}^{n-1}, \boldsymbol{\varphi}_{j,h}^{n+1}, \boldsymbol{\chi}_{j,h}) - b^*(\boldsymbol{w}_{j,h}^{'n}, \boldsymbol{\varphi}_{j,h}^{n+1} - 2\boldsymbol{\varphi}_{j,h}^{n} + \boldsymbol{\varphi}_{j,h}^{n-1}, \boldsymbol{\chi}_{j,h}) + \gamma\big(\nabla\cdot\boldsymbol{\varphi}_{j,h}^{n+1}, \nabla\cdot\boldsymbol{\chi}_{j,h}\big) \\
&= \frac{\nu_j - \nu_{m,j}}{2}\big((1+\theta)\nabla\boldsymbol{\eta}_{\boldsymbol{w},j}^{n} - \theta\nabla\boldsymbol{\eta}_{\boldsymbol{w},j}^{n-1}, \nabla\boldsymbol{\chi}_{j,h}\big) + \frac{\bar{\nu} + \bar{\nu}_m}{2}(\nabla\boldsymbol{\eta}_{\boldsymbol{v},j}^{n+1}, \nabla\boldsymbol{\chi}_{j,h}) \\
&+ \frac{\nu_j^{'} + \nu_{m,j}^{'}}{2}\big(\nabla(2\boldsymbol{\eta}_{\boldsymbol{v},j}^{n} - \boldsymbol{\eta}_{\boldsymbol{v},j}^{n-1}), \nabla\boldsymbol{\chi}_{j,h}\big) + b^*\big(2\boldsymbol{\eta}_{\boldsymbol{w},j}^{n} - \boldsymbol{\eta}_{\boldsymbol{w},j}^{n-1}, \boldsymbol{v}_j(t^{n+1}), \boldsymbol{\chi}_{j,h}\big) \\
&+ b^*(2\boldsymbol{w}_{j,h}^{n} - \boldsymbol{w}_{j,h}^{n-1}, \boldsymbol{\eta}_{\boldsymbol{v},j}^{n+1}, \boldsymbol{\chi}_{j,h}) - b^*(\boldsymbol{w}_{j,h}^{'n}, \boldsymbol{\eta}_{\boldsymbol{v},j}^{n+1} - 2\boldsymbol{\eta}_{\boldsymbol{v},j}^{n} + \boldsymbol{\eta}_{\boldsymbol{v},j}^{n-1}, \boldsymbol{\chi}_{j,h}) \\
&- \big(q_j(t^{n+1}), \nabla\cdot\boldsymbol{\chi}_{j,h}\big) + \gamma\big(\nabla\cdot\boldsymbol{\eta}_{\boldsymbol{v},j}^{n+1}, \nabla\cdot\boldsymbol{\chi}_{j,h}\big) + G_1(t, \boldsymbol{v}_j, \boldsymbol{w}_j, \boldsymbol{\chi}_{j,h}),
\end{aligned} \tag{3.23}
$$

and

$$
\begin{aligned}
&\Big(\frac{3\boldsymbol{\psi}_{j,h}^{n+1} - 4\boldsymbol{\psi}_{j,h}^{n} + \boldsymbol{\psi}_{j,h}^{n-1}}{2\Delta t}, \boldsymbol{l}_{j,h}\Big) + \frac{\bar{\nu} + \bar{\nu}_m}{2}(\nabla\boldsymbol{\psi}_{j,h}^{n+1}, \nabla\boldsymbol{l}_{j,h}) + \frac{\nu_j^{'} + \nu_{m,j}^{'}}{2}\big(\nabla(2\boldsymbol{\psi}_{j,h}^{n} - \boldsymbol{\psi}_{j,h}^{n-1}), \nabla\boldsymbol{l}_{j,h}\big) \\
&+ \frac{\nu_j - \nu_{m,j}}{2}\big((1+\theta)\nabla\boldsymbol{\varphi}_{j,h}^{n} - \theta\nabla\boldsymbol{\varphi}_{j,h}^{n-1}, \nabla\boldsymbol{l}_{j,h}\big) + b^*\big(2\boldsymbol{\varphi}_{j,h}^{n} - \boldsymbol{\varphi}_{j,h}^{n-1}, \boldsymbol{w}_j(t^{n+1}), \boldsymbol{l}_{j,h}\big) \\
&+ b^*(2\boldsymbol{v}_{j,h}^{n} - \boldsymbol{v}_{j,h}^{n-1}, \boldsymbol{\psi}_{j,h}^{n+1}, \boldsymbol{l}_{j,h}) - b^*(\boldsymbol{v}_{j,h}^{'n}, \boldsymbol{\psi}_{j,h}^{n+1} - 2\boldsymbol{\psi}_{j,h}^{n} + \boldsymbol{\psi}_{j,h}^{n-1}, \boldsymbol{l}_{j,h}) + \gamma\big(\nabla\cdot\boldsymbol{\psi}_{j,h}^{n+1}, \nabla\cdot\boldsymbol{l}_{j,h}\big) \\
&= \frac{\nu_j - \nu_{m,j}}{2}\big((1+\theta)\nabla\boldsymbol{\eta}_{\boldsymbol{v},j}^{n} - \theta\nabla\boldsymbol{\eta}_{\boldsymbol{v},j}^{n-1}, \nabla\boldsymbol{l}_{j,h}\big) + \frac{\bar{\nu} + \bar{\nu}_m}{2}(\nabla\boldsymbol{\eta}_{\boldsymbol{w},j}^{n+1}, \nabla\boldsymbol{l}_{j,h}) \\
&+ \frac{\nu_j^{'} + \nu_{m,j}^{'}}{2}\big(\nabla(2\boldsymbol{\eta}_{\boldsymbol{w},j}^{n} - \boldsymbol{\eta}_{\boldsymbol{w},j}^{n-1}), \nabla\boldsymbol{l}_{j,h}\big) + b^*\big(2\boldsymbol{\eta}_{\boldsymbol{v},j}^{n} - \boldsymbol{\eta}_{\boldsymbol{v},j}^{n-1}, \boldsymbol{w}_j(t^{n+1}), \boldsymbol{l}_{j,h}\big) \\
&+ b^*(2\boldsymbol{v}_{j,h}^{n} - \boldsymbol{v}_{j,h}^{n-1}, \boldsymbol{\eta}_{\boldsymbol{w},j}^{n+1}, \boldsymbol{l}_{j,h}) - b^*(\boldsymbol{v}_{j,h}^{'n}, \boldsymbol{\eta}_{\boldsymbol{w},j}^{n+1} - 2\boldsymbol{\eta}_{\boldsymbol{w},j}^{n} + \boldsymbol{\eta}_{\boldsymbol{w},j}^{n-1}, \boldsymbol{l}_{j,h}) \\
&- \big(r_j(t^{n+1}), \nabla\cdot\boldsymbol{l}_{j,h}\big) + \gamma\big(\nabla\cdot\boldsymbol{\eta}_{\boldsymbol{w},j}^{n+1}, \nabla\cdot\boldsymbol{l}_{j,h}\big) + G_2(t, \boldsymbol{v}_j, \boldsymbol{w}_j, \boldsymbol{l}_{j,h}).
\end{aligned} \tag{3.24}
$$

Choosing $\boldsymbol{\chi}_{j,h} = \boldsymbol{\varphi}_{j,h}^{n+1}, \boldsymbol{l}_{j,h} = \boldsymbol{\psi}_{j,h}^{n+1}$, we use the identity (3.11) in (3.23) and (3.24), to obtain

$$
\begin{aligned}
&\frac{1}{4\Delta t}\Big(\|\boldsymbol{\varphi}_{j,h}^{n+1}\|^2 - \|\boldsymbol{\varphi}_{j,h}^{n}\|^2 + \|2\boldsymbol{\varphi}_{j,h}^{n+1} - \boldsymbol{\varphi}_{j,h}^{n}\|^2 - \|2\boldsymbol{\varphi}_{j,h}^{n} - \boldsymbol{\varphi}_{j,h}^{n-1}\|^2 + \|\boldsymbol{\varphi}_{j,h}^{n+1} - 2\boldsymbol{\varphi}_{j,h}^{n} + \boldsymbol{\varphi}_{j,h}^{n-1}\|^2\Big) \\
&+ \frac{\bar{\nu} + \bar{\nu}_m}{2}\|\nabla\boldsymbol{\varphi}_{j,h}^{n+1}\|^2 + \gamma\|\nabla\cdot\boldsymbol{\varphi}_{j,h}^{n+1}\|^2 \le (1+\theta)\frac{|\nu_j - \nu_{m,j}|}{2}\Big\{|(\nabla\boldsymbol{\psi}_{j,h}^{n}, \nabla\boldsymbol{\varphi}_{j,h}^{n+1})| + |(\nabla\boldsymbol{\eta}_{\boldsymbol{w},j}^{n}, \nabla\boldsymbol{\varphi}_{j,h}^{n+1})|\Big\} \\
&+ \theta\frac{|\nu_j - \nu_{m,j}|}{2}\Big\{|(\nabla\boldsymbol{\psi}_{j,h}^{n-1}, \nabla\boldsymbol{\varphi}_{j,h}^{n+1})| + |(\nabla\boldsymbol{\eta}_{\boldsymbol{w},j}^{n-1}, \nabla\boldsymbol{\varphi}_{j,h}^{n+1})|\Big\} + \frac{|\nu_j^{'} + \nu_{m,j}^{'}|}{2}|\big(\nabla(2\boldsymbol{\varphi}_{j,h}^{n} - \boldsymbol{\varphi}_{j,h}^{n-1}), \nabla\boldsymbol{\varphi}_{j,h}^{n+1}\big)| \\
&+ \frac{\bar{\nu} + \bar{\nu}_m}{2}|(\nabla\boldsymbol{\eta}_{\boldsymbol{v},j}^{n+1}, \nabla\boldsymbol{\varphi}_{j,h}^{n+1})| + |b^*\big(2\boldsymbol{\eta}_{\boldsymbol{w},j}^{n} - \boldsymbol{\eta}_{\boldsymbol{w},j}^{n-1}, \boldsymbol{v}_j(t^{n+1}), \boldsymbol{\varphi}_{j,h}^{n+1}\big)| + |b^*\big(2\boldsymbol{w}_{j,h}^{n} - \boldsymbol{w}_{j,h}^{n-1}, \boldsymbol{\eta}_{\boldsymbol{v},j}^{n+1}, \boldsymbol{\varphi}_{j,h}^{n+1}\big)| \\
&+ |b^*\big(\boldsymbol{w}_{j,h}^{'n}, \boldsymbol{\eta}_{\boldsymbol{v},j}^{n+1} - 2\boldsymbol{\eta}_{\boldsymbol{v},j}^{n} + \boldsymbol{\eta}_{\boldsymbol{v},j}^{n-1}, \boldsymbol{\varphi}_{j,h}^{n+1}\big)| + |b^*\big(2\boldsymbol{\psi}_{j,h}^{n} - \boldsymbol{\psi}_{j,h}^{n-1}, \boldsymbol{v}_j(t^{n+1}), \boldsymbol{\varphi}_{j,h}^{n+1}\big)| \\
&+ |b^*\big(\boldsymbol{w}_{j,h}^{'n}, \boldsymbol{\varphi}_{j,h}^{n+1} - 2\boldsymbol{\varphi}_{j,h}^{n} + \boldsymbol{\varphi}_{j,h}^{n-1}, \boldsymbol{\varphi}_{j,h}^{n+1}\big)| + |\big(q_j(t^{n+1}), \nabla\cdot\boldsymbol{\varphi}_{j,h}^{n+1}\big)| + \gamma|\big(\nabla\cdot\boldsymbol{\eta}_{\boldsymbol{v},j}^{n+1}, \nabla\cdot\boldsymbol{\varphi}_{j,h}^{n+1}\big)| \\
&+ |G_1(t, \boldsymbol{v}_j, \boldsymbol{w}_j, \boldsymbol{\varphi}_{j,h}^{n+1})|,
\end{aligned} \tag{3.25}
$$

and

$$\begin{aligned}
&\frac{1}{4\Delta t}\Big(\|\boldsymbol{\psi}_{j,h}^{n+1}\|^2-\|\boldsymbol{\psi}_{j,h}^{n}\|^2+\|2\boldsymbol{\psi}_{j,h}^{n+1}-\boldsymbol{\psi}_{j,h}^{n}\|^2-\|2\boldsymbol{\psi}_{j,h}^{n}-\boldsymbol{\psi}_{j,h}^{n-1}\|^2+\|\boldsymbol{\psi}_{j,h}^{n+1}-2\boldsymbol{\psi}_{j,h}^{n}+\boldsymbol{\psi}_{j,h}^{n-1}\|^2\Big)\\
&+\frac{\bar{\nu}+\bar{\nu}_m}{2}\|\nabla\boldsymbol{\psi}_{j,h}^{n+1}\|^2+\gamma\|\nabla\cdot\boldsymbol{\psi}_{j,h}^{n+1}\|^2\leq(1+\theta)\frac{|\nu_j-\nu_{m,j}|}{2}\Big\{|(\nabla\boldsymbol{\varphi}_{j,h}^{n},\nabla\boldsymbol{\psi}_{j,h}^{n+1})|+|(\nabla\boldsymbol{\eta}_{\boldsymbol{v},j}^{n},\nabla\boldsymbol{\psi}_{j,h}^{n+1})|\Big\}\\
&+\theta\frac{|\nu_j-\nu_{m,j}|}{2}\Big\{|(\nabla\boldsymbol{\varphi}_{j,h}^{n-1},\nabla\boldsymbol{\psi}_{j,h}^{n+1})|+|(\nabla\boldsymbol{\eta}_{\boldsymbol{v},j}^{n-1},\nabla\boldsymbol{\psi}_{j,h}^{n+1})|\Big\}+\frac{|\nu_j^{'}+\nu_{m,j}^{'}|}{2}|\big(\nabla(2\boldsymbol{\psi}_{j,h}^{n}-\boldsymbol{\psi}_{j,h}^{n-1}),\nabla\boldsymbol{\psi}_{j,h}^{n+1}\big)|\\
&+\frac{\bar{\nu}+\bar{\nu}_m}{2}|(\nabla\boldsymbol{\eta}_{\boldsymbol{w},j}^{n+1},\nabla\boldsymbol{\psi}_{j,h}^{n+1})|+|b^*\big(2\boldsymbol{\eta}_{\boldsymbol{v},j}^{n}-\boldsymbol{\eta}_{\boldsymbol{v},j}^{n-1},\boldsymbol{w}_j(t^{n+1}),\boldsymbol{\psi}_{j,h}^{n+1}\big)|+|b^*\big(2\boldsymbol{v}_{j,h}^{n}-\boldsymbol{v}_{j,h}^{n-1},\boldsymbol{\eta}_{\boldsymbol{w},j}^{n+1},\boldsymbol{\psi}_{j,h}^{n+1}\big)|\\
&+|b^*\big(\boldsymbol{v}_{j,h}^{'n},\boldsymbol{\eta}_{\boldsymbol{w},j}^{n+1}-2\boldsymbol{\eta}_{\boldsymbol{w},j}^{n}+\boldsymbol{\eta}_{\boldsymbol{w},j}^{n-1},\boldsymbol{\psi}_{j,h}^{n+1}\big)|+|b^*\big(2\boldsymbol{\varphi}_{j,h}^{n}-\boldsymbol{\varphi}_{j,h}^{n-1},\boldsymbol{w}_j(t^{n+1}),\boldsymbol{\psi}_{j,h}^{n+1}\big)|\\
&+|b^*\big(\boldsymbol{w}_{j,h}^{'n},\boldsymbol{\psi}_{j,h}^{n+1}-2\boldsymbol{\psi}_{j,h}^{n}+\boldsymbol{\psi}_{j,h}^{n-1},\boldsymbol{\psi}_{j,h}^{n+1}\big)|+|\big(r_j(t^{n+1}),\nabla\cdot\boldsymbol{\psi}_{j,h}^{n+1}\big)|+\gamma|\big(\nabla\cdot\boldsymbol{\eta}_{\boldsymbol{w},j}^{n+1},\nabla\cdot\boldsymbol{\psi}_{j,h}^{n+1}\big)|\\
&+|G_2(t,\boldsymbol{v}_j,\boldsymbol{w}_j,\boldsymbol{\psi}_{j,h}^{n+1})|. \qquad (3.26)
\end{aligned}$$

We now turn our attention to finding bounds on the right-hand-side terms of (3.25). Applying Cauchy-Schwarz and Young's inequalities on the first six terms to provide

$$\begin{aligned}
(1+\theta)\frac{|\nu_j-\nu_{m,j}|}{2}|\big(\nabla\boldsymbol{\psi}_{j,h}^{n},\nabla\boldsymbol{\varphi}_{j,h}^{n+1}\big)|&\leq(1+\theta)\frac{|\nu_j-\nu_{m,j}|}{4}\big(\|\nabla\boldsymbol{\psi}_{j,h}^{n}\|^2+\|\nabla\boldsymbol{\varphi}_{j,h}^{n+1}\|^2\big),\\
\theta\frac{|\nu_j-\nu_{m,j}|}{2}|\big(\nabla\boldsymbol{\psi}_{j,h}^{n-1},\nabla\boldsymbol{\varphi}_{j,h}^{n+1}\big)|&\leq\theta\frac{|\nu_j-\nu_{m,j}|}{4}\big(\|\nabla\boldsymbol{\psi}_{j,h}^{n-1}\|^2+\|\nabla\boldsymbol{\varphi}_{j,h}^{n+1}\|^2\big),\\
(1+\theta)\frac{|\nu_j-\nu_{m,j}|}{2}|\big(\nabla\boldsymbol{\eta}_{\boldsymbol{w},j}^{n},\nabla\boldsymbol{\varphi}_{j,h}^{n+1}\big)|&\leq\frac{\alpha_j}{36}\|\nabla\boldsymbol{\varphi}_{j,h}^{n+1}\|^2+\frac{9(1+\theta)^2(\nu_j-\nu_{m,j})^2}{4\alpha_j}\|\nabla\boldsymbol{\eta}_{\boldsymbol{w},j}^{n}\|^2,\\
\theta\frac{|\nu_j-\nu_{m,j}|}{2}|\big(\nabla\boldsymbol{\eta}_{\boldsymbol{w},j}^{n-1},\nabla\boldsymbol{\varphi}_{j,h}^{n+1}\big)|&\leq\frac{\alpha_j}{36}\|\nabla\boldsymbol{\varphi}_{j,h}^{n+1}\|^2+\frac{9\theta^2(\nu_j-\nu_{m,j})^2}{4\alpha_j}\|\nabla\boldsymbol{\eta}_{\boldsymbol{w},j}^{n-1}\|^2,\\
\frac{\nu_j^{'}+\nu_{m,j}^{'}}{2}|\big(\nabla(2\boldsymbol{\varphi}_{j,h}^{n}-\boldsymbol{\varphi}_{j,h}^{n-1}),\nabla\boldsymbol{\varphi}_{j,h}^{n+1}\big)|&\leq\frac{|\nu_j^{'}+\nu_{m,j}^{'}|}{4}(3\|\nabla\boldsymbol{\varphi}_{j,h}^{n+1}\|^2+2\|\nabla\boldsymbol{\varphi}_{j,h}^{n}\|^2+\|\nabla\boldsymbol{\varphi}_{j,h}^{n-1}\|^2),\\
\frac{\bar{\nu}+\bar{\nu}_m}{2}|\big(\nabla\boldsymbol{\eta}_{\boldsymbol{v},j}^{n+1},\nabla\boldsymbol{\varphi}_{j,h}^{n+1}\big)|&\leq\frac{\alpha_j}{36}\|\nabla\boldsymbol{\varphi}_{j,h}^{n+1}\|^2+\frac{9(\bar{\nu}+\bar{\nu}_m)^2}{4\alpha_j}\|\nabla\boldsymbol{\eta}_{\boldsymbol{v},j}^{n+1}\|^2.
\end{aligned}$$

Applying Young's inequalities with (1.14) on the first three nonlinear terms yields

$$\begin{aligned}
|b^*\big(2\boldsymbol{\eta}_{\boldsymbol{w},j}^{n}-\boldsymbol{\eta}_{\boldsymbol{w},j}^{n-1},\boldsymbol{v}_j(t^{n+1}),\boldsymbol{\varphi}_{j,h}^{n+1}\big)|&\leq C\|\nabla(2\boldsymbol{\eta}_{\boldsymbol{w},j}^{n}-\boldsymbol{\eta}_{\boldsymbol{w},j}^{n-1})\|\|\nabla\boldsymbol{v}_j(t^{n+1})\|\|\nabla\boldsymbol{\varphi}_{j,h}^{n+1}\|\\
&\leq\frac{\alpha_j}{36}\|\nabla\boldsymbol{\varphi}_{j,h}^{n+1}\|^2+\frac{C}{\alpha_j}\|\nabla(2\boldsymbol{\eta}_{\boldsymbol{w},j}^{n}-\boldsymbol{\eta}_{\boldsymbol{w},j}^{n-1})\|^2\|\nabla\boldsymbol{v}_j(t^{n+1})\|^2,\\
|b^*\big(2\boldsymbol{w}_{j,h}^{n}-\boldsymbol{w}_{j,h}^{n-1},\boldsymbol{\eta}_{\boldsymbol{v},j}^{n+1},\boldsymbol{\varphi}_{j,h}^{n+1}\big)|&\leq C\|\nabla(2\boldsymbol{w}_{j,h}^{n}-\boldsymbol{w}_{j,h}^{n-1})\|\|\nabla\boldsymbol{\eta}_{\boldsymbol{v},j}^{n+1}\|\|\nabla\boldsymbol{\varphi}_{j,h}^{n+1}\|\\
&\leq\frac{\alpha_j}{36}\|\nabla\boldsymbol{\varphi}_{j,h}^{n+1}\|^2+\frac{C}{\alpha_j}\|\nabla(2\boldsymbol{w}_{j,h}^{n}-\boldsymbol{w}_{j,h}^{n-1})\|^2\|\nabla\boldsymbol{\eta}_{\boldsymbol{v},j}^{n+1}\|^2,\\
|b^*\big(\boldsymbol{w}_{j,h}^{'n},\boldsymbol{\eta}_{\boldsymbol{v},j}^{n+1}-\boldsymbol{\eta}_{\boldsymbol{v},j}^{n}+\boldsymbol{\eta}_{\boldsymbol{v},j}^{n-1},\boldsymbol{\varphi}_{j,h}^{n+1}\big)|&\leq C\|\nabla\boldsymbol{w}_{j,h}^{'n}\|\|\nabla(\boldsymbol{\eta}_{\boldsymbol{v},j}^{n+1}-\boldsymbol{\eta}_{\boldsymbol{v},j}^{n}+\boldsymbol{\eta}_{\boldsymbol{v},j}^{n-1})\|\|\nabla\boldsymbol{\varphi}_{j,h}^{n+1}\|\\
&\leq\frac{\alpha_j}{36}\|\nabla\boldsymbol{\varphi}_{j,h}^{n+1}\|^2+\frac{C}{\alpha_j}\|\nabla\boldsymbol{w}_{j,h}^{'n}\|^2\|\nabla(\boldsymbol{\eta}_{\boldsymbol{v},j}^{n+1}-\boldsymbol{\eta}_{\boldsymbol{v},j}^{n}+\boldsymbol{\eta}_{\boldsymbol{v},j}^{n-1})\|^2.
\end{aligned}$$

For the fourth nonlinear term, we use Hölder's inequality, Sobolev embedding theorems, Agmon's, Poincare's and Young's inequalities to reveal

$$
\begin{aligned}
&|b^*\big(2\boldsymbol{\psi}_{j,h}^n-\boldsymbol{\psi}_{j,h}^{n-1},\boldsymbol{v}_j(t^{n+1}),\boldsymbol{\varphi}_{j,h}^{n+1}\big)|\\
&\leq C\|2\boldsymbol{\psi}_{j,h}^n-\boldsymbol{\psi}_{j,h}^{n-1}\|\|\nabla\boldsymbol{v}_j(t^{n+1})\|_{\boldsymbol{L}^6}\|\boldsymbol{\varphi}_{j,h}^{n+1}\|_{\boldsymbol{L}^3}+C\|2\boldsymbol{\psi}_{j,h}^n-\boldsymbol{\psi}_{j,h}^{n-1}\|\|\nabla\boldsymbol{\varphi}_{j,h}^{n+1}\|\|\boldsymbol{v}_j(t^{n+1})\|_\infty\\
&\leq C\|2\boldsymbol{\psi}_{j,h}^n-\boldsymbol{\psi}_{j,h}^{n-1}\|\|\boldsymbol{v}_j(t^{n+1})\|_{\boldsymbol{H}^2}\|\boldsymbol{\varphi}_{j,h}^{n+1}\|^{1/2}\|\nabla\boldsymbol{\varphi}_{j,h}^{n+1}\|^{1/2}+C\|2\boldsymbol{\psi}_{j,h}^n-\boldsymbol{\psi}_{j,h}^{n-1}\|\|\nabla\boldsymbol{\varphi}_{j,h}^{n+1}\|\|\boldsymbol{v}_j(t^{n+1})\|_{\boldsymbol{H}^2}\\
&\leq C\|2\boldsymbol{\psi}_{j,h}^n-\boldsymbol{\psi}_{j,h}^{n-1}\|\|\boldsymbol{v}_j(t^{n+1})\|_{\boldsymbol{H}^2}\|\nabla\boldsymbol{\varphi}_{j,h}^{n+1}\|\\
&\leq \frac{\alpha_j}{36}\|\nabla\boldsymbol{\varphi}_{j,h}^{n+1}\|^2+\frac{C}{\alpha_j}\|\boldsymbol{v}_j(t^{n+1})\|_{\boldsymbol{H}^2}^2\|2\boldsymbol{\psi}_{j,h}^n-\boldsymbol{\psi}_{j,h}^{n-1}\|^2.
\end{aligned}
\tag{3.27}
$$

Applying inverse and Young's inequalities with (1.14) on the fifth nonlinear terms to yield

$$
\begin{aligned}
|b^*\big(\boldsymbol{w}_{j,h}^{'n},\boldsymbol{\varphi}_{j,h}^{n+1}-2\boldsymbol{\varphi}_{j,h}^n+\boldsymbol{\varphi}_{j,h}^{n-1},\boldsymbol{\varphi}_{j,h}^{n+1}\big)|&\leq C\|\nabla\boldsymbol{w}_{j,h}^{'n}\|\|\nabla(\boldsymbol{\varphi}_{j,h}^{n+1}-2\boldsymbol{\varphi}_{j,h}^n+\boldsymbol{\varphi}_{j,h}^{n-1})\|\|\nabla\boldsymbol{\varphi}_{j,h}^{n+1}\|\\
&\leq \frac{\alpha_j}{36}\|\nabla\boldsymbol{\varphi}_{j,h}^{n+1}\|^2+\frac{C}{\alpha_j h^2}\|\nabla\boldsymbol{w}_{j,h}^{'n}\|^2\|\boldsymbol{\varphi}_{j,h}^{n+1}-2\boldsymbol{\varphi}_{j,h}^n+\boldsymbol{\varphi}_{j,h}^{n-1}\|^2.
\end{aligned}
\tag{3.28}
$$

Since $\boldsymbol{\varphi}_{j,h}^{n+1}\in\boldsymbol{V}_h$, we rewrite the pressure term, apply Cauchy-Schwarz and Young's inequalities to get

$$
\begin{aligned}
|\big(q_j(t^{n+1}),\nabla\cdot\boldsymbol{\varphi}_{j,h}^{n+1}\big)|&=|\big(q_j(t^{n+1})-q_{j,h}^{n+1},\nabla\cdot\boldsymbol{\varphi}_{j,h}^{n+1}\big)|\\
&\leq\frac{\gamma}{4}\|\nabla\cdot\boldsymbol{\varphi}_{j,h}^{n+1}\|^2+\gamma^{-1}\|q_j(t^{n+1})-q_{j,h}^{n+1}\|^2,\quad\forall q_{j,h}^{n+1}\in Q_h.
\end{aligned}
$$

Next, we find the upper bound of the term with coefficient γ using Cauchy-Schwarz and Young's inequalities as

$$
\begin{aligned}
\gamma|\big(\nabla\cdot\boldsymbol{\eta}_{\boldsymbol{v},j}^{n+1},\nabla\cdot\boldsymbol{\varphi}_{j,h}^{n+1}\big)|&\leq\gamma\|\nabla\cdot\boldsymbol{\eta}_{\boldsymbol{v},j}^{n+1}\|\|\nabla\cdot\boldsymbol{\varphi}_{j,h}^{n+1}\|\\
&\leq\frac{\gamma}{2}\|\nabla\cdot\boldsymbol{\varphi}_{j,h}^{n+1}\|^2+\frac{\gamma}{2}\|\nabla\cdot\boldsymbol{\eta}_{\boldsymbol{v},j}^{n+1}\|^2.
\end{aligned}
$$

Using Taylor's series expansion about time-step size, Cauchy-Schwarz, Poincare's and Young's inequalities, the upper bound of the last term can be found as

$$
\begin{aligned}
|G_1(t,\boldsymbol{v}_j,\boldsymbol{w}_j,\boldsymbol{\varphi}_{j,h}^{n+1})|\leq{}&\frac{\alpha_j}{36}\|\nabla\boldsymbol{\varphi}_{j,h}^{n+1}\|^2+(\Delta t)^4\frac{45(\nu_j^{'}+\nu_{m,j}^{'})^2}{4\alpha_j}\|\nabla\boldsymbol{v}_{j,tt}(s_1^*)\|^2\\
&+(\Delta t)^2\frac{45(\nu_j-\nu_{m,j})^2(1-\theta)^2}{4\alpha_j}\|\nabla\boldsymbol{w}_{j,t}(s_2^*)\|^2\\
&+(\Delta t)^4\frac{C}{\alpha_j}\Big(\|\nabla\boldsymbol{w}_{j,tt}(s_3^*)\|^2\|\nabla\boldsymbol{v}_j(t^{n+1})\|^2+\|\nabla\boldsymbol{w}_{j,h}^{'n}\|^2\|\nabla\boldsymbol{v}_{j,tt}(s_4^*)\|^2+\|\boldsymbol{v}_{j,ttt}(s_5^*)\|^2\Big)
\end{aligned}
$$

with $s_1^*, s_2^*, s_3^*, s_4^*, s_5^* \in [t^{n-1}, t^{n+1}]$. Using these estimates in (3.25) and reducing, it produces

$$\begin{aligned}
&\frac{1}{4\Delta t}\left(\|\boldsymbol{\varphi}_{j,h}^{n+1}\|^2 - \|\boldsymbol{\varphi}_{j,h}^{n}\|^2 + \|2\boldsymbol{\varphi}_{j,h}^{n+1} - \boldsymbol{\varphi}_{j,h}^{n}\|^2 - \|2\boldsymbol{\varphi}_{j,h}^{n} - \boldsymbol{\varphi}_{j,h}^{n-1}\|^2\right)\\
&+\Big(\frac{1}{4\Delta t} - \frac{C}{\alpha_j h^2}\|\nabla \boldsymbol{w}_{j,h}^{'n}\|^2\Big)\|\boldsymbol{\varphi}_{j,h}^{n+1} - 2\boldsymbol{\varphi}_{j,h}^{n} + \boldsymbol{\varphi}_{j,h}^{n-1}\|^2 + \frac{\bar{\nu}+\bar{\nu}_m}{4}\|\nabla\boldsymbol{\varphi}_{j,h}^{n+1}\|^2 + \frac{\gamma}{4}\|\nabla\cdot\boldsymbol{\varphi}_{j,h}^{n+1}\|^2\\
&\le (1+\theta)\frac{|\nu_j-\nu_{m,j}|}{4}\|\nabla\boldsymbol{\psi}_{j,h}^{n}\|^2 + \theta\frac{|\nu_j-\nu_{m,j}|}{4}\|\nabla\boldsymbol{\psi}_{j,h}^{n-1}\|^2 + \frac{9(1+\theta)^2(\nu_j-\nu_{m,j})^2}{4\alpha_j}\|\nabla\boldsymbol{\eta}_{\boldsymbol{w},j}^{n}\|^2\\
&+\frac{9\theta^2(\nu_j-\nu_{m,j})^2}{4\alpha_j}\|\nabla\boldsymbol{\eta}_{\boldsymbol{w},j}^{n-1}\|^2 + \frac{|\nu_j^{'}+\nu_{m,j}^{'}|}{4}(2\|\nabla\boldsymbol{\varphi}_{j,h}^{n}\|^2 + \|\nabla\boldsymbol{\varphi}_{j,h}^{n-1}\|^2) + \frac{9(\bar{\nu}+\bar{\nu}_m)^2}{4\alpha_j}\|\nabla\boldsymbol{\eta}_{\boldsymbol{v},j}^{n+1}\|^2\\
&+\frac{C}{\alpha_j}\|\nabla(2\boldsymbol{\eta}_{\boldsymbol{w},j}^{n} - \boldsymbol{\eta}_{\boldsymbol{w},j}^{n-1})\|^2\|\nabla\boldsymbol{v}_j(t^{n+1})\|^2 + \frac{C}{\alpha_j}\|\nabla(2\boldsymbol{w}_{j,h}^{n} - \boldsymbol{w}_{j,h}^{n-1})\|^2\|\nabla\boldsymbol{\eta}_{\boldsymbol{v},j}^{n+1}\|^2\\
&+\frac{C}{\alpha_j}\|\nabla\boldsymbol{w}_{j,h}^{'n}\|^2\|\nabla(\boldsymbol{\eta}_{\boldsymbol{v},j}^{n+1} - \boldsymbol{\eta}_{\boldsymbol{v},j}^{n} + \boldsymbol{\eta}_{\boldsymbol{v},j}^{n-1})\|^2 + \frac{C}{\alpha_j}\|\boldsymbol{v}_j(t^{n+1})\|_{H^2}^2\|2\boldsymbol{\psi}_{j,h}^{n} - \boldsymbol{\psi}_{j,h}^{n-1}\|^2\\
&+(\Delta t)^4\frac{45(\nu_j^{'}+\nu_{m,j}^{'})^2}{4\alpha_j}\|\nabla\boldsymbol{v}_{j,tt}(s_1^*)\|^2 + (\Delta t)^2\frac{45(\nu_j-\nu_{m,j})^2(1-\theta)^2}{4\alpha_j}\|\nabla\boldsymbol{w}_{j,t}(s_2^*)\|^2\\
&+\frac{\gamma}{2}\|\nabla\cdot\boldsymbol{\eta}_{\boldsymbol{v},j}^{n+1}\|^2 + \gamma^{-1}\|q_j(t^{n+1}) - q_{j,h}^{n+1}\|^2\\
&+(\Delta t)^4\frac{C}{\alpha_j}\Big(\|\nabla\boldsymbol{w}_{j,tt}(s_3^*)\|^2\|\nabla\boldsymbol{v}_j(t^{n+1})\|^2 + \|\nabla\boldsymbol{w}_{j,h}^{'n}\|^2\|\nabla\boldsymbol{v}_{j,tt}(s_4^*)\|^2 + \|\boldsymbol{v}_{j,ttt}(s_5^*)\|^2\Big). \qquad (3.29)
\end{aligned}$$

Applying similar techniques to (3.26), we get

$$\begin{aligned}
&\frac{1}{4\Delta t}\left(\|\boldsymbol{\psi}_{j,h}^{n+1}\|^2 - \|\boldsymbol{\psi}_{j,h}^{n}\|^2 + \|2\boldsymbol{\psi}_{j,h}^{n+1} - \boldsymbol{\psi}_{j,h}^{n}\|^2 - \|2\boldsymbol{\psi}_{j,h}^{n} - \boldsymbol{\psi}_{j,h}^{n-1}\|^2\right)\\
&+\Big(\frac{1}{4\Delta t} - \frac{C}{\alpha_j h^2}\|\nabla \boldsymbol{v}_{j,h}^{'n}\|^2\Big)\|\boldsymbol{\psi}_{j,h}^{n+1} - \boldsymbol{\psi}_{j,h}^{n} + \boldsymbol{\psi}_{j,h}^{n-1}\|^2 + \frac{\bar{\nu}+\bar{\nu}_m}{4}\|\nabla\boldsymbol{\psi}_{j,h}^{n+1}\|^2 + \frac{\gamma}{4}\|\nabla\cdot\boldsymbol{\psi}_{j,h}^{n+1}\|^2\\
&\le (1+\theta)\frac{|\nu_j-\nu_{m,j}|}{4}\|\nabla\boldsymbol{\varphi}_{j,h}^{n}\|^2 + \theta\frac{|\nu_j-\nu_{m,j}|}{4}\|\nabla\boldsymbol{\varphi}_{j,h}^{n-1}\|^2 + \frac{9(1+\theta)^2(\nu_j-\nu_{m,j})^2}{4\alpha_j}\|\nabla\boldsymbol{\eta}_{\boldsymbol{v},j}^{n}\|^2\\
&+\frac{9\theta^2(\nu_j-\nu_{m,j})^2}{4\alpha_j}\|\nabla\boldsymbol{\eta}_{\boldsymbol{v},j}^{n-1}\|^2 + \frac{|\nu_j^{'}+\nu_{m,j}^{'}|}{4}(2\|\nabla\boldsymbol{\psi}_{j,h}^{n}\|^2 + \|\nabla\boldsymbol{\psi}_{j,h}^{n-1}\|^2) + \frac{9(\bar{\nu}+\bar{\nu}_m)^2}{4\alpha_j}\|\nabla\boldsymbol{\eta}_{\boldsymbol{w},j}^{n+1}\|^2\\
&+\frac{C}{\alpha_j}\|\nabla(2\boldsymbol{\eta}_{\boldsymbol{v},j}^{n} - \boldsymbol{\eta}_{\boldsymbol{v},j}^{n-1})\|^2\|\nabla\boldsymbol{w}_j(t^{n+1})\|^2 + \frac{C}{\alpha_j}\|\nabla(2\boldsymbol{v}_{j,h}^{n} - \boldsymbol{v}_{j,h}^{n-1})\|^2\|\nabla\boldsymbol{\eta}_{\boldsymbol{w},j}^{n+1}\|^2\\
&+\frac{C}{\alpha_j}\|\nabla\boldsymbol{v}_{j,h}^{'n}\|^2\|\nabla(\boldsymbol{\eta}_{\boldsymbol{w},j}^{n+1} - \boldsymbol{\eta}_{\boldsymbol{w},j}^{n} + \boldsymbol{\eta}_{\boldsymbol{w},j}^{n-1})\|^2 + \frac{C}{\alpha_j}\|\boldsymbol{w}_j(t^{n+1})\|_{H^2}^2\|2\boldsymbol{\varphi}_{j,h}^{n} - \boldsymbol{\varphi}_{j,h}^{n-1}\|^2\\
&+(\Delta t)^4\frac{45(\nu_j^{'}+\nu_{m,j}^{'})^2}{4\alpha_j}\|\nabla\boldsymbol{w}_{j,tt}(t_1^*)\|^2 + (\Delta t)^2\frac{45(\nu_j-\nu_{m,j})^2(1-\theta)^2}{4\alpha_j}\|\nabla\boldsymbol{v}_{j,t}(t_2^*)\|^2\\
&+\frac{\gamma}{2}\|\nabla\cdot\boldsymbol{\eta}_{\boldsymbol{w},j}^{n+1}\|^2 + \gamma^{-1}\|r_j(t^{n+1}) - r_{j,h}^{n+1}\|^2\\
&+(\Delta t)^4\frac{C}{\alpha_j}\Big(\|\nabla\boldsymbol{v}_{j,tt}(t_3^*)\|^2\|\nabla\boldsymbol{w}_j(t^{n+1})\|^2 + \|\nabla\boldsymbol{v}_{j,h}^{'n}\|^2\|\nabla\boldsymbol{w}_{j,tt}(t_4^*)\|^2 + \|\boldsymbol{w}_{j,ttt}(t_5^*)\|^2\Big), \qquad (3.30)
\end{aligned}$$

with $t_1^*, t_2^*, t_3^*, t_4^*, t_5^* \in [t^{n-1}, t^{n+1}]$. After add (3.29) and (3.30), assume

$$\Delta t \leq \frac{\alpha_{\min} h^2}{C \max\limits_{1\leq j\leq J} \left\{ \|\nabla \boldsymbol{v}_{j,h}^{'n}\|^2, \|\nabla \boldsymbol{w}_{j,h}^{'n}\|^2 \right\}}, \tag{3.31}$$

drops non-negative terms from left-hand-side, and rearrange, we have

$$\begin{aligned}
&\frac{1}{4\Delta t}\left(\|\boldsymbol{\varphi}_{j,h}^{n+1}\|^2 - \|\boldsymbol{\varphi}_{j,h}^{n}\|^2 + \|2\boldsymbol{\varphi}_{j,h}^{n+1} - \boldsymbol{\varphi}_{j,h}^{n}\|^2 - \|2\boldsymbol{\varphi}_{j,h}^{n} - \boldsymbol{\varphi}_{j,h}^{n-1}\|^2\right)\\
&+\frac{1}{4\Delta t}\left(\|\boldsymbol{\psi}_{j,h}^{n+1}\|^2 - \|\boldsymbol{\psi}_{j,h}^{n}\|^2 + \|2\boldsymbol{\psi}_{j,h}^{n+1} - \boldsymbol{\psi}_{j,h}^{n}\|^2 - \|2\boldsymbol{\psi}_{j,h}^{n} - \boldsymbol{\psi}_{j,h}^{n-1}\|^2\right)\\
&+\frac{\bar{\nu}+\bar{\nu}_m}{4}\left(\|\nabla\boldsymbol{\varphi}_{j,h}^{n+1}\|^2 - \|\nabla\boldsymbol{\varphi}_{j,h}^{n}\|^2 + \|\nabla\boldsymbol{\psi}_{j,h}^{n+1}\|^2 - \|\nabla\boldsymbol{\psi}_{j,h}^{n}\|^2\right)\\
&+\frac{\alpha_j+\theta|\nu_j-\nu_{m,j}|+|\nu_j^{'}+\nu_{m,j}^{'}|}{4}\left(\|\nabla\boldsymbol{\varphi}_{j,h}^{n}\|^2 - \|\nabla\boldsymbol{\varphi}_{j,h}^{n-1}\|^2 + \|\nabla\boldsymbol{\psi}_{j,h}^{n}\|^2 - \|\nabla\boldsymbol{\psi}_{j,h}^{n-1}\|^2\right)\\
&+\frac{\alpha_j}{4}\left(\|\nabla\boldsymbol{\varphi}_{j,h}^{n-1}\|^2 + \|\nabla\boldsymbol{\psi}_{j,h}^{n-1}\|^2\right) + \frac{\gamma}{4}\left(\|\nabla\cdot\boldsymbol{\varphi}_{j,h}^{n+1}\|^2 + \|\nabla\cdot\boldsymbol{\psi}_{j,h}^{n+1}\|^2\right)\\
&\leq \frac{9(1+\theta)^2(\nu_j-\nu_{m,j})^2}{4\alpha_j}\left(\|\nabla\boldsymbol{\eta}_{\boldsymbol{v},j}^{n}\|^2 + \|\nabla\boldsymbol{\eta}_{\boldsymbol{w},j}^{n}\|^2\right)\\
&+\frac{9\theta^2(\nu_j-\nu_{m,j})^2}{4\alpha_j}\left(\|\nabla\boldsymbol{\eta}_{\boldsymbol{v},j}^{n-1}\|^2 + \|\nabla\boldsymbol{\eta}_{\boldsymbol{w},j}^{n-1}\|^2\right) + \frac{9(\bar{\nu}+\bar{\nu}_m)^2}{4\alpha_j}\left(\|\nabla\boldsymbol{\eta}_{\boldsymbol{v},j}^{n+1}\|^2 + \|\nabla\boldsymbol{\eta}_{\boldsymbol{w},j}^{n+1}\|^2\right)\\
&+\frac{C}{\alpha_j}\|\nabla(2\boldsymbol{\eta}_{\boldsymbol{w},j}^{n} - \boldsymbol{\eta}_{\boldsymbol{w},j}^{n-1})\|^2\|\nabla\boldsymbol{v}_j(t^{n+1})\|^2 + \frac{C}{\alpha_j}\|\nabla(2\boldsymbol{\eta}_{\boldsymbol{v},j}^{n} - \boldsymbol{\eta}_{\boldsymbol{v},j}^{n-1})\|^2\|\nabla\boldsymbol{w}_j(t^{n+1})\|^2\\
&+\frac{C}{\alpha_j}\|\nabla(2\boldsymbol{w}_{j,h}^{n} - \boldsymbol{w}_{j,h}^{n-1})\|^2\|\nabla\boldsymbol{\eta}_{\boldsymbol{v},j}^{n+1}\|^2 + \frac{C}{\alpha_j}\|\nabla(2\boldsymbol{v}_{j,h}^{n} - \boldsymbol{v}_{j,h}^{n-1})\|^2\|\nabla\boldsymbol{\eta}_{\boldsymbol{w},j}^{n+1}\|^2\\
&+\frac{C}{\alpha_j}\|\nabla\boldsymbol{w}_{j,h}^{'n}\|^2\|\nabla(\boldsymbol{\eta}_{\boldsymbol{v},j}^{n+1} - \boldsymbol{\eta}_{\boldsymbol{v},j}^{n} + \boldsymbol{\eta}_{\boldsymbol{v},j}^{n-1})\|^2 + \frac{C}{\alpha_j}\|\nabla\boldsymbol{v}_{j,h}^{'n}\|^2\|\nabla(\boldsymbol{\eta}_{\boldsymbol{w},j}^{n+1} - \boldsymbol{\eta}_{\boldsymbol{w},j}^{n} + \boldsymbol{\eta}_{\boldsymbol{w},j}^{n-1})\|^2\\
&+\frac{C}{\alpha_j}\|\boldsymbol{v}_j(t^{n+1})\|_{H^2}^2\|2\boldsymbol{\psi}_{j,h}^{n} - \boldsymbol{\psi}_{j,h}^{n-1}\|^2 + \frac{C}{\alpha_j}\|\boldsymbol{w}_j(t^{n+1})\|_{H^2}^2\|2\boldsymbol{\varphi}_{j,h}^{n} - \boldsymbol{\varphi}_{j,h}^{n-1}\|^2\\
&+(\Delta t)^4\frac{45(\nu_j^{'}+\nu_{m,j}^{'})^2}{4\alpha_j}\left(\|\nabla\boldsymbol{v}_{j,tt}(s_1^*)\|^2 + \|\nabla\boldsymbol{w}_{j,tt}(t_1^*)\|^2\right)\\
&+(\Delta t)^2\frac{45(\nu_j-\nu_{m,j})^2(1-\theta)^2}{4\alpha_j}\left(\|\nabla\boldsymbol{v}_{j,t}(t_2^*)\|^2 + \|\nabla\boldsymbol{w}_{j,t}(s_2^*)\|^2\right)\\
&+\frac{\gamma}{2}\left(\|\nabla\cdot\boldsymbol{\eta}_{\boldsymbol{v},j}^{n+1}\|^2 + \|\nabla\cdot\boldsymbol{\eta}_{\boldsymbol{w},j}^{n+1}\|^2\right) + \frac{1}{\gamma}\left(\|q_j(t^{n+1}) - q_{j,h}^{n+1}\|^2 + \|r_j(t^{n+1}) - r_{j,h}^{n+1}\|^2\right)\\
&+(\Delta t)^4\frac{C}{\alpha_j}\Big(\|\nabla\boldsymbol{w}_{j,tt}(s_3^*)\|^2\|\nabla\boldsymbol{v}_j(t^{n+1})\|^2 + \|\nabla\boldsymbol{w}_{j,h}^{'n}\|^2\|\nabla\boldsymbol{v}_{j,tt}(s_4^*)\|^2 + \|\boldsymbol{v}_{j,ttt}(s_5^*)\|^2\Big)\\
&+(\Delta t)^4\frac{C}{\alpha_j}\Big(\|\nabla\boldsymbol{v}_{j,tt}(t_3^*)\|^2\|\nabla\boldsymbol{w}_j(t^{n+1})\|^2 + \|\nabla\boldsymbol{v}_{j,h}^{'n}\|^2\|\nabla\boldsymbol{w}_{j,tt}(t_4^*)\|^2 + \|\boldsymbol{w}_{j,ttt}(t_5^*)\|^2\Big).
\end{aligned} \tag{3.32}$$

Multiply both sides by $4\Delta t$, use stability and regularity assumptions, $\|\boldsymbol{\varphi}_{j,h}^0\| = \|\boldsymbol{\psi}_{j,h}^0\| = \|\boldsymbol{\varphi}_{j,h}^1\| =$

$\|\boldsymbol{\psi}_{j,h}^1\| = 0$, $\Delta t M = T$, and sum over the time steps to find

$$
\begin{aligned}
&\|\boldsymbol{\varphi}_{j,h}^M\|^2 + \|2\boldsymbol{\varphi}_{j,h}^M - \boldsymbol{\varphi}_{j,h}^{M-1}\|^2 + \|\boldsymbol{\psi}_{j,h}^M\|^2 + \|2\boldsymbol{\psi}_{j,h}^M - \boldsymbol{\psi}_{j,h}^{M-1}\|^2 \\
&+ \alpha_j \Delta t \sum_{n=2}^{M} (\|\nabla \boldsymbol{\varphi}_{j,h}^n\|^2 + \|\nabla \boldsymbol{\psi}_{j,h}^n\|^2) + \gamma \Delta t \sum_{n=2}^{M} \big(\|\nabla \cdot \boldsymbol{\varphi}_{j,h}^n\|^2 + \|\nabla \cdot \boldsymbol{\psi}_{j,h}^n\|^2\big) \\
&\leq \frac{C(1+\theta)^2(\nu_j - \nu_{m,j})^2}{\alpha_j} h^{2k} + \frac{C\theta^2(\nu_j - \nu_{m,j})^2}{\alpha_j} h^{2k} + \frac{C(\bar{\nu} + \bar{\nu}_m)^2}{\alpha_j} h^{2k} \\
&+ \frac{C}{\alpha_j} h^{2k} \left(\|\boldsymbol{v}_j(t)\|^2_{L^\infty\left(0,T;\boldsymbol{H}^1(\Omega)^d\right)} + \|\boldsymbol{w}_j(t)\|^2_{L^\infty\left(0,T;\boldsymbol{H}^1(\Omega)^d\right)} \right) + \frac{C}{\alpha_j} h^{2k} \\
&+ \frac{C}{\alpha_j} \Delta t \sum_{n=1}^{M-1} \left\{ \|\boldsymbol{v}_j(t)\|^2_{L^\infty\left(0,T;\boldsymbol{H}^2(\Omega)^d\right)} \|2\boldsymbol{\psi}_{j,h}^n - \boldsymbol{\psi}_{j,h}^{n-1}\|^2 + \|\boldsymbol{w}_j(t)\|^2_{L^\infty\left(0,T;\boldsymbol{H}^2(\Omega)^d\right)} \|2\boldsymbol{\varphi}_{j,h}^n - \boldsymbol{\varphi}_{j,h}^{n-1}\|^2 \right\} \\
&+ C\big((\Delta t)^4 + (\nu_j - \nu_{m,j})^2(1-\theta)^2(\Delta t)^2\big) + C\gamma h^{2k} + \frac{C}{\gamma} h^{2k}. \qquad (3.33)
\end{aligned}
$$

Using triangular and Young's inequalities, dropping non-negative terms from left-hand-side, and simplifying yield

$$
\begin{aligned}
&\|\boldsymbol{\varphi}_{j,h}^M\|^2 + \|\boldsymbol{\psi}_{j,h}^M\|^2 + \alpha_j \Delta t \sum_{n=2}^{M} (\|\nabla \boldsymbol{\varphi}_{j,h}^n\|^2 + \|\nabla \boldsymbol{\psi}_{j,h}^n\|^2) + \gamma \Delta t \sum_{n=2}^{M} \big(\|\nabla \cdot \boldsymbol{\varphi}_{j,h}^n\|^2 + \|\nabla \cdot \boldsymbol{\psi}_{j,h}^n\|^2\big) \\
&\qquad \leq \Delta t \sum_{n=2}^{M-1} \frac{C}{\alpha_j} \big(\|\boldsymbol{\varphi}_{j,h}^n\|^2 + \|\boldsymbol{\psi}_{j,h}^n\|^2\big) + C\big(h^{2k} + (\Delta t)^4 + (\nu_j - \nu_{m,j})^2(1-\theta)^2(\Delta t)^2\big). \qquad (3.34)
\end{aligned}
$$

Applying the discrete Grönwall Lemma 1.1, we have

$$
\begin{aligned}
&\|\boldsymbol{\varphi}_{j,h}^M\|^2 + \|\boldsymbol{\psi}_{j,h}^M\|^2 + \alpha_j \Delta t \sum_{n=2}^{M} (\|\nabla \boldsymbol{\varphi}_{j,h}^n\|^2 + \|\nabla \boldsymbol{\psi}_{j,h}^n\|^2) + \gamma \Delta t \sum_{n=2}^{M} \big(\|\nabla \cdot \boldsymbol{\varphi}_{j,h}^n\|^2 + \|\nabla \cdot \boldsymbol{\psi}_{j,h}^n\|^2\big) \\
&\qquad \leq C \exp\left(\frac{CT}{\alpha_j}\right) \big(h^{2k} + (\Delta t)^4 + (\nu_j - \nu_{m,j})^2(1-\theta)^2(\Delta t)^2\big). \qquad (3.35)
\end{aligned}
$$

Use of triangle and Young's inequalities allows us to write

$$
\begin{aligned}
&\|\boldsymbol{e}_{\boldsymbol{v},j}^M\|^2 + \|\boldsymbol{e}_{\boldsymbol{w},j}^M\|^2 + \alpha_j \Delta t \sum_{n=2}^{M} \big(\|\nabla \boldsymbol{e}_{\boldsymbol{v},j}^n\|^2 + \|\nabla \boldsymbol{e}_{\boldsymbol{w},j}^n\|^2\big) + \gamma \Delta t \sum_{n=2}^{M} \big(\|\nabla \cdot \boldsymbol{e}_{\boldsymbol{v},j}^n\|^2 + \|\nabla \cdot \boldsymbol{e}_{\boldsymbol{w},j}^n\|^2\big) \\
&\leq 2\Bigg(\|\boldsymbol{\varphi}_{j,h}^M\|^2 + \|\boldsymbol{\psi}_{j,h}^M\|^2 + \alpha_j \Delta t \sum_{n=2}^{M} \big(\|\nabla \boldsymbol{\varphi}_{j,h}^n\|^2 + \|\nabla \boldsymbol{\psi}_{j,h}^n\|^2\big) + \gamma \Delta t \sum_{n=2}^{M} \big(\|\nabla \cdot \boldsymbol{\varphi}_{j,h}^n\|^2 + \|\nabla \cdot \boldsymbol{\psi}_{j,h}^n\|^2\big) \\
&+ \|\boldsymbol{\eta}_{\boldsymbol{v},j}^M\|^2 + \|\boldsymbol{\eta}_{\boldsymbol{w},j}^M\|^2 + \alpha_j \Delta t \sum_{n=2}^{M} \big(\|\nabla \boldsymbol{\eta}_{\boldsymbol{v},j}^n\|^2 + \|\nabla \boldsymbol{\eta}_{\boldsymbol{w},j}^n\|^2\big) + \gamma \Delta t \sum_{n=2}^{M} \big(\|\nabla \cdot \boldsymbol{\eta}_{\boldsymbol{v},j}^n\|^2 + \|\nabla \cdot \boldsymbol{\eta}_{\boldsymbol{w},j}^n\|^2\big) \Bigg) \\
&\leq C\big(h^{2k} + (\Delta t)^4 + (\nu_j - \nu_{m,j})^2(1-\theta)^2(\Delta t)^2\big). \qquad (3.36)
\end{aligned}
$$

Define $< \boldsymbol{e}_v >^n := \frac{1}{J} \sum_{j=1}^{J} (2\boldsymbol{e}_{\boldsymbol{v},j}^n - \boldsymbol{e}_{\boldsymbol{v},j}^{n-1})$, and $< \boldsymbol{e}_w >^n := \frac{1}{J} \sum_{j=1}^{J} (2\boldsymbol{e}_{\boldsymbol{w},j}^n - \boldsymbol{e}_{\boldsymbol{w},j}^{n-1})$, use triangle inequality and

equation (3.36), we have

$$\begin{aligned}\| < \boldsymbol{e_v} >^M \|^2 + \| < \boldsymbol{e_w} >^M \|^2 + \alpha_{\min}\Delta t \sum_{n=2}^{M} \left(\|\nabla < \boldsymbol{e_v} >^n \|^2 + \|\nabla < \boldsymbol{e_w} >^n \|^2\right) \\ +\gamma\Delta t \sum_{n=2}^{M} \left(\|\nabla\cdot < \boldsymbol{e_v} >^n \|^2 + \|\nabla\cdot < \boldsymbol{e_w} >^n \|^2\right) \\ \leq C\left(h^{2k} + (\Delta t)^4 + \frac{(1-\theta)^2(\Delta t)^2}{J}\sum_{j=1}^{J}(\nu_j - \nu_{m,j})^2\right). \qquad (3.37)\end{aligned}$$

By substituting the original variables, we complete the proof.

□

3.4 Numerical Experiments of the θ-scheme

To test the proposed Algorithm and the associated theories, in this section, we present results of numerical experiments. We employ a first-order backward-Euler timestepping scheme given in [37] to compute the first timestep solution so that the proposed second order Algorithms gets the required number of initial conditions for further timestep evolution.

We will use stable weakly divergence-free Taylor-hood (TH) element (P_2, P_1) for the velocity-pressure and magnetic field-magnetic pressure pairs on regular unstructured triangular mesh with grad-div stabilization parameter $\gamma = 10^5$. To estimate the viscosity parameters ν, and ν_m, we draw an independent sample of size $J = 20$ from a uniform distribution for each parameter.

3.4.1 Convergence Rate Verification

We will utilize the same manufactured analytical functions as (2.52). We will also be implementing noise, forcing functions, boundary conditions, and initial conditions just as we did in the convergence rate verification for Algorithm 2.

For each two-dimensional random sample of the viscosity parameters, the Algorithm 3 picks a maximum value of the parameter θ so that the condition

$$\frac{\theta}{1+\theta} < \frac{\bar{\nu}}{\bar{\nu}_m} < \frac{1+\theta}{\theta}$$

holds true. Then, we record the errors, compute the convergence rates, and present them in Tables 3.1-3.10. In Tables 3.1-3.5, we observe the second order temporal convergence which is an excellent agreement with the theoretical claim, and in Tables 3.6-3.10 we observe a second order spatial convergence which is also consistent with the theory as we have used (P_2, P_1) element.

We append Tables 3.1 to 3.10 to provide the temporal and spatial convergence at various ϵ values.

Table 3.1: θ-Scheme: Temporal errors and convergence rates for $\boldsymbol{v}$ and $\boldsymbol{w}$ with $\gamma = 100000$. $\nu_j \in [0.0009, 0.0011]$ utilizes $\theta = 1.0$ while $\nu_j \in [0.009, 0.011]$ utilizes $\theta = 0.109191$.

Temporal convergence (fixed $h = 1/64$, $T = 1$) with $j = 1, 2, \cdots, 20$								
$\epsilon = 0.0$	$\{(\nu_j, \nu_{m,j}) \in [0.0009, 0.0011] \times [0.0009, 0.0011]\}$				$\{(\nu_j, \nu_{m,j}) \in [0.009, 0.011] \times [0.0009, 0.0011]\}$			
Δt	$\|<\boldsymbol{e_v}>\|_{2,1}$	rate	$\|<\boldsymbol{e_w}>\|_{2,1}$	rate	$\|<\boldsymbol{e_v}>\|_{2,1}$	rate	$\|<\boldsymbol{e_w}>\|_{2,1}$	rate
$\frac{T}{4}$	5.5202e-01		4.3600e-01		2.8883e-01		2.4935e-01	
$\frac{T}{8}$	1.3842e-01	2.00	1.1773e-01	1.89	8.5909e-01	1.75	7.8401e-01	1.67
$\frac{T}{16}$	3.4930e-02	1.99	3.0991e-02	1.93	2.4315e-02	1.82	2.2833e-02	1.78
$\frac{T}{32}$	8.7272e-03	2.00	7.9073e-03	1.97	6.1903e-03	1.92	6.1903e-03	1.88
$\frac{T}{64}$	2.1852e-03	2.00	2.0048e-03	1.98	1.5919e-03	1.98	1.5919e-03	1.96

Table 3.2: θ-Scheme: Temporal errors and convergence rates for $\boldsymbol{v}$ and $\boldsymbol{w}$ with $\gamma = 100000$. $\nu_j \in [0.0009, 0.0011]$ utilizes $\theta = 1.0$ while $\nu_j \in [0.009, 0.011]$ utilizes $\theta = 0.109191$.

Temporal convergence (fixed $h = 1/64$, $T = 1$) with $j = 1, 2, \cdots, 20$								
$\epsilon = 0.001$	$\{(\nu_j, \nu_{m,j}) \in [0.0009, 0.0011] \times [0.0009, 0.0011]\}$				$\{(\nu_j, \nu_{m,j}) \in [0.009, 0.011] \times [0.0009, 0.0011]\}$			
Δt	$\|<\boldsymbol{e_v}>\|_{2,1}$	rate	$\|<\boldsymbol{e_w}>\|_{2,1}$	rate	$\|<\boldsymbol{e_v}>\|_{2,1}$	rate	$\|<\boldsymbol{e_w}>\|_{2,1}$	rate
$\frac{T}{4}$	5.5179e-01		4.3490e-01		2.8877e-01		2.4924e-01	
$\frac{T}{8}$	1.3840e-01	2.00	1.1762e-01	1.89	8.5897e-02	1.75	7.8383e-02	1.67
$\frac{T}{16}$	3.4927e-02	1.99	3.0977e-02	1.92	2.4311e-02	1.82	2.2828e-02	1.78
$\frac{T}{32}$	8.7270e-03	2.00	7.9061e-03	1.97	6.4450e-03	1.92	6.1895e-03	1.88
$\frac{T}{64}$	2.1849e-03	2.00	2.0038e-03	1.98	1.6308e-03	1.98	1.5908e-03	1.96

Table 3.3: θ-Scheme: Temporal errors and convergence rates for $\boldsymbol{v}$ and $\boldsymbol{w}$ with $\gamma = 100000$. $\nu_j \in [0.0009, 0.0011]$ utilizes $\theta = 1.0$ while $\nu_j \in [0.009, 0.011]$ utilizes $\theta = 0.109191$.

Temporal convergence (fixed $h = 1/64$, $T = 1$) with $j = 1, 2, \cdots, 20$								
$\epsilon = 0.01$	$\{(\nu_j, \nu_{m,j}) \in [0.0009, 0.0011] \times [0.0009, 0.0011]\}$				$\{(\nu_j, \nu_{m,j}) \in [0.009, 0.011] \times [0.0009, 0.0011]\}$			
Δt	$\|<\boldsymbol{e_v}>\|_{2,1}$	rate	$\|<\boldsymbol{e_w}>\|_{2,1}$	rate	$\|<\boldsymbol{e_v}>\|_{2,1}$	rate	$\|<\boldsymbol{e_w}>\|_{2,1}$	rate
$\frac{T}{4}$	5.3441e-01		3.7628e-01		2.8835e-01		2.4023e-01	
$\frac{T}{8}$	1.3666e-01	1.97	1.1013e-01	1.77	8.5000e-02	1.74	7.7062e-02	1.64
$\frac{T}{16}$	3.4748e-02	1.98	3.0106e-02	1.87	2.4158e-02	1.81	2.2607e-02	1.77
$\frac{T}{32}$	8.7029e-03	2.00	7.7806e-03	1.95	6.4120e-03	1.91	6.1414e-03	1.88
$\frac{T}{64}$	2.1803e-03	2.00	1.9790e-03	1.98	1.6224e-03	1.98	1.5786e-03	1.96

Table 3.4: θ-Scheme: Temporal errors and convergence rates for $\boldsymbol{v}$ and $\boldsymbol{w}$ with $\gamma = 100000$. $\nu_j \in [0.0009, 0.0011]$ utilizes $\theta = 1.0$ while $\nu_j \in [0.009, 0.011]$ utilizes $\theta = 0.109191$.

Temporal convergence (fixed $h = 1/64$, $T = 1$) with $j = 1, 2, \cdots, 20$								
$\epsilon = 0.05$	$\{(\nu_j, \nu_{m,j}) \in [0.0009, 0.0011] \times [0.0009, 0.0011]\}$				$\{(\nu_j, \nu_{m,j}) \in [0.009, 0.011] \times [0.0009, 0.0011]\}$			
Δt	$\|<\boldsymbol{e_v}>\|_{2,1}$	rate	$\|<\boldsymbol{e_w}>\|_{2,1}$	rate	$\|<\boldsymbol{e_v}>\|_{2,1}$	rate	$\|<\boldsymbol{e_w}>\|_{2,1}$	rate
$\frac{T}{4}$	4.5861e-01		2.5152e-01		2.3957e-01		1.8070e-01	
$\frac{T}{8}$	1.2363e-01	1.89	7.5345e-02	1.74	7.4468e-02	1.69	6.2555e-02	1.53
$\frac{T}{16}$	3.2391e-02	1.93	2.1357e-02	1.82	2.1563e-02	1.79	1.8910e-02	1.73
$\frac{T}{32}$	8.2462e-03	1.97	5.6715e-03	1.91	5.7364e-03	1.91	5.1628e-03	1.87
$\frac{T}{64}$	2.0818e-03	1.99	1.4682e-03	1.95	1.4422e-03	1.99	1.3162e-03	1.97

Table 3.5: θ-Scheme: Temporal errors and convergence rates for $\boldsymbol{v}$ and $\boldsymbol{w}$ $\gamma = 100000$. $\nu_j \in [0.0009, 0.0011]$ utilizes $\theta = 1.0$ while $\nu_j \in [0.009, 0.011]$ utilizes $\theta = 0.109191$.

Temporal convergence (fixed $h = 1/64$, $T = 1$) with $j = 1, 2, \cdots, 20$								
$\epsilon = 0.1$	$\{(\nu_j, \nu_{m,j}) \in [0.0009, 0.0011] \times [0.0009, 0.0011]\}$				$\{(\nu_j, \nu_{m,j}) \in [0.009, 0.011] \times [0.0009, 0.0011]\}$			
Δt	$\|<\boldsymbol{e_v}>\|_{2,1}$	rate	$\|<\boldsymbol{e_w}>\|_{2,1}$	rate	$\|<\boldsymbol{e_v}>\|_{2,1}$	rate	$\|<\boldsymbol{e_w}>\|_{2,1}$	rate
$\frac{T}{4}$	3.9623e-01		1.7459e-01		1.9591e-01		1.4800e-01	
$\frac{T}{8}$	1.0823e-01	1.87	5.3527e-02	1.71	6.0773e-02	1.69	4.9441e-02	1.58
$\frac{T}{16}$	2.8624e-02	1.92	1.7192e-02	1.64	1.7427e-02	1.80	1.4725e-02	1.75
$\frac{T}{32}$	7.3330e-03	1.96	4.9390e-03	1.80	4.6126e-03	1.92	4.0379e-03	1.87
$\frac{T}{64}$	1.8625e-03	1.98	1.2988e-03	1.93	1.1654e-03	1.98	1.0480e-03	1.95

Table 3.6: θ-Scheme: Spatial errors and convergence rates for $\boldsymbol{v}$ and $\boldsymbol{w}$ with $\gamma = 1000000$. $\nu_j \in [0.0009, 0.0011]$ utilizes $\theta = 1.0$ while $\nu_j \in [0.009, 0.011]$ utilizes $\theta = 0.109191$.

Spatial convergence (fixed $T = 0.001$, $\Delta t = T/8$) with $j = 1, 2, \cdots, 20$								
$\epsilon = 0.0$	$\{(\nu_j, \nu_{m,j}) \in [0.0009, 0.0011] \times [0.0009, 0.0011]\}$				$\{(\nu_j, \nu_{m,j}) \in [0.009, 0.011] \times [0.0009, 0.0011]\}$			
h	$\|<\boldsymbol{e_v}>\|_{2,1}$	rate	$\|<\boldsymbol{e_w}>\|_{2,1}$	rate	$\|<\boldsymbol{e_v}>\|_{2,1}$	rate	$\|<\boldsymbol{e_w}>\|_{2,1}$	rate
$\frac{1}{4}$	1.0074e-04		1.9305e-04		1.0074e-04		1.9305e-04	
$\frac{1}{8}$	2.5324e-05	1.99	4.8228e-05	2.00	2.5324e-05	1.99	4.8228e-05	2.00
$\frac{1}{16}$	6.3396e-06	2.00	1.2055e-05	2.00	6.3396e-06	2.00	1.2055e-05	2.00
$\frac{1}{32}$	1.5855e-06	2.00	3.0136e-06	2.00	1.5855e-06	2.00	3.0136e-06	2.00
$\frac{1}{64}$	3.9649e-07	2.00	7.5342e-07	2.00	3.9645e-07	2.00	7.5341e-07	2.00

Table 3.7: θ-Scheme: Spatial errors and convergence rates for $\boldsymbol{v}$ and $\boldsymbol{w}$ with $\gamma = 1000000$. $\nu_j \in [0.0009, 0.0011]$ utilizes $\theta = 1.0$ while $\nu_j \in [0.009, 0.011]$ utilizes $\theta = 0.109191$.

Spatial convergence (fixed $T = 0.001$, $\Delta t = T/8$) with $j = 1, 2, \cdots, 20$								
$\epsilon = 0.001$	$\{(\nu_j, \nu_{m,j}) \in [0.0009, 0.0011] \times [0.0009, 0.0011]\}$				$\{(\nu_j, \nu_{m,j}) \in [0.009, 0.011] \times [0.0009, 0.0011]\}$			
h	$\|<\boldsymbol{e_v}>\|_{2,1}$	rate	$\|<\boldsymbol{e_w}>\|_{2,1}$	rate	$\|<\boldsymbol{e_v}>\|_{2,1}$	rate	$\|<\boldsymbol{e_w}>\|_{2,1}$	rate
$\frac{1}{4}$	1.0074e-04		1.9305e-04		1.0074e-04		1.9305e-04	
$\frac{1}{8}$	2.5324e-05	1.99	4.8228e-05	2.00	2.5324e-05	1.99	4.8228e-05	2.00
$\frac{1}{16}$	6.3396e-06	2.00	1.2055e-05	2.00	6.3396e-06	2.00	1.2055e-05	2.00
$\frac{1}{32}$	1.5855e-06	2.00	3.0136e-06	2.00	1.5855e-06	2.00	3.0136e-06	2.00
$\frac{1}{64}$	3.9649e-07	2.00	7.5342e-07	2.00	3.9645e-07	2.00	7.5341e-07	2.00

Table 3.8: θ-Scheme: Spatial errors and convergence rates for $\boldsymbol{v}$ and $\boldsymbol{w}$ with $\gamma = 1000000$. $\nu_j \in [0.0009, 0.0011]$ utilizes $\theta = 1.0$ while $\nu_j \in [0.009, 0.011]$ utilizes $\theta = 0.109191$.

Spatial convergence (fixed $T = 0.001$, $\Delta t = T/8$) with $j = 1, 2, \cdots, 20$								
$\epsilon = 0.01$	$\{(\nu_j, \nu_{m,j}) \in [0.0009, 0.0011] \times [0.0009, 0.0011]\}$				$\{(\nu_j, \nu_{m,j}) \in [0.009, 0.011] \times [0.0009, 0.0011]\}$			
h	$\|<\boldsymbol{e_v}>\|_{2,1}$	rate	$\|<\boldsymbol{e_w}>\|_{2,1}$	rate	$\|<\boldsymbol{e_v}>\|_{2,1}$	rate	$\|<\boldsymbol{e_w}>\|_{2,1}$	rate
$\frac{1}{4}$	1.0074e-04		1.9305e-04		1.0074e-04		1.9305e-04	
$\frac{1}{8}$	2.5324e-05	1.99	4.8228e-05	2.00	2.5324e-05	1.99	4.8228e-05	2.00
$\frac{1}{16}$	6.3396e-06	2.00	1.2055e-05	2.00	6.3396e-06	2.00	1.2055e-05	2.00
$\frac{1}{32}$	1.5855e-06	2.00	3.0136e-06	2.00	1.5855e-06	2.00	3.0136e-06	2.00
$\frac{1}{64}$	3.9649e-07	2.00	7.5342e-07	2.00	3.9645e-07	2.00	7.5341e-07	2.00

Table 3.9: θ-Scheme: Spatial errors and convergence rates for $\boldsymbol{v}$ and $\boldsymbol{w}$ with $\gamma = 1000000$. $\nu_j \in [0.0009, 0.0011]$ utilizes $\theta = 1.0$ while $\nu_j \in [0.009, 0.011]$ utilizes $\theta = 0.109191$.

Spatial convergence (fixed $T = 0.001$, $\Delta t = T/8$) with $j = 1, 2, \cdots, 20$								
$\epsilon = 0.05$	$\{(\nu_j, \nu_{m,j}) \in [0.0009, 0.0011] \times [0.0009, 0.0011]\}$				$\{(\nu_j, \nu_{m,j}) \in [0.009, 0.011] \times [0.0009, 0.0011]\}$			
h	$\|<\boldsymbol{e_v}>\|_{2,1}$	rate	$\|<\boldsymbol{e_w}>\|_{2,1}$	rate	$\|<\boldsymbol{e_v}>\|_{2,1}$	rate	$\|<\boldsymbol{e_w}>\|_{2,1}$	rate
$\frac{1}{4}$	1.0074e-04		1.9305e-04		1.0074e-04		1.9305e-04	
$\frac{1}{8}$	2.5324e-05	1.99	4.8228e-05	2.00	2.5324e-05	1.99	4.8228e-05	2.00
$\frac{1}{16}$	6.3396e-06	2.00	1.2055e-05	2.00	6.3396e-06	2.00	1.2055e-05	2.00
$\frac{1}{32}$	1.5855e-06	2.00	3.0136e-06	2.00	1.5855e-06	2.00	3.0136e-06	2.00
$\frac{1}{64}$	3.9649e-07	2.00	7.5342e-07	2.00	3.9645e-07	2.00	7.5341e-07	2.00

Table 3.10: θ-Scheme: Spatial errors and convergence rates for $\boldsymbol{v}$ and $\boldsymbol{w}$ with $\gamma = 1000000$. $\nu_j \in [0.0009, 0.0011]$ utilizes $\theta = 1.0$ while $\nu_j \in [0.009, 0.011]$ utilizes $\theta = 0.109191$.

Spatial convergence (fixed $T = 0.001$, $\Delta t = T/8$) with $j = 1, 2, \cdots, 20$								
$\epsilon = 0.1$	$\{(\nu_j, \nu_{m,j}) \in [0.0009, 0.0011] \times [0.0009, 0.0011]\}$				$\{(\nu_j, \nu_{m,j}) \in [0.009, 0.011] \times [0.0009, 0.0011]\}$			
h	$\|<\boldsymbol{e_v}>\|_{2,1}$	rate	$\|<\boldsymbol{e_w}>\|_{2,1}$	rate	$\|<\boldsymbol{e_v}>\|_{2,1}$	rate	$\|<\boldsymbol{e_w}>\|_{2,1}$	rate
$\frac{1}{4}$	1.0074e-04		1.9305e-04		1.0074e-04		1.9305e-04	
$\frac{1}{8}$	2.5324e-05	1.99	4.8228e-05	2.00	2.5324e-05	1.99	4.8228e-05	2.00
$\frac{1}{16}$	6.3396e-06	2.00	1.2055e-05	2.00	6.3396e-06	2.00	1.2055e-05	2.00
$\frac{1}{32}$	1.5855e-06	2.00	3.0136e-06	2.00	1.5855e-06	2.00	3.0136e-06	2.00
$\frac{1}{64}$	3.9649e-07	2.00	7.5342e-07	2.00	3.9645e-07	2.00	7.5341e-07	2.00

4 Comparison Tables

We append Tables 4.1 to 4.4 to provide a comparison between the the SPP-FEM and BE-MHD algorithm. Each simulations is ran using a fixed $\epsilon = 0.01$ and varying stabilization parameter γ.

Table 4.1: Difference between the BE-MHD and SPP algorithms and the convergence rates with varying γ, fixed $\epsilon = 0.01$ and two different samples $\{(\nu_j, \nu_{m,j}) \in [0.9, 1.1] \times [0.9, 1.1]\}$and $\{(\nu_j, \nu_{m,j}) \in [0.009, 0.011] \times [0.09, 0.11]\}$.

Fixed $T = 1.0$ and $\Delta t = T/10$ with $j = 1, 2, \cdots, 20$								
$\epsilon = 0.01$	$\{(\nu_j, \nu_{m,j}) \in [0.9, 1.1] \times [0.9, 1.1]\}$				$\{(\nu_j, \nu_{m,j}) \in [0.009, 0.011] \times [0.09, 0.11]\}$			
γ	$\|<\boldsymbol{v}_h - \hat{\boldsymbol{v}}_h>\|_{2,1}$	rate	$\|<\boldsymbol{w}_h - \hat{\boldsymbol{w}}_h>\|_{2,1}$	rate	$\|<\boldsymbol{v}_h - \hat{\boldsymbol{v}}_h>\|_{2,1}$	rate	$\|<\boldsymbol{w}_h - \hat{\boldsymbol{w}}_h>\|_{2,1}$	rate
1	5.5784e-01		5.32025e-01		1.5279		1.4276	
10	1.5396e-01	0.56	1.4646e-01	0.56	2.0998e-01	0.86	1.8832e-01	0.88
10^2	1.9221e-02	0.90	1.8249e-02	0.90	2.1919e-02	0.98	1.9578e-02	0.98
10^3	1.9734e-03	0.99	1.8733e-03	0.99	2.2018e-03	1.00	1.9660e-03	1.00
10^4	1.9785e-04	1.00	1.8782e-04	1.00	2.2026e-04	1.00	1.9668e-04	1.00
10^5	1.9784e-05	1.00	1.8790e-05	1.00	2.2036e-05	1.00	1.9649e-05	1.00
10^6	2.0850e-06	0.98	2.0272e-06	0.97	3.8125e-06	0.76	3.1253e-06	0.80

Table 4.2: Difference between the BE-MHD and SPP algorithms and the convergence rates with varying γ, fixed $\epsilon = 0.01$ and two different samples $\{(\nu_j, \nu_{m,j}) \in [0.9, 1.1] \times [0.9, 1.1]\}$and $\{(\nu_j, \nu_{m,j}) \in [0.009, 0.011] \times [0.09, 0.11]\}$.

Fixed $T = 1.0$ and $\Delta t = T/10$ with $j = 1, 2, \cdots, 20$								
$\epsilon = 0.01$	$\{(\nu_j, \nu_{m,j}) \in [0.009, 0.011] \times [0.0009, 0.0011]\}$				$\{(\nu_j, \nu_{m,j}) \in [0.0009, 0.0011] \times [0.0009, 0.0011]\}$			
γ	$\|<\boldsymbol{v}_h - \hat{\boldsymbol{v}}_h>\|_{2,1}$	rate	$\|<\boldsymbol{w}_h - \hat{\boldsymbol{w}}_h>\|_{2,1}$	rate	$\|<\boldsymbol{v}_h - \hat{\boldsymbol{v}}_h>\|_{2,1}$	rate	$\|<\boldsymbol{w}_h - \hat{\boldsymbol{w}}_h>\|_{2,1}$	rate
1	2.5284		1.8966		4.0012		2.2296	
10	3.7455e-01	0.83	3.2483e-01	0.77	5.8161e-01	0.84	3.5660e-01	0.80
10^2	3.9501e-02	0.98	3.5633e-02	0.96	6.0928e-02	0.98	3.9328e-02	0.96
10^3	3.9690e-03	1.00	3.5951e-03	1.00	6.1112e-03	1.00	3.9715e-03	1.00
10^4	3.9450e-04	1.00	3.5761e-04	1.00	6.0112e-04	1.01	3.9731e-04	1.00
10^5	3.8554e-05	1.01	3.6154e-05	1.00	5.5968e-05	1.03	4.7789e-05	0.92

Table 4.3: Difference between the BE-MHD and SPP algorithms and the convergence rates with varying γ, fixed $\epsilon = 0.01$ and two different samples $\{(\nu_j, \nu_{m,j}) \in [0.9, 1.1] \times [0.9, 1.1]\}$and $\{(\nu_j, \nu_{m,j}) \in [0.009, 0.011] \times [0.09, 0.11]\}$.

Fixed $T = 1.0$ and $\Delta t = T/10$ with $j = 1, 2, \cdots, 20$				
$\epsilon = 0.01$	$\{(\nu_j, \nu_{m,j}) \in [0.9, 1.1] \times [0.9, 1.1]\}$			
γ	$\|<\boldsymbol{v}_h - \hat{\boldsymbol{v}}_h>\|_{\infty,1}$	rate	$\|<\boldsymbol{w}_h - \hat{\boldsymbol{w}}_h>\|_{\infty,1}$	rate
1	5.0649e-01		4.6206e-01	
10	3.8430e-02	1.12	3.4736e-02	1.12
10^2	5.9807e-04	1.81	5.3806e-04	1.81
10^3	6.3024e-06	1.98	5.6685e-06	1.98
10^4	6.3352e-08	2.00	5.6982e-08	2.00
10^5	6.3359e-10	2.00	5.7041e-10	2.00
10^6	7.2035e-12	1.94	6.7268e-12	1.93

Table 4.4: Difference between the BE-MHD and SPP algorithms and the convergence rates with varying γ, fixed $\epsilon = 0.01$ and two different samples $\{(\nu_j, \nu_{m,j}) \in [0.009, 0.011] \times [0.0009, 0.0011]\}$and $\{(\nu_j, \nu_{m,j}) \in [0.0009, 0.0011] \times [0.0009, 0.0011]\}$.

Fixed $T = 1.0$ and $\Delta t = T/10$ with $j = 1, 2, \cdots, 20$								
$\epsilon = 0.01$	$\{(\nu_j, \nu_{m,j}) \in [0.009, 0.011] \times [0.0009, 0.0011]\}$				$\{(\nu_j, \nu_{m,j}) \in [0.0009, 0.0011] \times [0.0009, 0.0011]\}$			
γ	$\|<\boldsymbol{v}_h - \hat{\boldsymbol{v}}_h>\|_{\infty,1}$	rate	$\|<\boldsymbol{w}_h - \hat{\boldsymbol{w}}_h>\|_{\infty,1}$	rate	$\|<\boldsymbol{v}_h - \hat{\boldsymbol{v}}_h>\|_{\infty,1}$	rate	$\|<\boldsymbol{w}_h - \hat{\boldsymbol{w}}_h>\|_{\infty,1}$	rate
1	4.0601		3.6191		27.5591		11.6088	
10	7.5828e-02	1.73	6.0896e-02	1.77	6.0567e-01	1.66	3.0238e-01	1.58
10^2	8.3137e-04	1.96	6.6591e-04	1.96	6.6928e-03	1.96	3.7597e-03	1.91
10^3	8.3960e-06	2.00	6.7259e-06	2.00	6.7529e-05	2.00	3.8453e-05	1.99
10^4	8.4048e-08	2.00	6.7339e-08	2.00	6.6685e-07	2.01	3.8563e-07	2.00
10^5	8.3719e-10	2.00	6.8263e-10	1.99	5.9057e-09	2.05	4.1964e-09	1.96

5 Conclusions and Future Works

In this thesis, we have proposed, analyzed, and tested two novel efficient algorithms for magnetohydrodynamic flow simulations, both of which are fully discrete, and decoupled time stepping schemes. The first of being the grad-div stabilize penalty projection algorithm, which utilized grad-div stabilization and ensemble eddy-viscosity terms to compute MHD flow ensemble. This algorithm: (1) Is decoupled into four sub problems, which are solved simultaneously. (2) Solves the velocity, magnetic field, and pressure separately. (3) Keeps the system matrix common to all ensemble members with different right-hand-side vectors. The second of which being the fully discrete θ-scheme. This algorithm: (1) Solves both Step 1 and Step 2 simultaneously. (2) Exhibits second order temporal convergence for practical flow. (3) Makes the system matrix on the left-hand-side independent of j, while the right-hand-side vector becomes j dependent. Future works may include using machine learning techniques, such as random forest and convolutional neural network, which should result in a more accurate simulation. We plan to utilize distinct segments of the data for the purpose of testing and training a model during various iterations. We plan to propose and investigate a penalty-projection-based Uncertainty Quantification (UQ) for Navier-Stokes (NS) flow problems. The use of the stochastic collocation method in conjunction with the proposed penalty projection method for the UQ of NS and MHD flow problems.

REFERENCES

[1] M. Akbas, S. Kaya, M. Mohebujjaman, and L. Rebholz. Numerical analysis and testing of a fully discrete, decoupled penalty-projection algorithm for MHD in Elsässer variable. International Journal of Numerical Analysis & Modeling, 13(1):90–113, 2016.

[2] A. V. Arefiev and B. N. Breizman. Magnetohydrodynamic scenario of plasma detachment in a magnetic nozzle. physics of plasmas, 12(4), 2005.

[3] D. Arnold and J. Qin. Quadratic velocity/linear pressure Stokes elements. Advances in Computer Methods for Partial Differential Equations, 7:28–34, 1992.

[4] M. J. Balajewicz, E. H Dowell, and B. R. Noack. Low-dimensional modelling of high-Reynolds-number shear flows incorporating constraints from the Navier-Stokes equation. Journal of Fluid Mechanics, 729:285, 2013.

[5] L. Barleon, V. Casal, and L. Lenhart. MHD flow in liquid-metal-cooled blankets. Fusion Engineering and Design, 14:401–412, 1991.

[6] D. Biskamp. Magnetohydrodynamic Turbulence. Cambridge University Press, Cambridge, 2003.

[7] H. Branover, A. Eidelman, M. Nagorny, and M. Kireev. Magnetohydrodynamic simulation of quasi-two-dimensional geophysical turbulence. Progress in Turbulence Research, 162:64, 1994.

[8] S. C. Brenner and L. R. Scott. The Mathematical Theory of Finite Element Methods. Texts in Applied Mathematics, 15. Springer Science+Business Media, LLC, 2008.

[9] M. Case, A. Labovsky, L. G. Rebholz, and N. Wilson. A high physical accuracy method for incompressible magnetohydrodynamics. Int. J. Numer. Anal. Model. Ser. B, 1(2):219–238, 2010.

[10] M. A. Case, V. J. Ervin, A. Linke, and L. G. Rebholz. A connection between Scott–Vogelius and grad-div stabilized Taylor–Hood FE approximations of the Navier–Stokes equations. SIAM Journal on Numerical Analysis, 49(4):1461–1481, 2011.

[11] P. A. Davidson. An introduction to magnetohydrodynamics. Cambridge Texts in Applied Mathematics, Cambridge University Press, Cambridge, 2001.

[12] P.A. Davidson. An Introduction to Magnetohydrodynamics. Cambridge University Press, 2001.

[13] W. M. Elsässer. The hydromagnetic equations. Phys. Rev., 79:183, 1950.

[14] D. Erkmen, S. Kaya, and A. Çıbık. A second order decoupled penalty projection method based on deferred correction for MHD in Elsässer variable. Journal of Computational and Applied Mathematics, 371:112694, 2020.

[15] D. Erkmen and A. Labovsky. Note on the usage of grad-div stabilization for the penalty-projection algorithm in magnetohydrodynamics. Applied Mathematics and Computation, 349:48–52, 2019.

[16] L. Fick, Y. Maday, A. T. Patera, and T. Taddei. A stabilized POD model for turbulent flows over a range of Reynolds numbers: Optimal parameter sampling and constrained projection. Journal of Computational Physics, 371:214–243, 2018.

[17] V. Girault and P.-A.Raviart. Finite Element Methods for Navier-Stokes Equations: Theory and Algorithms. Springer-Verlag, 1986.

[18] H. Hashizume. Numerical and experimental research to solve MHD problem in liquid blanket system. Fusion Engineering and Design, 81:1431–1438, 2006.

[19] T. Heister, M. Mohebujjaman, and L. Rebholz. Decoupled, unconditionally stable, higher order discretizations for MHD flow simulation. Journal of Scientific Computing, 71:21–43, 2017.

[20] J. G. Heywood and R. Rannacher. Finite-Element approximation of the nonstationary Navier-Stokes problem part IV: error analysis for second-order time discretization. SIAM Journal on Numerical Analysis, 27:353–384, 1990.

[21] E. W. Jenkins, V. John, A. Linke, and L. G. Rebholz. On the parameter choice in grad-div stabilization for the

Stokes equations. Advances in Computational Mathematics, 40(2):491–516, 2014.

[22] N. Jiang and W. Layton. An algorithm for fast calculation of flow ensembles. International Journal for Uncertainty Quantification, 4:273–301, 2014.

[23] N. Jiang and W. Layton. Numerical analysis of two ensemble eddy viscosity numerical regularizations of fluid motion. Numerical Methods for Partial Differential Equations, 31:630–651, 2015.

[24] N. Jiang and M. Schneier. An efficient, partitioned ensemble algorithm for simulating ensembles of evolutionary MHD flows at low magnetic Reynolds number. Numerical Methods for Partial Differential Equations, 34(6):2129–2152, 2018.

[25] P. Kuberry, A. Larios, L. G. Rebholz, and N. E. Wilson. Numerical approximation of the Voigt regularization for incompressible Navier–Stokes and magnetohydrodynamic flows. Computers & Mathematics with Applications, 64(8):2647–2662, 2012.

[26] L. D. Landau and E. M. Lifshitz. Electrodynamics of Continuous Media. Pergamon Press, Oxford, 1960.

[27] M. W. Lee, E. H. Dowell, and M. J. Balajewicz. A study of the regularized lid-driven cavity's progression to chaos. Communications in Nonlinear Science and Numerical Simulation, 71:50–72, 2019.

[28] J. M. Lewis. Roots of ensemble forecasting. Monthly Weather Review, 133:1865 – 1885, 2005.

[29] Y. Li and C. Trenchea. Partitioned second order method for magnetohydrodynamics in elsässer variables. Discrete & Continuous Dynamical Systems-B, 23(7):2803, 2018.

[30] T. F. Lin, J. B. Gilbert, and R. Kossowsky. Sea-water magnetohydrodynamic propulsion for next-generation undersea vehicles. Technical report, PENNSYLVANIA STATE UNIV STATE COLLEGE APPLIED RESEARCH LAB, 1990.

[31] T. F. Lin, J. B. Gilbert, R. Kossowsky, and PENNSYLVANIA STATE UNIV STATE COLLEGE. Sea-Water Magnetohydrodynamic Propulsion for Next-Generation Undersea Vehicles. Defense Technical Information Center, 1990.

[32] A. Linke. Collision in a cross-shaped domain–A steady 2d Navier–Stokes example demonstrating the importance of mass conservation in CFD. Computer Methods in Applied Mechanics and Engineering, 198(41-44):3278–3286, 2009.

[33] A. Linke, M. Neilan, L. Rebholz, and N. Wilson. A connection between coupled and penalty projection timestepping schemes with FE spacial discretization for the Navier-Stokes equations. submitted, 2014.

[34] T. N. Palmer M. Leutbecher. Ensemble forecasting. Journal of Computational Physics, 227:3515–3539, 2008.

[35] M. Mohebujjaman. High order efficient algorithm for computation of MHD flow ensembles. Advances in Applied Mathematics and Mechanics, in press, 2021.

[36] M. Mohebujjaman and L. G. Rebholz. An efficient algorithm for computation of MHD flow ensembles. Computational Methods in Applied Mathematics, 17:121–137, 2017.

[37] M. Mohebujjaman, H. Wang, L. G. Rebholz, and M. A. A. Mahbub. An efficient algorithm for parameterized magnetohydrodynamic flow ensembles simulation. Computers & Mathematics with Applications, 112:167–180, 2022.

[38] J. C. Robinson, J. L. Rodrigo, and W. Sadowski. The Three-Dimensional Navier-Stokes Equations. Cambridge University Press, 2016.

[39] K. Sankaran, L. Martinelli, S. C. Jardin, and E. Y. Choueiri. A flux-limited numerical method for solving the mhd equations to simulate propulsive plasma flows. International journal for numerical methods in engineering, 53(6):1415–1432, 2002.

[40] S. Smolentsev, R. Moreau, L. Buhler, and C. Mistrangelo. MHD thermofluid issues of liquid-metal blankets: phe-

nomena and advances. Fusion Engineering and Design, 85:1196–1205, 2010.

[41] Z. Sun, J. A. Salami, A. Khodak, F. Saenz, B. Wynne, R. Maingi, K. Hanada, C. H. Hu, and E. Kolemen. Magnetohydrodynamics in free surface liquid metal flow relevant to plasma-facing components. Nuclear Fusion, 63(7):076022, 2023.

[42] C. Trenchea. Unconditional stability of a partitioned IMEX method for magnetohydrodynamic flows. Applied Mathematics Letters, 27:97–100, 2014.

[43] N. Wilson, A. Labovsky, and C. Trenchea. High accuracy method for magnetohydrodynamics system in Elsässer variables. Computational Methods in Applied Mathematics, 15(1):97–110, 2015.

[44] X. Wu, P. Tao, J. Zhu, C. Wu, Y. Wei, Y. Peng, and B. Gao. In vitro study on the dynamics of blood flow impelled by an alternating current magnetohydrodynamic blood pump. Artificial organs, 42(11):E349–E356, 2018.

[45] S. Zhang. A new family of stable mixed finite elements for the 3D Stokes equations. Mathematics of Computation, 74:543–554, 2005.

[46] B. Zheng and Y. Shang. Two-level defect-correction stabilized algorithms for the simulation of 2D/3D steady Navier-Stokes equations with damping. Applied Numerical Mathematics, 163:182–203, 2021.

6 Appendix

In the appendix, necessary G-Calculations for θ-Scheme are provided.

6.1 G-Calculations for θ-Scheme

$$
\begin{aligned}
G_1(t,\boldsymbol{v}_j,\boldsymbol{w}_j,\boldsymbol{\chi}_{j,h}) := &((\boldsymbol{w}_j(t^{n+1}) - 2\boldsymbol{w}_j(t^n) + \boldsymbol{w}_j(t^{n-1}))\cdot\nabla\boldsymbol{v}_j(t^{n+1}),\boldsymbol{\chi}_{j,h}) \\
&+ (\boldsymbol{w}_{j,h}^{'n}\cdot\nabla(\boldsymbol{v}_j(t^{n+1}) - 2\boldsymbol{v}_j(t^n) + \boldsymbol{v}_j(t^{n-1})),\boldsymbol{\chi}_{j,h}) \\
&+ \frac{\nu_j^{'} + \nu_{m,j}^{'}}{2}\Big(\nabla\big(\boldsymbol{v}_j(t^{n+1}) - 2\boldsymbol{v}_j(t^n) + \boldsymbol{v}_j(t^{n-1})\big),\nabla\boldsymbol{\chi}_{j,h}\Big) \\
&+ \frac{\nu_j - \nu_{m,j}}{2}\big(\nabla(\boldsymbol{w}_j(t^{n+1}) - (1+\theta)\boldsymbol{w}_j(t^n) + \theta\boldsymbol{w}_j(t^{n-1})),\nabla\boldsymbol{\chi}_{j,h}\big) \\
&+ \left(\boldsymbol{v}_{j,t}(t^{n+1}) - \frac{3\boldsymbol{v}_j(t^{n+1}) - 4\boldsymbol{v}_j(t^n) + \boldsymbol{v}_j(t^{n-1})}{2\Delta t},\boldsymbol{\chi}_{j,h}\right),
\end{aligned}
\tag{6.1}
$$

$$
\boldsymbol{w}_j(t^{n+1}) = \boldsymbol{w}_j(t^n + \Delta t) = \boldsymbol{w}_j(t^n) + \boldsymbol{w}_{j,t}(t^n)\frac{\Delta t}{1!} + \boldsymbol{w}_{j,tt}(s^*)\frac{(\Delta t)^2}{2!}, \tag{6.2}
$$

$$
\boldsymbol{w}_j(t^{n-1}) = \boldsymbol{w}_j(t^n - \Delta t) = \boldsymbol{w}_j(t^n) - \boldsymbol{w}_{j,t}(t^n)\frac{\Delta t}{1!} + \boldsymbol{w}_{j,tt}(s^*)\frac{(\Delta t)^2}{2!}. \tag{6.3}
$$

Adding (6.2) and (6.3) gives

$$
\boldsymbol{w}_j(t^{n+1}) - 2\boldsymbol{w}_j(t^n) + \boldsymbol{w}_j(t^{n-1}) = \boldsymbol{w}_{j,tt}(s^*)(\Delta t)^2. \tag{6.4}
$$

Similarly,

$$
\boldsymbol{v}_j(t^{n+1}) - 2\boldsymbol{v}_j(t^n) + \boldsymbol{v}_j(t^{n-1}) = \boldsymbol{v}_{j,tt}(t^*)(\Delta t)^2. \tag{6.5}
$$

Again,

$$
\boldsymbol{v}_j(t^n) = \boldsymbol{v}_j(t^{n+1} - \Delta t) = \boldsymbol{v}_j(t^{n+1}) - \boldsymbol{v}_{j,t}(t^{n+1})\frac{\Delta t}{1!} + \boldsymbol{v}_{j,tt}(t^{n+1})\frac{(\Delta t)^2}{2!} + \boldsymbol{v}_{j,ttt}(s^{**})\frac{(\Delta t)^3}{3!}, \tag{6.6}
$$

$$
\boldsymbol{v}_j(t^{n-1}) = \boldsymbol{v}_j(t^{n+1} - 2\Delta t) = \boldsymbol{v}_j(t^{n+1}) - \boldsymbol{v}_{j,t}(t^{n+1})\frac{2\Delta t}{1!} + 2\boldsymbol{v}_{j,tt}(t^{n+1})(\Delta t)^2 - \boldsymbol{v}_{j,ttt}(s^{**})\frac{4(\Delta t)^3}{3}. \tag{6.7}
$$

If we subtract 4×(6.6) from equation (6.7), we will be left with

$$
\boldsymbol{v}_j(t^{n-1}) - 4\boldsymbol{v}_j(t^n) = -3\boldsymbol{v}_j(t^{n+1}) + 2\boldsymbol{v}_{j,t}(t^{n+1})\Delta t - 2\boldsymbol{v}_{j,ttt}(s^{**})(\Delta t)^3,
$$

which gives

$$\boldsymbol{v}_{j,t}(t^{n+1}) - \frac{3\boldsymbol{v}_j(t^{n+1}) - 4\boldsymbol{v}_j(t^n) + \boldsymbol{v}_j(t^{n-1})}{2\Delta t} = 2\boldsymbol{v}_{j,ttt}(s^{**})(\Delta t)^2. \tag{6.8}$$

Also,

$$\boldsymbol{w}_j(t^{n+1}) - (1+\theta)\boldsymbol{w}_j(t^n) + \theta\boldsymbol{w}_j(t^{n-1}) = (1-\theta)\boldsymbol{w}_{j,t}(s^{***})\Delta t.$$

Then,

$$\begin{aligned}|G_1(t,\boldsymbol{v}_j,\boldsymbol{w}_j,\boldsymbol{\varphi}_{j,h}^{n+1})| \le (\Delta t)^2|\big(\boldsymbol{w}_{tt}(s^*)\cdot\nabla\boldsymbol{v}_j(t^{n+1}),\boldsymbol{\varphi}_{j,h}^{n+1}\big)| + (\Delta t)^2|(\boldsymbol{w}_{j,h}^{'n}\cdot\nabla\boldsymbol{v}_{tt}(t^*),\boldsymbol{\varphi}_{j,h}^{n+1})|\\ +\frac{|\nu_j^{'}+\nu_{m,j}^{'}|}{2}(\Delta t)^2|\Big(\nabla\boldsymbol{v}_{tt}(t^*),\nabla\boldsymbol{\varphi}_{j,h}^{n+1}\Big)| + \frac{|\nu_j-\nu_{m,j}|}{2}(1-\theta)\Delta t\|\big(\nabla\boldsymbol{w}_{j,t}(s^{***}),\nabla\boldsymbol{\varphi}_{j,h}^{n+1}\big)|\\ +2(\Delta t)^2|\Big(\boldsymbol{v}_{ttt}(s^{**}),\boldsymbol{\varphi}_{j,h}^{n+1}\Big)|\end{aligned}$$

$$\begin{aligned}|G_1(t,\boldsymbol{v}_j,\boldsymbol{w}_j,\boldsymbol{\varphi}_{j,h}^{n+1})| \le C(\Delta t)^2\|\nabla\boldsymbol{w}_{tt}(s^*)\|\|\nabla\boldsymbol{v}_j(t^{n+1})\|\|\nabla\boldsymbol{\varphi}_{j,h}^{n+1}\| + C(\Delta t)^2\|\nabla\boldsymbol{w}_{j,h}^{'n}\|\|\nabla\boldsymbol{v}_{tt}(t^*)\|\|\nabla\boldsymbol{\varphi}_{j,h}^{n+1}\|\\ +\frac{|\nu_j^{'}+\nu_{m,j}^{'}|}{2}(\Delta t)^2\|\nabla\boldsymbol{v}_{tt}(t^*)\|\|\nabla\boldsymbol{\varphi}_{j,h}^{n+1}\| + \frac{|\nu_j-\nu_{m,j}|}{2}(1-\theta)\Delta t\|\nabla\boldsymbol{w}_t(s^{***})\|\|\nabla\boldsymbol{\varphi}_{j,h}^{n+1}\|\\ +2C(\Delta t)^2\|\boldsymbol{v}_{ttt}(s^{**})\|\|\nabla\boldsymbol{\varphi}_{j,h}^{n+1}\|\end{aligned}$$

$$\begin{aligned}|G_1(t,\boldsymbol{v}_j,\boldsymbol{w}_j,\boldsymbol{\varphi}_{j,h}^{n+1})| \le \frac{\alpha_j}{44}\|\nabla\boldsymbol{\varphi}_{j,h}^{n+1}\|^2 + (\Delta t)^4\frac{C}{\alpha_j}\|\nabla\boldsymbol{w}_{tt}(s^*)\|^2\|\nabla\boldsymbol{v}_j(t^{n+1})\|^2\\ +(\Delta t)^4\frac{C}{\alpha_j}\|\nabla\boldsymbol{w}_{j,h}^{'n}\|^2\|\nabla\boldsymbol{v}_{tt}(t^*)\|^2 + (\Delta t)^4\frac{55(\nu_j^{'}+\nu_{m,j}^{'})^2}{4\alpha_j}\|\nabla\boldsymbol{v}_{tt}(t^*)\|^2\\ +(\Delta t)^2\frac{55(\nu_j-\nu_{m,j})^2(1-\theta)^2}{4\alpha_j}\|\nabla\boldsymbol{w}_t(s^{***})\|^2 + (\Delta t)^4\frac{C}{\alpha_j}\|\boldsymbol{v}_{ttt}(s^{**})\|^2\end{aligned}$$

VITA

Julián Vicente Miranda

Major Specialization

Mathematics

Educational Background

Texas A&M International University (TAMIU), August 2017 - May 2022

Bachelor of Science, Mathematics

Minor in Applied Physics

Professional Experience

Graduate Research Assistant

TAMIU, June 2022 - August 2023

Undergraduate Research Assistant

TAMIU, Sep 2021 - June 2022

Mathematics Tutor

TAMIU, Sep 2021 - May 2022

Contact info: Miranda.V.Julian@gmail.com